

Disaster & Development

Volume 4 • Number 2 • November 2010

ISSN: 0973-6700

Aster Stereo Images for Landslide Hazard Assessment in the Central Alborz Mountains, Iran

Vegetation & Agriculture Health Monitoring using Worldview-2 Satellite Image derived indices:
An Approach for Drought Assessment in Jharkhand, India

Geospatial Modelling for Flood Management in a Rural Development Block of Orissa, India

Use of Multi-Source Data Sets for Land Use/Land Cover Classification in a Hilly Terrain for
Landslide Study

Application of GIS and Remote Sensing for Disaster Prone Areas: A Case Study in Coastal Kerala

Accuracy Aspects in the use of GPS Technology for Geoinformation System

GIS-based slope stability evaluation of a landslide complex - case study from Paglajhora,
Darjeeling Himalaya, India

Village Information System (VIS): Development of Village Economy through Space Technology

Remote Sensing Based Hazard Assessment of Glacial Lakes - A Case Study from Kumaon
Himalaya, India

Disaster & Development

Journal of the National Institute of Disaster Management, New Delhi

Editorial Advisory Board

Lt. Gen. (Dr.) J.R. Bhardwaj

Former Member
National Disaster Management Authority
New Delhi

Prof. A.S. Arya

Professor Emeritus
Indian Institute of Technology, Roorkee

Prof. S.K. Dube

Former Director
Tata Institute of Social Sciences, Mumbai

Prof. Debarati Guha-Sapir

Director
Centre for Research on the Epidemiology
of Disasters, Université Catholique de Louvain,
Brussels, Belgium

Dr. P.S. Roy

Director
Indian Institute of Remote Sensing
Department of Space, GOI, Dehradun

Dr. R.K. Pachauri

Director General
The Energy and Resources Institute, New Delhi

Dr. T.S. Murty

Adjunct Professor
Department of Earth Sciences and Civil Engineering
University of Ottawa, Canada

Dr. R.K. Bhandari

Former Chairman
Centre for Disaster Management Vellore Institute
of Technology

Dr. K. Sekar

Professor
National Institute of Mental Health and Neuro
Sciences, Bangalore

Editor

P.G. Dhar Chakrabarti

Executive Director
National Institute of Disaster Management

Associate Editors

Santosh Kumar

santosh.nidm@nic.in

Chandan Ghosh

chandan.nidm@nic.in

Anil K. Gupta

anil.nidm@nic.in

Surya Prakash

surya.nidm@nic.in

K.J. Anandha Kumar

anadha.nidm@nic.in

Sreeja S. Nair

sreeja.nidm@nic.in



Mailing Address

Disaster & Development
National Institute of Disaster Management
Ministry of Home Affairs
Government of India
IIPA Campus, I.P. Estate, Mahatma Gandhi Marg, New Delhi - 110002
Phone: 91- 11 -23702445, Fax: 91- 11- 23702446

Disaster & Development

Journal of the National Institute of Disaster Management

Volume 4 • Number 2 • November 2010

©National Institute of Disaster Management (NIDM), New Delhi.

All rights reserved. No part of this publication may be reproduced or transmitted in any form or by any means, electronic or mechanical, including photocopying, recording or by any information storage and retrieval system without permission from National Institute of Disaster Management (NIDM), New Delhi.

ISSN: 0973-6700

Disaster & Development Journal is published two times a year and is distributed by
KW Publishers Pvt Ltd.
www.kwpublishers.com

Published in India by

Kalpana Shukla
KW Publishers Pvt Ltd
5A/4A, Ansari Road, Daryaganj, New Delhi 110002
email: knowledgeworld@vsnl.net / online.kw@gmail.com

Typeset by Black Innovation, New Delhi

Printed and Published by Mr. P.G. Dhar Chakrabarti on behalf of National Institute of Disaster Management (NIDM), New Delhi and Printed by Glorious Printers, A-13, Jhil Mil, Delhi 110 095 and Published at NIDM, IIPA Campus, I.P. Estate, Mahatma Gandhi Marg, New Delhi 110 002.
Editor: P.G. Dhar Chakrabarti

Contents

Volume 4 No.2 November 2010

Editorial Note	vii
1. Aster Stereo Images for Landslide Hazard Assessment in the Central Alborz Mountains, Iran <i>Seyed Ramzan Mousavi, Saeid Pirasteh, Shattri Bin Mansor, Ahamad Rodzi Mahmud, Ali Amani and Khalegh Arvin</i>	1
2. Vegetation & Agriculture Health Monitoring using Worldview-2 Satellite Image derived indices: An Approach for Drought Assessment in Jharkhand, India <i>Vivek Kumar Singh, Rajat Satpathy, Reshma Parveen and Sreeja S. Nair</i>	11
3. Geospatial Modelling for Flood Management in a Rural Development Block of Orissa, India <i>Ansuman Satapathy, Kiranmay Sarma, and Gopal Krishna Panda</i>	23
4. Use of Multi-Source Data Sets for Land Use/Land Cover Classification in a Hilly Terrain for Landslide Study <i>D. P. Kanungo and S. Sarkar</i>	35
5. Application of GIS and Remote Sensing for Disaster Prone Areas: A Case Study in Coastal Kerala <i>Manjush Koshy, Aneesh A and Jayalekshmi AB</i>	53
6. Accuracy Aspects in the use of GPS Technology for Geoinformation System <i>Dr. S. K. Katiyar</i>	65

Contents

7. GIS-based slope stability evaluation of a landslide complex - 77
case study from Paglajhora, Darjeeling Himalaya, India
Saibal Ghosh, Niroj K. Sarkar and Chinmoy Paul
8. VILLAGE INFORMATION SYSTEM(VIS) 91
Development of Village Economy through Space Technology
Kiran Jalem and Dr. A.K. Singh
9. Remote Sensing Based Hazard Assessment of Glacial Lakes - 113
A Case Study from Kumaon Himalaya, India
K. Babu Govindha Raj

Contributors

- **Seyed Ramzan Mousavi** Institute of Advanced Technology (ITMA), University Putra Malaysia (UPM) 43400 Serdang, Selangor, Malaysia E-mail: srmmousavi@gmail.com
- **Saeid Pirasteh** Institute of Advanced Technology (ITMA), University Putra Malaysia (UPM) 43400 Serdang, Selangor, Malaysia E-mail: srmmousavi@gmail.com
- **Shattri Bin Mansor** Department of Civil Engineering, University Putra Malaysia (UPM) 43400 Serdang, Selangor, Malaysia
- **Ahamad Rodzi Mahmud** Department of Civil Engineering, University Putra Malaysia (UPM) 43400 Serdang, Selangor, Malaysia
- **Ali Amani** Institute of Advanced Technology (ITMA), University Putra Malaysia (UPM) 43400 Serdang, Selangor, Malaysia E-mail: srmmousavi@gmail.com
- **Khalegh Arvin** Institute of Advanced Technology (ITMA), University Putra Malaysia (UPM) 43400 Serdang, Selangor, Malaysia E-mail: srmmousavi@gmail.com
- **Vivek Kumar Singh** Jharkhand Space Application Centre, Dept. of IT, Govt. of Jharkhand, Dhurwa-834004
- **Rajat Satpathy** Department of Remote Sensing, Vidyasagar University, Midnapur, West Bengal-721102
- **Reshma Parveen** Department of Remote Sensing, Vidyasagar University, Midnapur, West Bengal-721102
- **Sreeja S. Nair** National Institute of Disaster Management, New Delhi
- **Ansuman Satapathy** School of Environment Management, GGS Indraprastha University, New Delhi-110075
- **Kiranmay Sarma** School of Environment Management, GGS Indraprastha University, New Delhi-110075
- **Gopal Krishna Panda** Department of Geography, Utkal University, Bhubaneswar, Orissa
- **D. P. Kanungo** Geotechnical Engineering Division, CSIR-Central Building Research Institute, Roorkee 247 667, India
- **S. Sarkar** Geotechnical Engineering Division, CSIR-Central Building Research Institute, Roorkee 247 667, India
- **Manjush Koshy** Project Fellow*Geomatics Laboratory, Centre for Earth Science Studies, Akkulam, Thiruvananthapuram- 695031, Kerala

Contributors

- **Aneesh A** Project Fellow*Geomatics Laboratory, Centre for Earth Science Studies, Akkulam, Thiruvananthapuram- 695031, Kerala
- **Jayalekshmi AB** Project Fellow*Geomatics Laboratory, Centre for Earth Science Studies, Akkulam, Thiruvananthapuram- 695031, Kerala
- **Dr. S. K. Katiyar** Associate Professor, Civil Engineering Department, Maulana Azad National Institute of Technology, Bhopal (M.P.) - 462051 Email- skatiyar7@rediffmail.com
- **Saibal Ghosh** Corresponding author. mail_id: ghosh@itc.nl
- **Niroj K. Sarkar** Engineering Geology Division, Geological Survey of India, Kolkata, India, DK-6, Sector - II, Salt Lake, Kolkata - 700091
- **Chinmoy Paul** Engineering Geology Division, Geological Survey of India, Kolkata, India, DK-6, Sector - II, Salt Lake, Kolkata - 700091
- **Kiran Jalem** Asstt. Professor, Disaster Management Centre (DMC), Shri Krishna Institute of Public Administration (SKIPA), ATI Main Building, Meur's Road, Ranchi-834008.
- **Dr. A.K. Singh** Director General, Shri Krishna Institute of Public Administration (SKIPA), ATI Main Building, Meur's Road, Ranchi-834008
- **K. Babu Govindha Raj** RS & GIS APPLICATIONS AREA, National Remote Sensing Centre, Indian Space Research Organisation (ISRO), Balanagar, Hyderabad - 500 625. email: babugovindraaj@gmail.com

Editorial Note

Geoinformatics technology includes Geographic Information Systems (GIS), Remote Sensing (RS) and Global positioning systems (GPS provides applications ranging from collection, collation and interpretation of data, managing large amount of information in form of maps and tables, providing comparability and overlaying of various spatial information and combining various Geographical, socio-economic, environmental and administrative datasets.

Space technology i.e. Remote sensing and Global positioning systems has added advantage of comparing various geo-environmental and man-made features on various spatial and time-scales and when combined with GIS, it helps in understanding changing hazards scenario, vulnerability and is rapid assessment of disaster related damages and losses. The advanced high-resolution and multispectral sensors have provided immense scope to the scientists for mapping and analysis of earth surface features. Hyper-spectral analysis helps in near accurate identification of various objects. With the help of Geographic Information Systems (GIS) it is now possible to model, develop scenario related to floods, drought, earthquake, landslides, coastal hazards and industrial/chemical accidents, in an interactive manner that significantly helps in planning and implementation process. Modern Geoinformatics softwares and customized applications are user friendly and capable of addressing the needs of wide range of users not only limited to scientists or technocrats but equally to the administrators and field level managers.

The special issue on Geoinformation Systems include nine research papers from scientists, researchers and practitioners covering the applications Remote Sensing, GIS and GPS for management of wide range of disasters including flood, drought, landslides coastal hazards, glacial Lake Outburst Floods etc. I would like to express my sincere thanks to all the authors who have kindly contributed by providing papers to this journal. I would also like to express my sincere gratitude to the members of Advisory Council for their creative advice and guidance and I thank all the editorial board members for their cooperation and understanding in bringing out this special issue on Geoinformatics applications in Disaster Management. We would request all the readers to give your and suggestions and feedback to for the improvement in the next issues of the journal.

**Executive Director
NIDM**



Aster Stereo Images for Landslide Hazard Assessment in the Central Alborz Mountains, Iran

Seyed Ramzan Mousavi¹, Saeid Pirasteh¹, Shattri Bin Mansor¹,
Ahamad Rodzi Mahmud¹, Ali Amani¹ and Khalegh Arvin¹

Abstract

This research investigates and demonstrates the abilities of the ASTER stereo images using remote sensing techniques for detailed landslide hazard assessment in Central Alborz Mountains north of Iran. Since the most common methods of landslide hazard assessment using simple inventories and weighted overlays have been heavily depended on three-dimensional terrain visualization and analysis, stereo satellite images from the ASTER High Resolution sensor are used for this study. The Digital Elevation Models (DEMs) generated from ASTER stereo images appear to be much more accurate and sensitive to micro-scale terrain features than a DEM created from digital contour data with a 10 m contour interval. Stereo pair ASTER images permit interpretation of recent landslides as small as 10-15 m in width as well as relict landslides older than 30 years. A cost-benefit analysis comparing stereo air photo interpretation with stereo satellite image interpretation suggests that stereo satellite imagery is usually more cost-effective for detailed landslide hazard assessment over large mountain areas.

Keywords: Landslide hazard, Remote Sensing, ASTER Stereo Images, DEM, Central Alborz.

Introduction

ASTER as multispectral satellite remote sensors is providing high spectral and spatial resolutions for landslide hazard assessment. Nowadays, Methods for landslide hazard assessment need the collection of highly detailed information over large areas. The 14 bands of the ASTER data cover the visible and near infrared (VNIR; 3 bands with 15m

¹ Institute of Advanced Technology (ITMA), University Putra Malaysia (UPM) 43400 Serdang, Selangor, Malaysia E-mail: srmousavi@gmail.com

spatial resolution), shortwave infrared (SWIR; 6 bands with 30m spatial resolution), and thermal infrared (TIR; 5 bands with 90m spatial resolution) and allow for 364 Red-Green-Blue (RGB) color combinations. ASTER imagery is along-track stereo. So the two images that make up the stereo pair have been taken very closely together in time. Thus atmospheric, ground surface condition and illumination changes between the two images will be minimal. The downside of along-track stereo is that the stereo separation of the images may not be as optimal for DEM generation as across-track stereo can provide.

Soeters and Cornelis¹ illustrated four scales of slope instability assessment for landslide hazard: national, regional, medium and local. At the local level, only a few tens of square kilometers can be studied, and areas as small as 10 ha or less should be clearly defined. The most useful direct indicators of landslide susceptibility are considered to be evidence of past landslides as well as tension cracks and other detectable earth movement. Therefore, the simplest type of landslide hazard assessment includes an inventory of previous landslides and signs of mass movement, based on the premise that an area with past landslides is landslide prone and has a high probability of new landslides.² McCalpin³ showed that for planning purposes, any landslides with historic movement during the last 100 years have been considered active. Except in arid zones or under thick forest,⁴ recent landslides can be readily identified on air photos due to high contrast with the darker vegetated background, although, they become increasingly indistinct with time.⁵ The integration of observations, field measurements and stereo air photo interpretation can satisfy the demands for landslide studies. For example, approximately 230 photo prints at a scale of about 1: 8,000 are required for a complete stereo cover of an area of 80 km². Moreover, such a detailed air photo cover is expensive, and manual methods of stereo air photo interpretation are time-consuming, especially if the results of the interpretation are to be input to a GIS database for weighted overlay analyses. In such a case, a DEM is also required for Ortho-rectification and the production of a slope map. Moreover, generation an accurate DEM is available, Ortho-rectification of a stereo pair air photo may take more than 6 hours of professional work. Although some researcher such as Mantovani et al.⁶ implied that satellite images are unsuitable for landslide studies, But Nichol and Wong presented that most of landslides in forested areas could be detected by automated change detection using SPOT multispectral satellite images with a 20 m spatial resolution. The "identification" and "interpretation" of the features as landslides would require higher deductive processes based on stereo viewing of the topographic position and slope morphology.^{8 9 10}

The stereo capability of air photos that aids interpretation of slope morphology, as well as their higher resolution has mitigated against the use of satellite images.

However, the improved spatial resolution and stereo capability of recent satellite sensors such as Terra ASTER, IRS P5, SPOT-5 HRG, and IKONOS may give topographic details comparable to air photos in both 2D and 3D, with the advantage of a single mapping base covering large areas. To enable precise interpretation and visualization of slope morphology, 3D viewing is available using one of several techniques such as (i) direct stereo viewing of the image on a stereo-plotter, (ii) anaglyph construction, and (iii) draping the image over the DEM created from the same stereo satellite images. Measurement of elevations can be done either from the generated DEMs, or if ERDAS Imagine and PCI Geomatica software are available, directly from the digital anaglyph. Manual technique is considered to be more accurate than automatically processed DEMs. However, if the DEM is accurate and detailed enough to show minor changes in terrain height, the traces of small landslides are able to be detected.

This study describes an approach using high resolution stereo satellite images for assessment of landslide hazard. This paper emphasizes on detecting of meter scale micro-relief features and differences in surface texture indicative of micro-scale surface. This paper also tries to evaluate the costs and benefits of applying techniques for detailed landslide surveys over larger areas.

Study area

The study area is situated in Haraz Highway, Central Alborz, and Northern Iran that covers a 60 km² mountain area (Fig. 1). This area has high potential seism-tectonic activity. Rangelands and rocky outcrops cover most valleys in the study area. The area is underlain by Jurassic sedimentary rocks and Quaternary volcanic tuff and lava.

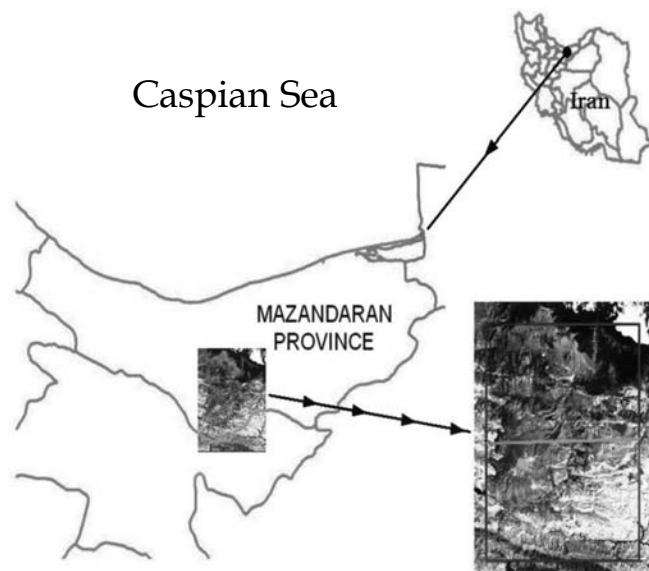


Fig. 1: Location of study area in Central Alborz, Northern Iran.

Materials and Methodology

Stereo ASTER L1A and L1B images acquired in August 2006 and have been used in this research. The DEM was generated at 15 meters resolution with the highest possible level of detail, and the holes are filled by automated interpolation.

24 well-distributed ground control points (GCPs) and 32 checkpoints were digitized from recent 1:10000 digital topography maps produced by the Iranian Survey Organization. The points correspond to clearly identifiable intersections and landmarks between roads or footpaths. The elevations of these points have been taken from a DEM with a grid resolution of 5 meters, produced from recent digital topographic maps (Iranian Survey Organization) with a contour interval of 5 meters.

Automatic image matching was conducted to define points in the overlap area between the two stereo images. Although the matching process has produced a number of tie points, small areas with highly variable terrain elevations could not be matched. Therefore, 32 additional points are manually digitized in these areas and are used for interpolation to produce a 5 meters DEM for the overlap area. The quality of the generated DEM (Fig2) was then assessed by comparing the elevations of 32 well-distributed checkpoints with those on a 5 meters DEM generated photographically from false colour dispositive air photos with a very high (2 meters) resolution. The accuracy of this DEM is assessed by comparing the elevations of 14 locations along a longitudinal section of a landslide trail and four points along a section across the landslide crown (Fig. 3) with (i) the existing DEM from 2 m contour maps, (ii) measurements on the anaglyph generated from ASTER stereo images, and (iii) measurements on an anaglyph generated from the 2 m resolution air photos. The Landslide database of the Geotechnical Engineering Office of the Iran, Mazandaran Province Watershed Management Department and Natural Resources Research Center, Iran, which includes records of all landslides since 1972, has been also used as a reference for the proportion of landslides, which could be identified using either stereoscopic air photos or ASTER images with both planimetric and stereoscopic viewing.

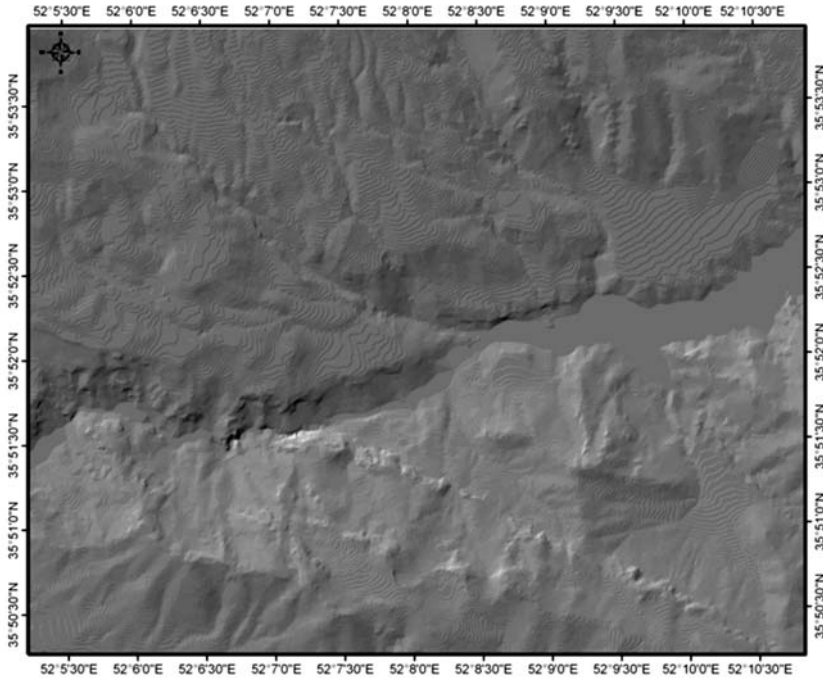


Fig. 2: Showing shaded relief models of DEMs generated from ASTER stereo images over study area (40 km²) with cell size of 5 m.

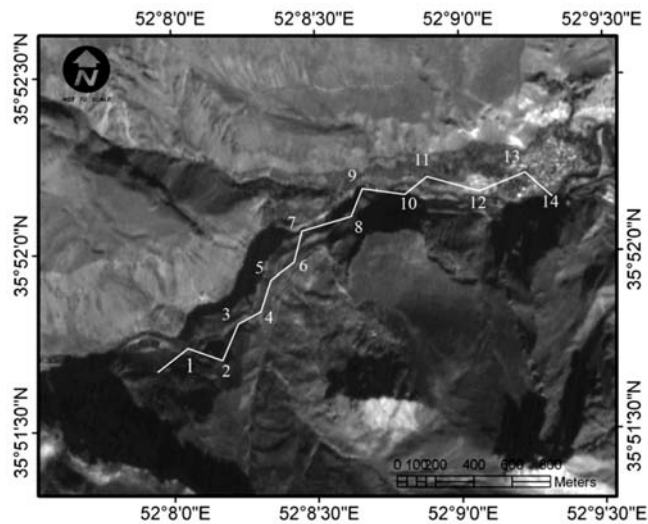


Fig. 3: Showing position of 14 traverse points and cross section on ASTER image.

Results and Discussion

The results of the orientation process gave total RMS errors at the checkpoints of 5, 8 and 15 m and maximum residual errors of 6, 9 and 18 m in X, Y and Z directions, respectively. This was achieved by using only four appropriate GCPs and there has been almost no improvement in the accuracy by adding more GCPs. Assessment of the ASTER 15 meters DEM at 32 checkpoints using the DEM from the air photos as reference shows that most of the points have height errors between 2.50 and 3.5 meters, but a few steeply sloping areas have larger errors up to 7.0 meters. The total RMS error and the linear error with a 79% level of confidence of the 15 meters DEM were 20 and 25 meters, respectively.

The mean height difference between the measurement on the ASTER anaglyph and that on the air-photo anaglyph was ca. 5.0 meters along the longitudinal section (Fig 4). The contour-based DEM suggests a 15 meters deep, V-shaped topography along the cross section, whereas the measurements from the ASTER anaglyph indicate a 15 m deep U-shaped topography (Fig 4). The difference would be crucial for volumetric studies, since the ASTER stereo suggests a much greater volume of material removed from the landslide crown. Thus, for detailed morphometric analyses, ASTER stereo images seem to be more useful than existing DEMs and give similar accuracy to the stereo air photos.

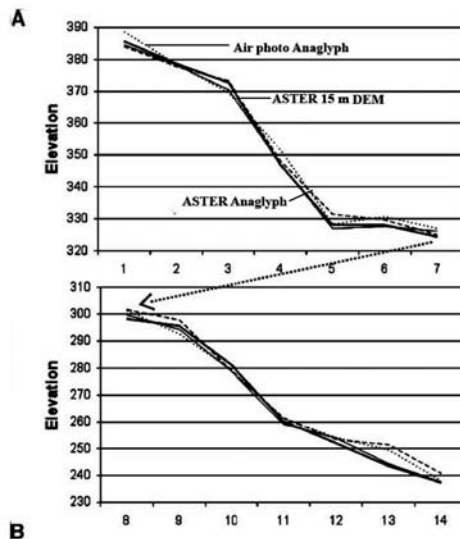


Fig. 4: Comparison of elevations (meter) obtained at stations along and across landslide trail among ASTER anaglyph, ASTER 15 meters DEM, existing DEM from 2 meters contour maps, and anaglyph from high-resolution air photos. (See Fig. 3 for their locations).

ASTER stereo images can be visualized using three different approaches: a. creating anaglyphs (Fig. 5), b. draping the ASTER ortho-images over the generated DEM (Fig. 6) and c. creating stereograms (Fig. 7). The main aim of the 3D visualization is to contribute additional contextual, locational and morphological information to planimetric image interpretation.

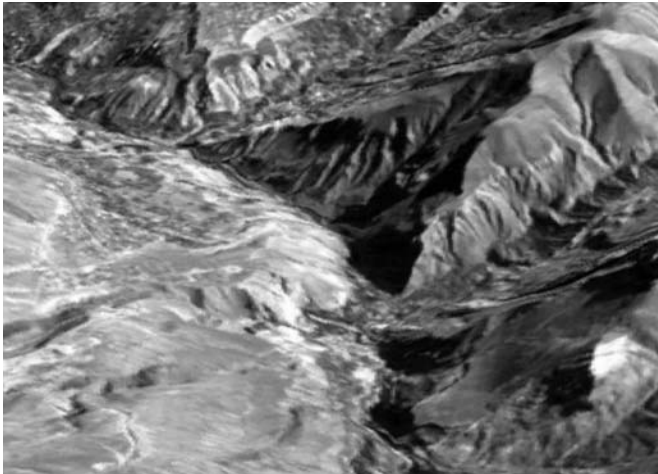


Fig. 5: Anaglyph produced from ASTER stereo imagery (See Fig6, Landslide Lake on two days after occurrence in 2001).

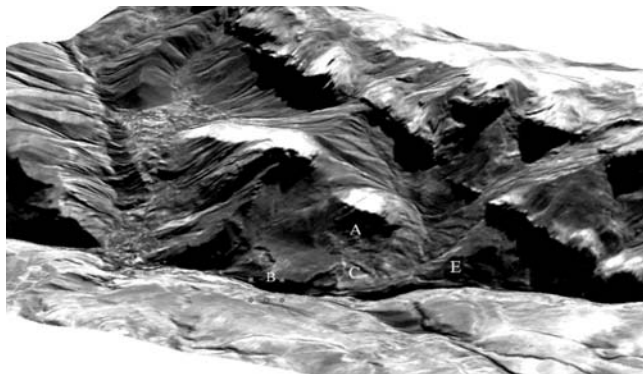


Fig. 6: Ortho-image draped over ASTER derived DEM showing detailed terrain information. Landslide trail in image centre is ca. 7 m wide, and footpath crossing from left to right is 1-2 meters wide. Landslides older than 50 years can be detected; inverted Vshaped scarp (A) and inverted spoon-shaped concavities (B, C, D and E).

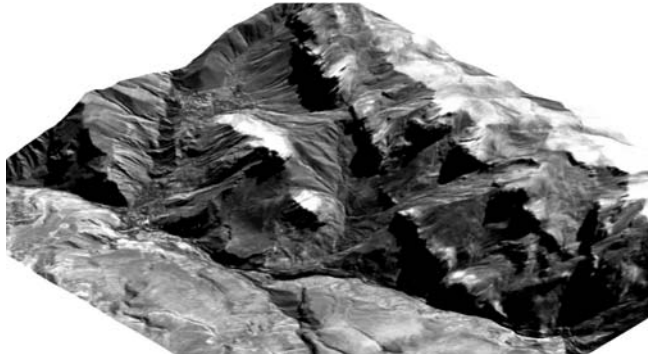


Fig. 7: Stereogram from ASTER stereo imagery, for 3D viewing using stereoscope.



Fig. 8: Showing Landslide in Ask, Haraz high way, Central Alborz two days after occurrence in 2001).

The database shows that 23 landslides occurred in the area covered by the 15 meters DEM, between 1972 and the image date (August 2006). Only the large and recent landslides (about 35%) can be identified on the ASTER image. However, with the direct 3D viewing of the ASTER images on the stereo plotter, the colour, shape, topographic position, and vegetative details are visible, permitting an experienced interpreter to identify approximately 50% of the landslides. Additionally, some old landslides which occurred before 1972 could be identified. These include a landslide at A on Fig. 6 and 8, in the form of a marked inverted V-shaped scarp, and smaller spoon-shaped concavities elongated downslope at B, C, D and E (Fig.8).

All the landslides less than eight years old including those with a small width of 20-30 meters are identified. Sub-meter features such as tension cracks are not visible. Although, the air photos potentially have a very high spatial resolution of 63 line pairs per mm, or 8 cm on the ground, they didn't lead to a significantly improved result. In addition, their interpretation is often tedious due to the restricted field of view under the binoculars and the fixed viewing base of standard mirror stereoscopes. On the other hand, ASTER stereo images are easier to manipulate since they can be viewed at various scales and fields of view. Anaglyphs are also available for detailed 3D viewing of small areas such as scarps, rocky outcrops and tension cracks. Furthermore, the 4-band, 11-bit data format of ASTER gives better image quality to air photos. The watershed and Natural Resources Center, Iran, database records only the length and position of landslides, not the width and volume. However, the volume of material removed are calculated automatically using digital cross sections from the ASTER DEM (Fig. 4) and can be used to estimate sedimentation rates and water quality in the lower catchments.

Conclusion

This study has shown that ASTER stereo images are satisfactory to study the requirements of landslide hazard and its assessment at local and medium scales where the scale of observations is between 10 and 100 meters. It can be used also for detecting micro-scale features that have dimensions of 10 to 20 meters. The ASTER images viewed in 3D were adequate for identifying all recent landslides as well as some very old landslides in the study area, based on slope morphology and re-growing vegetation. The level of 3D spatial detail achieved is deemed to be similar to that of 1: 10,000 scale air photos, but ASTER images surpass air photos in terms of spectral quality, ease of manipulation, a single image base for generation of a DEM, and cost. The DEM created from ASTER appears to be highly accurate, surpassing even that created from digital contour data with an interval of 15 meters. Since ASTER, IRS AND SPOT satellites can be programmed to image any area, and the repeat cycle of both is within three days (off-nadir mode), stereo satellite images now provide a viable alternative to air photos for creating detailed landslide inventories at a range of scales. Terms of structural integrity these are issues concerning fatigue design approaches i.e. infinite life, safe life, fail safe and damage tolerant design, which need to be resolved quickly. In countries such as Iran, air photos are routinely taken by the government and distributed free of charge to various institutes. It is easy to understand why air photos remain the preferred medium for creating landslide inventories. However, in areas where the availability of such data is low, or when the objective of the project is to integrate a landslide inventory with other

digital data for regional landslide hazard assessment, the use of satellite images is a viable option. If air photos have already been taken and are available, the overall cost of the air-photo-based approach is similar to that of the ASTER-based approach. If flying costs to take new air photos are added, the cost of the air-photo-based approach becomes 46% higher or 41% higher if tasking of IKONOS is required. A comparison of all image types for the total job cost indicates that the use of Terra ASTER stereo images is incomparably cheap.

Acknowledgements

The authors wish to thank Department of Geographic Organization, Iran for providing the Satellite data, Aerial photography and Topographic maps in this research.

References

1. A. Soeters, and J.W. Cornelis, Slope instability recognition, analysis and zonation. In: Schuster, R.L., Turner, A.K. (Eds.), Landslides Investigation and Mitigation. Transportation Research Board, Special Report 247. National Academy Press, Washington DC, 1996. p. 129-177.
2. T. Odajima, and S. Tsuchida, Y. Yamaguchi, T. Kamai, and Y.O.P. Siagian, GIS and remote sensing based analysis of landslide hazards in Cianjur, West Java, Indonesia. Proceedings of International Symposium on Application of Remote Sensing and Geographic Information System to Disaster Reduction, 1998. p. 185-190.
3. J. McCalpin, Preliminary age classification of landslides for inventory mapping: 21st Annual Symposium on Engineering Geology and Soils Engineering. Proceedings, University of Idaho, Moscow, Idaho, USA, 1974. p. 99-111.
4. F. Brardinoni, O. Slaymaker, and M.A. Hassan, Landslide inventory in rugged forested watershed: a comparison between air photo and field survey data. *Geomorphology*, 2003. 54: p. 179-196.
5. B.D. Malamud, D.L. Turcotte, F. Guzzetti, and P. Reichenback, Landslide inventories and their statistical properties. *Earth Surface Processes and Landforms*, 2004. 29: p. 687-711.
6. F. Mantovani, R. Soeters, and C.J. Van Westen, Remote sensing techniques for landslide studies and hazard zonation in Europe. *Geomorphology*, 1996. 15: p. 213-225.
7. J.E. Nichol, and M.S. Wong, Satellite remote sensing for detailed landslide inventories using change detection and image fusion. *International Journal of Remote Sensing*, 2005. 26: p. 1913-1926.
8. D. Brunsten, J.C. Doornkamp, P.G. Fookes, D.K.C. Jones, and J.M.H. Kelly, Large scale geomorphological mapping and highway engineering design. *Quarterly Journal of Engineering Geology*, 1975. 8: p. 227-253.
9. Mousavi S. R., Pirasteh S., Shattari, M. and Amani A., 2009, Landslides and Active Faults Using Remote Sensing and GIS Techniques in Central Alborz Mountains, Iran, *International Disaster Advances Journal*, Vol.2, No.3, page.24-29

Vegetation & Agriculture Health Monitoring using Worldview-2 Satellite Image derived indices: An Approach for Drought Assessment in Jharkhand, India

Vivek Kumar Singh¹, Rajat Satpathy²,
Reshma Parveen¹ and Sreeja S. Nair³

Abstract

Drought is a recurrent phenomenon in Jharkhand. It affects the livelihoods of the majority of its people, particularly tribals and dalits living in rural areas. Twelve of the 24 districts of the state, covering 43% of the total land area, are covered under the Drought Prone Areas Programme (DPAP). Hunger and starvation deaths are reported almost every year. Because of the pervasive and varying degree of drought effects, it is important to develop methods for drought assessment. Vegetation chlorophyll content and moisture status is one of the key parameters in drought monitoring, agricultural modelling and forest health mapping. In the present study three new indices was developed to predict the drought. All the indices are evaluated in the GIS environment using weighted overlay technique to produce the final result. The final result is validated by correlating the monthly rainfall data and irrigation condition of the study area. The satellite data used for this study is 8 band Worldview-2 was provided by Digital Globe.

Introduction

Periods of persistent abnormally dry weather known as droughts, can produce a serious agricultural, ecological and hydrological imbalance. Drought harshness depends upon the degree of moisture deficiency, duration and the size of the affected area [Wilhite, D. A., and M. H. Glantz, 1985]. Remote sensing is now widely used to monitor and predict vegetation characteristics for sustainable development. Imaging spectrometry has great potential for monitoring vegetation type and biophysical characteristics [Goetz, A.F.H.,

1. Jharkhand Space Application Centre, Dept. of IT, Govt. of Jharkhand, Dhurwa-834004
2. Department of Remote Sensing, Vidyasagar University, Midnapur, West Bengal-721102
3. National Institute of Disaster Management, New Delhi

1995]. Vegetation reflectance spectra are often quite informative, containing information on the vegetation chlorophyll absorption bands in the visible region, the sustained high reflectance in the near infrared band, and the effects of plant water absorption in the middle infrared region.

Leaf chlorophyll and moisture content is one of the key parameters in forest health mapping, agricultural modelling and drought monitoring. The incident energy is absorbed in the Blue (0.4-0.5 μ m) and Red (0.6-0.7 μ m) region due to the absorption band of chlorophyll whereas the Near-Infrared region (0.7-1.3 μ m) shows a peak reflectance characteristics due to the spongy mesophyll layer. Using that absorption and reflection characteristics of vegetation many researcher has define many vegetation indices for monitoring vegetation parameters.

The researcher used classical indices method to measure the chlorophyll content and moisture status within the leaves. Now, the availability of 8 spectral bands of the Worldview-2 will create an opportunity to analyze and modify the indices previously used. The three new bands namely Yellow, Red-Edge and NIR-2 will be used for this study to analyze the vegetation characteristics. The yellow band is very much useful for detecting the yellowness of the plant leaves. The red-edge band has a strong reflectance of vegetations. It is used for measuring the red edge stress over vegetations and agriculture. The NIR-2 band is less affected by atmospheric influences and within the spectral range (0.86-1.047 μ m) water absorption portion (0.97 μ m) is found. So, this band is useful for vegetation water content estimation.

Study Area:

The present study area is a part of Hazaribag and Chatra district, Jharkhand (figure-1). Geographically the area is located in the north east part of the Chotanagpur Plateau. The area drained by Barka River and its tributaries. Maximum height of the area is 850 meter. The maximum temperature in summer rises to above 40 $^{\circ}$ c and the minimum in winter falls to 08 - 10 $^{\circ}$ c. The average annual rainfall is about 800 mm. The latitudinal and longitudinal extent of the study area is as follows - Latitudinal extent - 23 $^{\circ}$ 55' N - 24 $^{\circ}$ N and Longitudinal extent - 85 $^{\circ}$ E - 85 $^{\circ}$ 06'25"E.

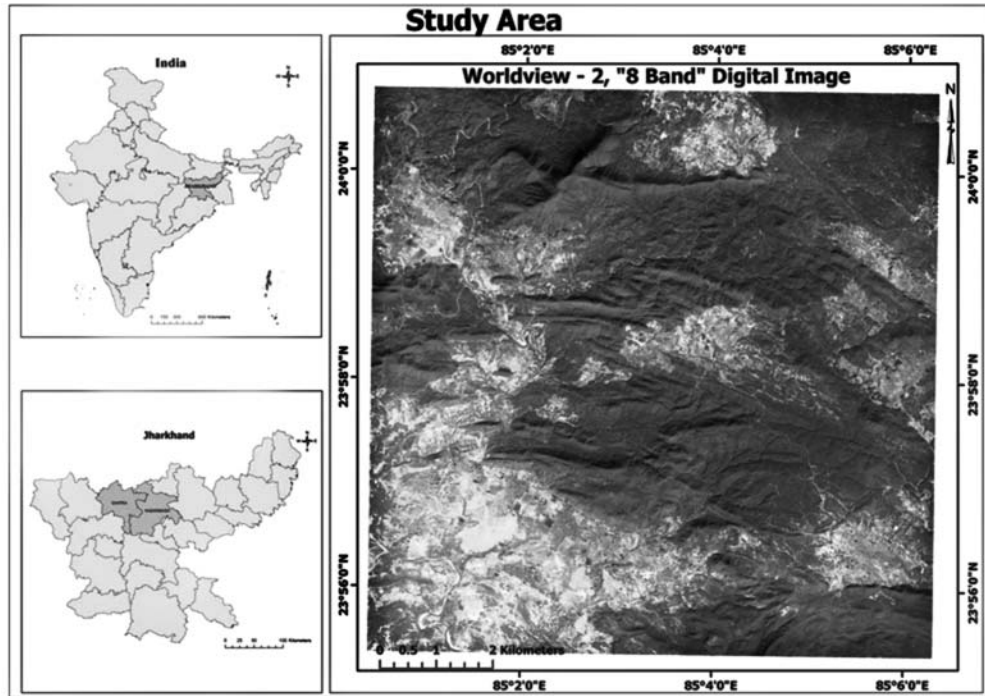


Fig 1. Location of the study area.

Data used and Methodology

Worldview-2, 8 band raw digital imagery provided by Digital Globe is used for this study. Apart from the satellite data Rainfall data and Jharkhand Agriculture Information System published report is used for this study. The flow chart shown in figure 2 illustrates the procedures followed in this study to monitor the drought condition of the area. The specification [Worldview white paper, 2010] of worldview-2 datasets is illustrated in table-1.

Table 1. Showing the specification of Worldview - 2 datasets.

Name of Bands	Spectral Bandwidths (nm)	Center Wavelength (nm)	Other Specification
Coastal Blue	400 - 450	427	Launch Date: October 8, 2009. Spatial Resolution: PAN - 0.46 Mts. MUL - 1.84 Mts. Quantization Level: 11 Bits. Swath Width: 16.4 Km. Revisit: 1.1 Days. New Bands: Coastal, Yellow, Red Edge and NIR - 2.
Blue	450 - 510	478	
Green	510 - 580	546	
Yellow	585 - 625	608	
Red	630 - 690	659	
Red Edge	705 - 745	724	
NIR-1	770 - 895	831	
NIR-2	860 - 1040	908	

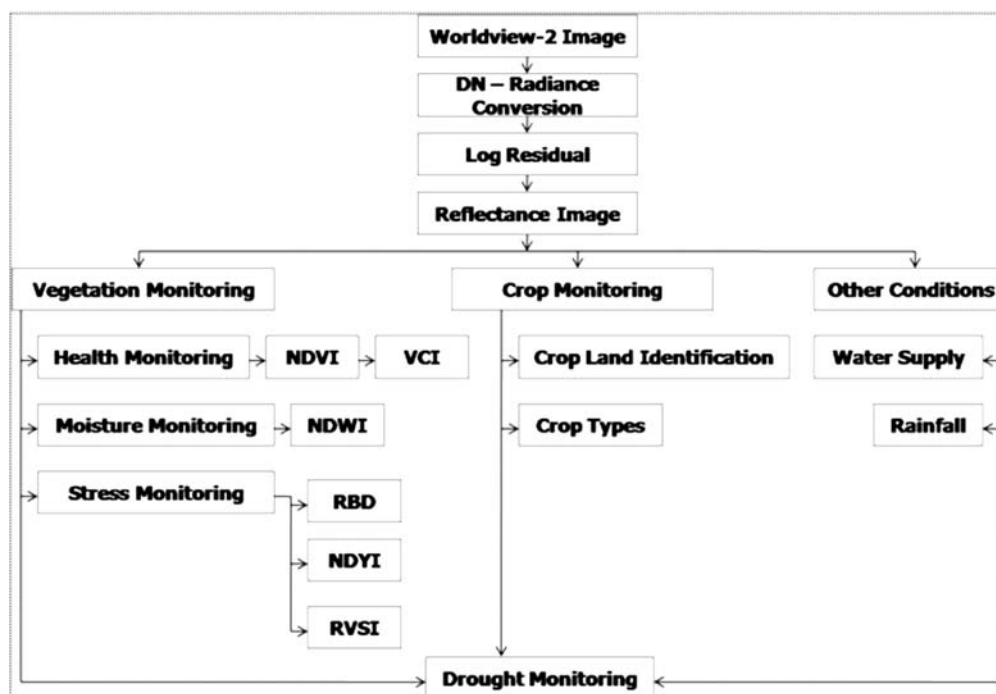


Fig 2. Processing flow of overall methodology

Pre-Processing

The DN values of Worldview-2 digital image is converted to the radiance values using ENVI based Worldview radiance conversion algorithm. The absolute calibration factor values (within the .imd file) are used to calculate the radiance image. The surface reflectance is calculated using ENVI based Log Residual method. The Log Residuals calibration tool is designed to remove solar irradiance, atmospheric transmittance, instrument gain, topographic effects, and albedo effects from radiance data [Envi User Guide, 2008]. This transform creates a pseudo reflectance image that is useful for analyzing vegetation related absorption features.

The logarithmic residuals of a dataset are defined as the input spectrum divided by the spectral geometric mean, then divided by the spatial geometric mean. The geometric mean is used because the transmittance and other effects are considered multiplicative; it is calculated using logarithms of the data values. The spectral mean is the mean of all bands for each pixel and removes topographic effects. The spatial mean is the mean of all pixels for each band and accounts for the solar irradiance, atmospheric transmittance, and instrument gain.

Health Monitoring

Normalised Difference Vegetation Index:

The most common vegetation index in use today is the Normalized Difference Vegetation Index, or NDVI [Rouse, 1972]. It is defined as:

$$NDVI = \frac{NIR_{\rho} - R_{\rho}}{NIR_{\rho} + R_{\rho}}$$

Where, NIR_{ρ} stands for the reflectance in the near-infrared band and R_{ρ} stands for the reflectance in the red band. This index is based on healthy vegetation having a high reflectance in the infrared band and a low reflectance in the red band, while stressed vegetation will have a lower IR reflectance and progressively higher red band reflectance. The NDVI values (figure-3, A&B) range from -1 to 1, with values below 0 indicating poor vegetation conditions or non-vegetation targets such as soil. Higher the NIR reflectance indicates the better forest/crop growth and lower the red reflectance indicates higher the biomass of the forest/crop. The index is sensitive to the presence of green vegetation [Sellers, 1987] and permits the prediction of agricultural crops (Tucker and Sellers, 1986). It has also been used to predict monthly evaporation [Szilagyi, *et al*, 1998] and used as the basis for drought detection using remote sensing [Wan *et al*, 2004].

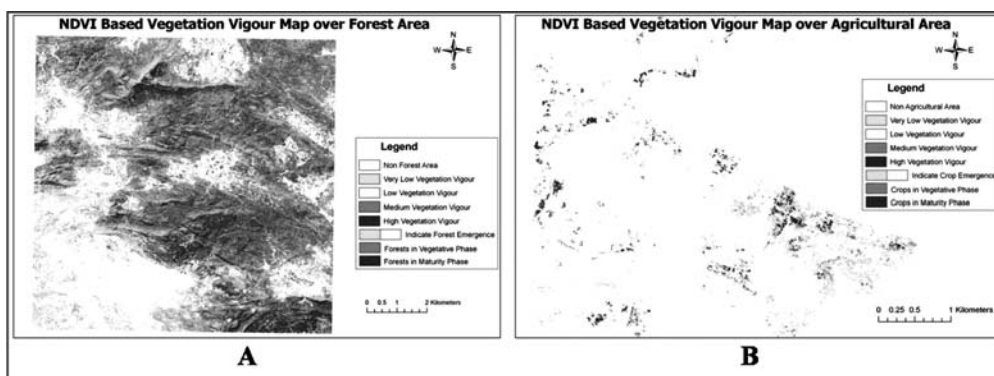


Fig 3. A- Showing the forest health of the study area and B- Showing the agriculture health of the study area.

Vegetation Condition Index:

Kogan [1997] developed the Vegetation Condition Index (VCI) which is defined in terms of NDVI. This index compares the vegetation of a region to the maximum values thus:

$$VCI = \frac{NDVI - NDVI_{min}}{NDVI_{max} - NDVI_{min}} * 100$$

Where, $NDVI_{max}$ and $NDVI_{min}$ the maximum and minimum NDVI measured in the study area respectively.

Moisture Monitoring:

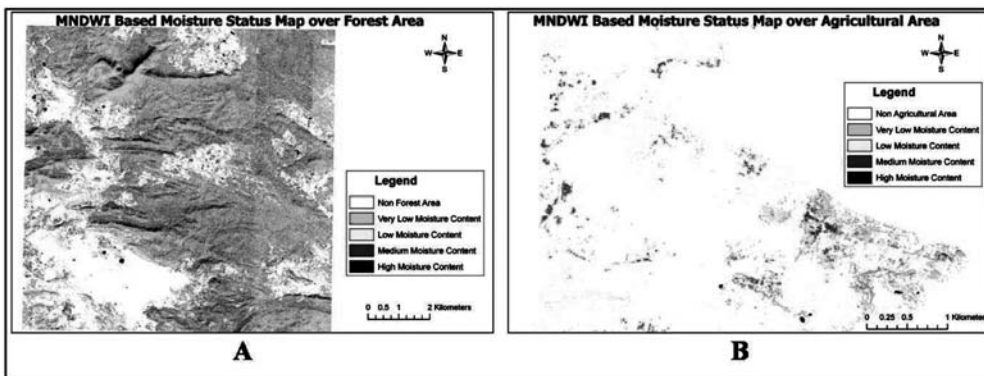
NDWI:

When radiation corresponding to the wavelengths of the water absorption bands is incident upon green vegetation, the reflectance is reduced to a varying extent, depending on the tissue water content [Thomas *et al.* 1971; Tucker 1980]. Therefore, the measurement of radiation reflected by leaves and canopies provides a basis for estimating leaf and canopy water contents. The Normalized Difference Water Index (NDWI) was proposed by Gao [1996] for remote sensing of vegetation liquid water from space. It uses two infra-red channels, one at 0.86 μm and the other at 1.24 μm . The index is defined as:

$$NDWI = \frac{\rho(0.86 \mu m) - \rho(1.24 \mu m)}{\rho(0.86 \mu m) + \rho(1.24 \mu m)}$$

Where, $\rho(0.86 \mu m)$ and $\rho(1.24 \mu m)$ is the reflectance at the given wavelength. These wavelengths were chosen because of their reflectance properties when considering absorption by water. . The one fundamental vibrational water absorption band ($0.97\mu m$) [Gates *et al.* 1965] was exist within the NIR-2 band of the Worldview-2. So, there is a possibility to measure the water content within the plant leaves using NIR-1 and NIR-2 band. The modified normalised difference water index (MNDWI) is developed in this study to measure the moisture status within the plant leaf (figure 4, A&B).

$$MNDWI = \frac{\rho_{NIR1} - \rho_{NIR2}}{\rho_{NIR1} + \rho_{NIR2}}$$



Where, ρ_{NIR1} and ρ_{NIR2} are the relectance of Worldview-2 NIR band 1 and 2 respectively.

Stress Monitoring:

Normalized Difference Yellowness Index (NDYI):

The Normalized Difference Yellowness Index (figure-5, C&D) is generated in this study for measuring the yellowness of the plant leaves. When the chlorophyll content within the plant leaves are decreased, the yellowness of the leaves are become increased. So, this index also measures the vegetation health. This index is defined as:

$$NDYI = \frac{Yellow_{\rho} - Red_{\rho}}{Yellow_{\rho} + Red_{\rho}}$$

Where, $Yellow_{\rho}$ and Red_{ρ} are the surface reflectance of yellow and red band of worldview -2 respectively.

Relative-absorption Band Depth (RBD)

This concept is used in Remote Sensing to map the mineral assemblages on the basis of their unique absorption and reflectance characteristics. It is seen that in the yellow and red-edge band of Worldview-2 having reflectance and absorption characteristics respectively. So, using this absorption and reflectance pattern of vegetation and crop spectra an attempt is made to map the yellowness stress of vegetations in the study area.

$$RBD = \frac{\rho_{Yellow} + \rho_{Red\ Edge}}{\rho_{Red}}$$

Where, ρ_{Yellow} , $\rho_{Red\ Edge}$ and ρ_{Red} are the reflectance of the yellow, red-edge and red band respectively.

Red Edge Vegetation Stress Detection:

The red-edge, centered at the largest change in reflectance per wavelength change, is located between the widely used red band and NIR band and may hold valuable information that may benefit aspects of vegetation stress study. The RVSI was developed to identify inter- and intra-community vegetation stress trends based on spectral changes in upper red-edge geometry [Merton and Huntington, 2002]. It is defined by them using AVIRIS data as-

$$RVSI = \left(\frac{\rho_{714} + \rho_{752}}{2} \right) - \rho_{733}$$

But that ratio is not applicable here. So, we developed a modified Red-Edge Vegetation Stress Index (MRVSI) index based on the worldview-2 data.

$$MRVSI = \left(\frac{\rho_{Red-Edge} + \rho_{NIR}}{2} \right) - \rho_{Red}$$

Where, ρ_{Red} , ρ_{NIR} and $\rho_{Red\ Edge}$ are the surface reflectance of the Red, NIR and Red-Edge band respectively. This ratio is better able to discriminate between healthy trees, and those impacted by disease (figure-5, A&B). In simple terms, reflectance spectra with upper red-edge convexity calculate negative RVSI values indicating low vegetation stress, whereas upper red-edge spectra with near-linear or concave curves indicate an “apparent stress” response.

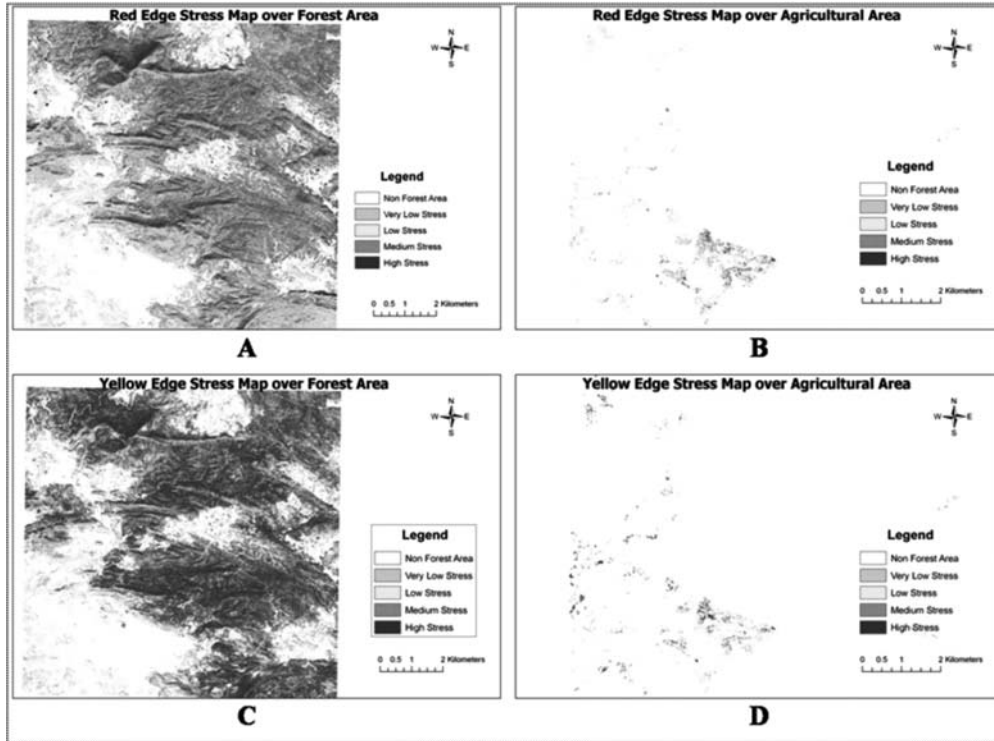


Fig 5. A & B - Red-Edge Vegetation and Crop stress and C & D - Yellow-Edge vegetation and crop stress.

Result and Discussion:

The land use & land cover classification using spectral angle mapper technique shows that the study area covered 7107.03 hectare forest land and 127.85 hectare agricultural land. The three methods Vegetation and Crop health, moisture status and stress analysis shows that the study area is under stress.

Table 2. Showing the statistics of different indices.

Methods	Over Forest		Over Crop	
	Max	Min	Max	Min
NDVI	0.47	-0.39	0.63	-0.24
MNDWI	0.19	-0.47	0.26	-0.32
NDYI	0.47	0.005	0.31	0.17
MRVSI	0.82	-0.16	0.69	-0.23

The comparative NDVI values (table-2) indicate that the crops having much vegetation vigour than the forest areas. MNDWI values shows that the water contents are less within the leaves than the crops. The NDYI and MRSVI value shows that forests are under stress. The crop areas are healthier due to the Barka river. Irrigation facilities are provided by the government in the crop lands. According to Jharkhand Agriculture Information System published report the major crop types in this area is Paddy and Maize, which require less water for growing.

As per Indian Metrological Department (IMD) in 2009 monsoon season the study area received significantly less rainfall than normal (figure-6). According to IMD advice to farmers Arhar, Moong, Paddy, Maize etc are best suitable for farming in December, 2009.

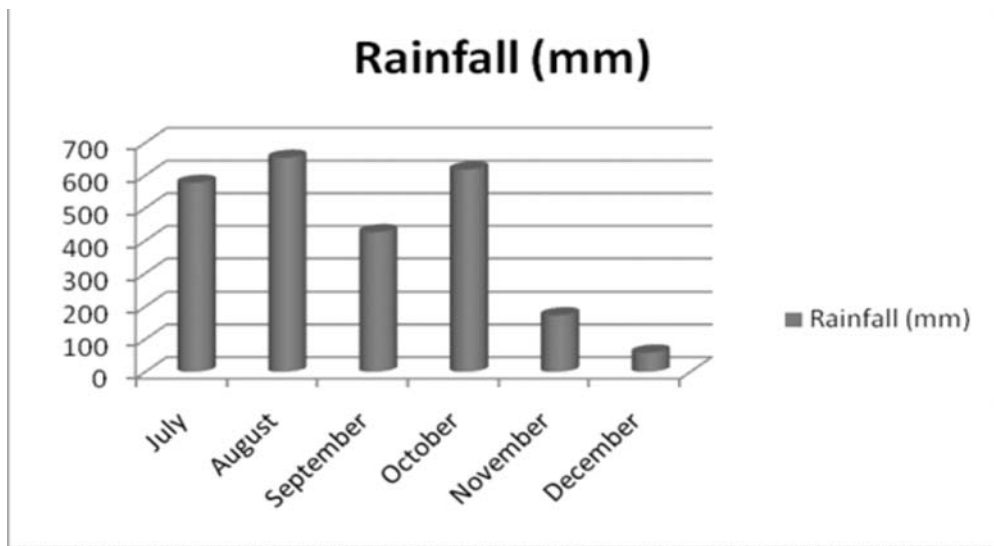


Fig 6. Showing the month wise rainfall distribution over the study area.

So, by analyzing the measured vegetation indices in correlation with other conditions such as irrigation facilities, rainfall amount, it is clear that the area under unhealthy plants and crops, low water content within the plant leaves. The leaves are yellow due to low chlorophyll content.

All the raster indices maps are imported to the GIS environment and a weighted overly method is applied to generate the drought prone map (figure-7). The weight (table-3) of each class is assigned on the basis of their influence for producing drought.

Table 3: Showing the weightage values assigned for overlay analysis

Methods Used	Weightage
NDVI	17
VCI	15
MNDWI	25
MRVSI	16
NDYI	13
RBD	14

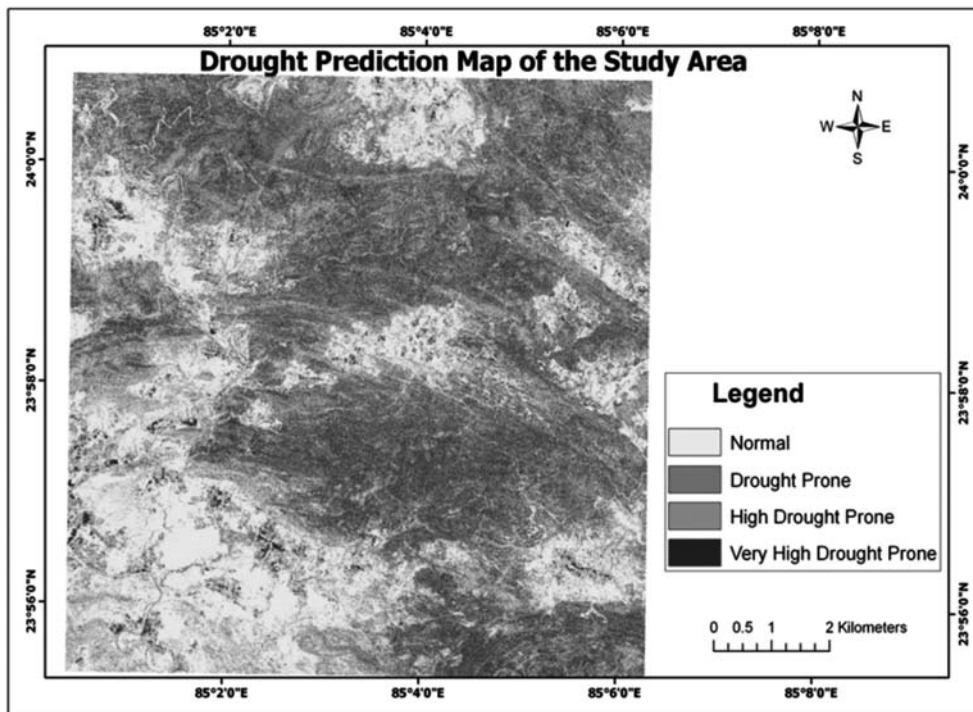


Fig 7. Showing the drought prediction maps of the study area.

Conclusion:

Meanwhile the area suffer drought year after year. So, for identifying the situation of drought, this study was carried out. It is concluded that NDVI, MNDWI, MRVSI, NDYI and RBD are good proxy indicators of drought. The red-edge stress detection is very

good for measuring the forest and crop health whether these are affected by disease or not. The yellow band is very much useful measuring the yellowness of the leaves. The Worldview-2, 8 band data analysis has revealed some new findings on the prediction of droughts using Remote Sensing.

For better studying the drought time series data is needed from the growing season to the maturity season. Three new indices are generated for this study and a future research is needed.

Acknowledgments:

Authors are thankful to Digital Globe for providing the imagery and giving the opportunity for participation in 8 band challenge. First author is thankful to Director, Jharkhand Space Application Center, Department of Information Technology, and Government of Jharkhand for their support and guidance.

References:

1. Gates, D. M., Keegan, H. J., Schleter, J. C., and Weidner, V. P. (1965). Spectral properties of plants. *Applied Optics* 4, 11.20.
2. Goetz, A.E.H., (1995), "Imaging spectrometry for Remote sensing vision to reality in 15 years", SPIE International Society for Optical Engineers, 2480:12 pp.
3. Gao, B.-C. (1996). NDWI.a normalised difference water index for remote sensing of vegetation liquid water from space. *Remote Sensing of Environment* 58, 257.266.
4. ITT Visual Information Solutions (2008), ENVI user's guide, version 4.5, 2008.
5. Kogan, F. (1997). "Global Drought Watch from Space." *Bulletin of the American Meteorological Society* 78(4): 621-635.
6. Merton, R., Huntington, J. (2002). Early Simulation Results Of the ARIES-1 Satellite Sensor for Multi-Temporal Vegetation Research derived from AVIRIS, CSIRO Exploration and Minig, and ARIES Consortium: 10 pp.
7. Rouse, J. W., Haas, R.H., Deering, D.W., Schell, J.A., Harlan, J.C. (1972). Monitoring the Vernal Advancement and Retrogradation of Natural Vegetation. College Station, Texas, Remote Sensing Center, Texas A&M University: 200 pp.
8. Sellers, P. J. (1987). "Canopy reflectance, photosynthesis and transpiration II: The role of biophysics in the linearity of their interdependence." *Remote Sensing of Environment* 21: 143-183.
9. Szilagyi, J., Rindquist, D.C., Gosselin, D.C., Parlange, M.B. (1998). "NDVI Relationship to Monthly Evaporation." *Geophysical Research Letters* 25(10): 1753-1756.
10. Thomas, J. R., Namken L. N., Oerther, G. F., and Brown, R. G. (1971). Estimating leaf water content by reflectance measurements. *Agronomy Journal* 63, 845.847.
11. Tucker, C. J., Sellers, P.J. (1986). "Satellite remote sensing of primary production." *International Journal of Remote Sensing* 7: 1395-1416.
12. Tucker, C. J. (1980). Remote sensing of leaf water content in the near infrared. *Remote Sensing of Environment* 10, 23.32.
13. Wan, Z., Wang, P., Li X. (2004). "Using MODIS Land Surface Temperature and Normalized Difference Vegetation Index products for monitoring drought in the Southern Great Plains, USA." *International Journal of Remote Sensing* 25(1): 61-72.
14. White paper, The Benefits of the 8 Spectral Bands of WorldView-2, March 2010.
15. Wilhite, D. A., and M. H. Glantz, (1985), Understanding the drought phenomenon: The role of definitions, *Water Int.*, 10, 111-120.

Geospatial Modelling for Flood Management in a Rural Development Block of Orissa, India

Ansuman Satapathy¹, Kiranmay Sarma^{2,*}
and Gopal Krishna Panda³

Abstract

The research examines the use of GIS and spatial statistics for management of flood vulnerability and risk in a rural environment. Housing, critical facility, economic, environmental and health, societal, relief and rescue vulnerability and risk are taken into account in this study. Location and priority quotients of vulnerability and risk and their spatial representation using spatial analysis are found to be providing significant support in decision making process. The spatial context of vulnerability, risk and related maps and database created are found to be highly necessary in generating valuable and timely information for effective disaster management practice. Specific research directions in the line of advanced spatial and attribution analysis are also suggested in this research.

Keywords: GIS; flood; vulnerability; risk; management priority; location quotient, priority quotient

Introduction

Geospatial modelling and prioritization of policies are necessary for effective disaster management practice. It is evident from the increasing attention received by GIS and spatial statistics in hazard research. A key role of GIS has been in devising ways to manage and analyze the data produced in disaster management situations. Vulnerability and risk assessment coming under prevention phase are the most important steps in the six phased disaster management process.

¹ & ² School of Environment Management, GGS Indraprastha University, New Delhi-110075

³ Department of Geography, Utkal University, Bhubaneswar, Orissa

* Corresponding author: kiranmayipu@gmail.com

Flood disaster has maximum frequency and has caused maximum amount of damage in India, as compared to other natural disasters (NIDM, 2009). According to Dhar *et al.* (2003), monsoon rainfall magnitude is not the only cause of flooding in the coastal Orissa. Lower channel depth and slope value, human intervention in the form of deforestation and commercial exploitation of silts deposited on natural levees also enhance the risk of flooding. Disaster risk reduction and more robust development planning are crucial in adapting to the increasing risks associated with climate change. This is particularly important in the face of mounting vulnerability to flood hazards, as reflected, for instance, in rising numbers of people affected and escalating levels of economic damage (Aalst, 2009). The essence of this paper is to propose a geospatial model for assisting the decision making process of flood managers.

Geospatial technology is necessary for immediate as well as long term response to natural hazards. GIS application in disaster risk management ranges from database creation, inventory, overlay, risk analysis, cost benefit analysis, scenario analysis, decision matrix, sensitivity analysis, geoprocessing, spatial statistics and many other complex spatial decision making tools and algorithms (Menon & Sahay, 2006). Management of disaster data include data integration, ingestion, information retrieval, filtering and data mining for decision support.

According to Islam and Sado (2004), flood hazard assessment can be done using flood frequency, depth, land cover, physiographic and geologic divisions also. Weighted score on the basis of flood frequency and depth can be given to each division for calculating hazard ranks. 'Analytical Hierarchical Process' is another important method used for hazard zonation. Decision factors such as geomorphic features, elevation, vegetation and land cover can be used and their relative importance weights are calculated using this method.

Vulnerability is defined as the degree of loss to a given element of risk or set of such elements, resulting from the occurrence of natural phenomenon of a given magnitude (UN, 1991). Risk is the chance of loss as defined as a measure of the probability and severity of adverse effect to health, property, environment and other things of value. It is a function of both natural hazard and vulnerability. Spatial pattern of vulnerability and risk provide important information about risk elements and prioritization of mitigation process (Ross, 1987). 'Risk and vulnerability assessment tools' prepared by NOAA, USA (1999), describes the process in six steps as hazard analysis, critical facilities analysis, economic analysis, environmental analysis, societal analysis and mitigation opportunities analysis. 'Hazard, risk and vulnerability assessment tool kit', prepared by Ministry of Public Safety and Solicitor General, Provincial Emergency Program, State of

British Columbia , Canada (2004) uses simple ranking method on the basis of risk profiles drawn from likelihood of disaster occurrence and consequent impact.

Oswald and Sinclair (2005) proposed seven broad categories of values in flood plain management. They are community identity and community attributes, community economic development, technical and non-structural approaches, civic engagement, flood legacy, personal rights & liberties and shared values. According to Hall *et al.* (2003), flood risk to environment, society and economy are cumulative effects of change. Hence, long term scenarios are required for sustainable flood management policies. Environmental vulnerability embraces various political, social, economic and biophysical dimensions that shape and conjure risk to hazards. Lack of resource in community decreases the resilience to hazards. Policy and institutional reforms and improved knowledge management are required to sustainably address the risks.

Materials and Methods

Study area and data

The area under study is Mahakalapada block belonging to the coastal district of Kendrapada in Orissa state (Fig. 1). The area comes under Mahanadi delta region. The block consists of 26 gram panchayats or GPs (Administrative unit consisting of some villages). The river Mahanadi passes through the area which comes under its flood velocity zone. Agriculture is the principal land use and aquaculture is practised in coastal GPs (Fig. 2). Total population of the area accounts to 1,91,745 (Census of India, 2001). A symbiotic relationship exists between flood, cyclone and economic backwardness of the area (Satapathy, 2007).

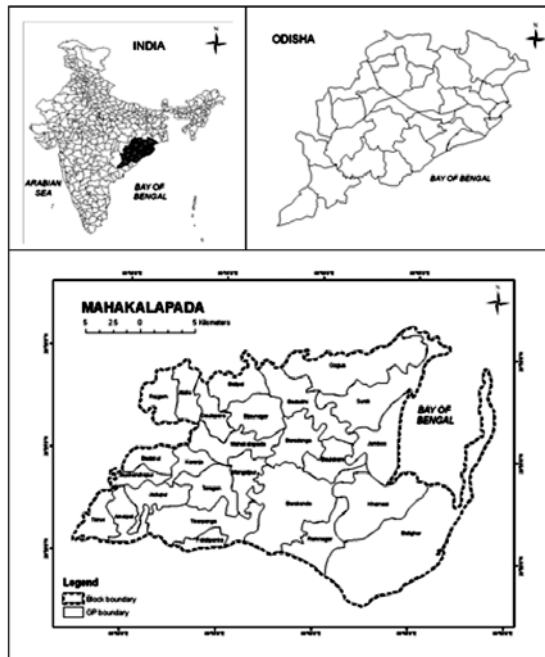


Fig 1. Location of the study area

IRS ID LISS III imagery of 2003 and relevant Survey of India toposheets are used for land use analysis and reference. Data regarding flood frequency is collected from District Emergency office. Census of India, 2001 data is used for acquiring socio-economic information. District Revenue office data is used to estimate the economic impacts of hazard and primary survey was carried out to collect data not available in secondary form.

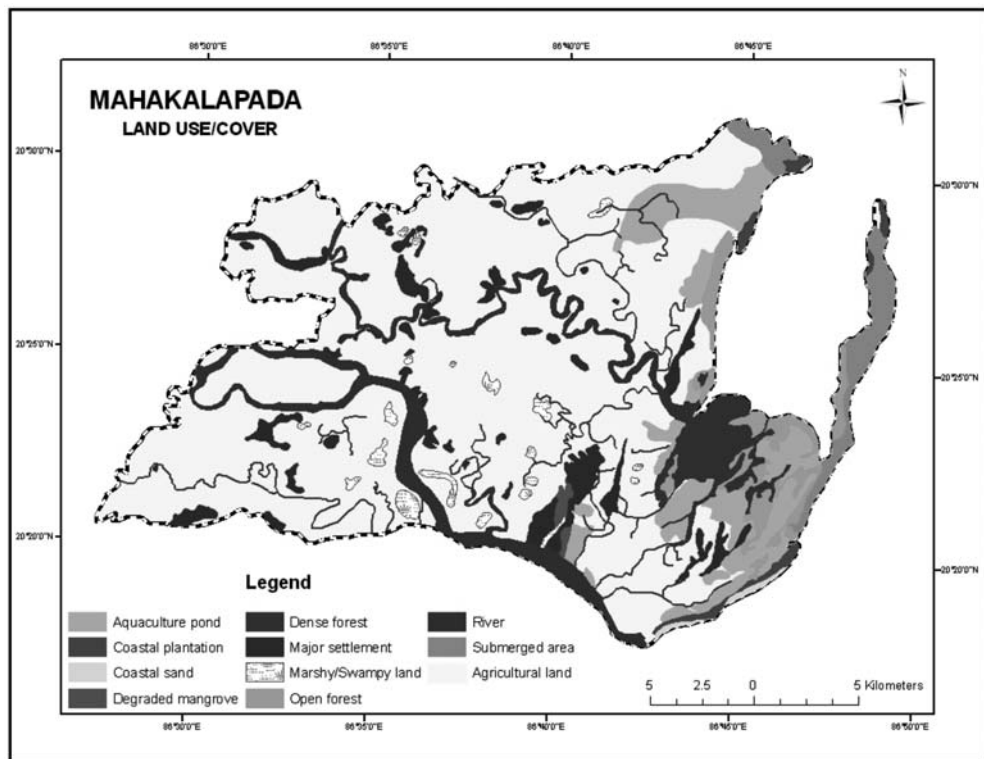


Fig 2. Land use / cover map of Mahakalapada

Methods

Hazard zonation of the area is done using a simple method which can be performed with easily available data. Two basic types of hazard factors are used for hazard zonation. Flood frequency and depth are considered as hydraulic factors and quality of flood water drainage is taken as geomorphic factor for hazard zonation. Quality of flood water

drainage is evaluated on the basis of percentage of area of each GP under high soil moisture in post flood scenario, which is acquired from the IRS 1D LISS III imagery (2003) of the study area. Ranking matrix in three dimensional multiplication modes (Table 1) has been used to calculate the composite flood hazard index, using hazard ranks of individual hazard factors. A scheme of progressive weightage (Sanyal & Lu, 2003) has been adopted for the variable 'hazard rank (HR)' so that the hazard curve becomes progressively steeper at the higher values of 'hazard factors'. The exponential function (e^x) is used to model hazard phenomena because a constant change in the independent variables (hazard factors) give the same proportional change (increase or decrease) in the dependent variable (hazard rank). Ranks of hazard, vulnerability and risk are simplified to a 5 point scale from low to high.

Table 1. Concept of ranking matrix

X		XY									
HR	0.12	0.34	0.94	2.57	7.08	HR	0.84	2.40	6.65	18.19	50.12
0.12	0.01	0.04	0.11	0.30	0.84	0.12	0.10	0.28	0.79	2.18	6.01
0.34	0.04	0.11	0.31	0.87	2.40	0.34	0.28	0.81	2.26	6.18	17.04
0.94	0.11	0.31	0.88	2.41	6.65	0.94	0.78	2.25	6.25	17.09	47.11
2.57	0.30	0.87	2.41	6.60	18.19	2.57	2.15	6.16	17.09	46.74	128.8
7.08	0.84	2.40	6.65	18.19	50.12	7.08	5.94	16.99	47.08	128.78	354.84

Gram panchayat wise vulnerability and risk assessment for elements, such as houses, critical facility, economy, environment, society, relief and rescue are carried out separately. Vulnerability is determined in the face of high flood hazard. In case of housing study the predominant material of roof and wall, damage history are taken as components of structural vulnerability and position with respect to base flood level is taken as component of operational vulnerability. Health Centre, school building, road, community building, telecommunication facility are taken under critical facility category and their structural and operational vulnerability are calculated using the codes prescribed by Vulnerability Atlas of India (1997).

Crop damage history, agricultural efficiency, live stock vulnerability on the basis of availability of shelter and medical care are considered to assess economic vulnerability. Availability of sanitation facility, drainage connectivity for waste water outlet and

livestock vulnerability is taken as factors for determining environmental and health vulnerability.

Population density, population under critical age group, population below poverty line, crime incidence and intensity, mental preparedness are considered as elements of societal vulnerability. Vulnerability of road, level of road network development, disaster cognizance level, efficiency history of relief distribution system are taken into account for calculating relief and rescue vulnerability. Level of road network development is determined by calculating cyclomatic number ($\mu = \text{no. of edges} - \text{no. of vertices} + \text{no. of graphs}$) for each GP and behavioural matrix is used to determine cognizance level. Literacy percentage, used as the determining factor for ability use incoming information and quality of incoming information are taken as components of the matrix.

Itemized and relative rating scales are used for ranking individual factors. These are principally knowledge based ranks. Combined vulnerability score is calculated from these values and then multiplied with composite hazard indices to determine risk scores. Categorization of risk scores is carried out by using ranking matrix in two dimensional multiplication modes. On the basis of vulnerability and risk scores, maps showing these categories are prepared and high priority elements are shown for different GPs. GIS and remote sensing techniques such as classification, topology building, fuzzy analysis, query and categorization are applied in Arc GIS and ERDAS environment to develop thematic maps. Structured questionnaire and group discussion methods are used for primary data collection from the samples selected by stratified random sampling method. Self rating method is used for collection of behavioural data. 5 point Likert scale is used to rank them. Likert scale measures the level of agreements of respondents to questionnaire statements (Kerlinger, 1986).

Solution matrices are prepared for vulnerability and risk scores by standardising the rank of individual vulnerable category on the basis of qualitative index (Table 2). The qualitative indices are transformed into quantitative ranks of 1 to 5. These values are used in the solution matrices, to calculate location quotient for GPs and priority quotient for vulnerable categories. Severity of a risk component with respect to average value of risks prevailing in the area is represented by priority quotient. Vulnerability and risk representation of a GP with respect to average representation levels of the block is represented by location quotient. On the basis of these quotients priority ranks are assigned. Priority ranks of individual vulnerability and risk category are also assigned using combined scores of these categories for all the GPs, which reveals block level scenario of vulnerability and risk. This will help in block level disaster management program. The formulae used for calculating location and priority quotients are as follows:

$$P = \frac{\sum v \text{ or } r \text{ ranks for all individual categories in the GP}}{\sum v \text{ or } r \text{ ranks of all the GPs} \div \text{Total number of GPs}}$$

$$r \text{ category} = \frac{\sum \text{ ranks of all the GPs for that category}}{\sum \text{ ranks of all the categories of } v \text{ or } r \div \sum v \text{ or } r \text{ categories}}$$

ation Quotient; PQ: Priority Quotient; v: vulnerability; r: risk)

On the basis of the above quotients, priority ranks are assigned. Using these ranks management priority maps is prepared. The term 'management priority' is used in the sense that in mitigation programs the ranks will determine priority elements. Also during an unexpected disaster in a low hazard risk area, vulnerability score will help to determine priority functions of disaster management. Product moment correlation coefficient between combined vulnerability and risk scores is calculated to test the effectiveness of the ranking system used. Relationship between vulnerable and risk elements have been estimated by using Spearman's rank difference method. The overall methodology framework is given in Fig. 3.

Table 2. Framework for solution matrix for vulnerability / risk analysis

Vulnerable element	Vulnerability / risk ranks of individual gram panchayats on 5 point scale						Total (GP1 to GP26)	Priority quotient	Priority rank
	GP1	GP2	GP3	GP4	GP5	GP6.....			
Housing facility	4	5	1	3	2	1	82	1.01	2
Critical facility	3	4	1	2	1	1	62	0.76	3
Economy	4	5	1	3	2	1	82	1.01	2
Environment & health	5	5	2	3	2	2	94	1.16	1
Society	4	5	1	3	2	1	82	1.01	2
Relief & rescue	4	5	1	3	2	1	82	1.01	2
Total	24	29	7	17	11	7			
Location quotient	1.28	1.55	0.37	0.90	0.58	0.37			
Priority rank	2	1	7	4	6	7			

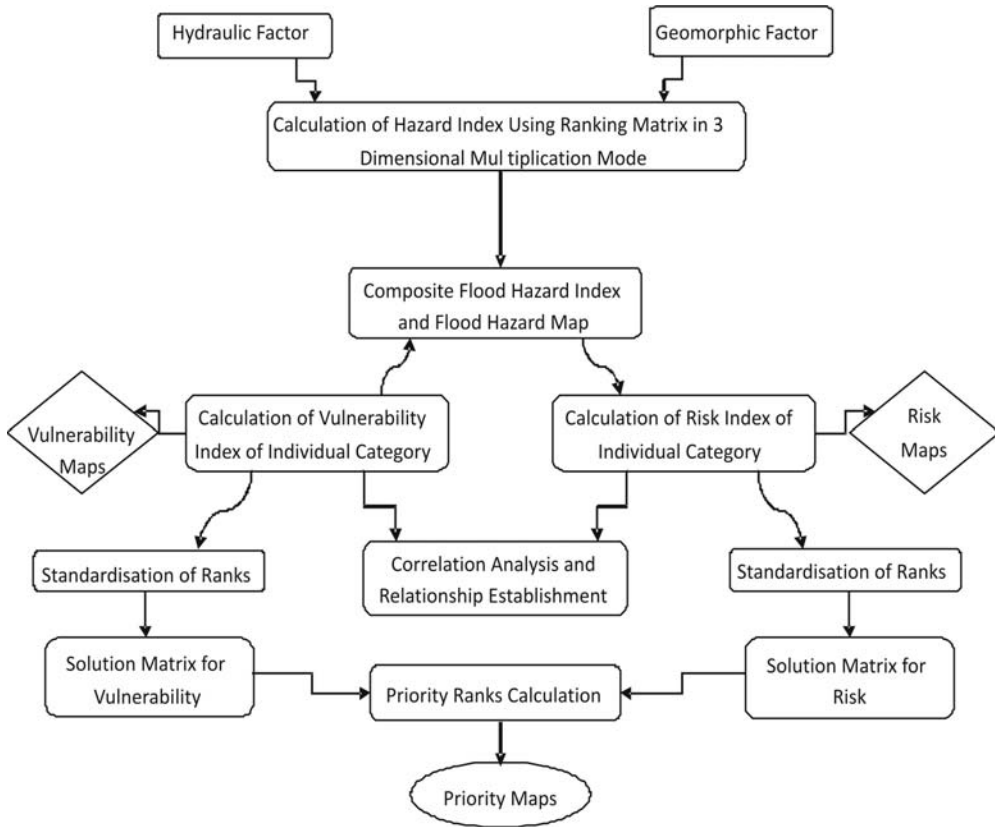


Fig 3. Methodology framework

Results and Discussion

The composite flood hazard indices showed high and medium risk in most of the GPs. The GPs of north east portion are comparatively low risk areas due to relatively higher altitude (Fig. 4). Most of the GPs come under moderately high to high housing risk. The critical facility vulnerability is found to be moderately low. This is because of hazard resilient construction works carried out in post super cyclone that hit the state in 1999.

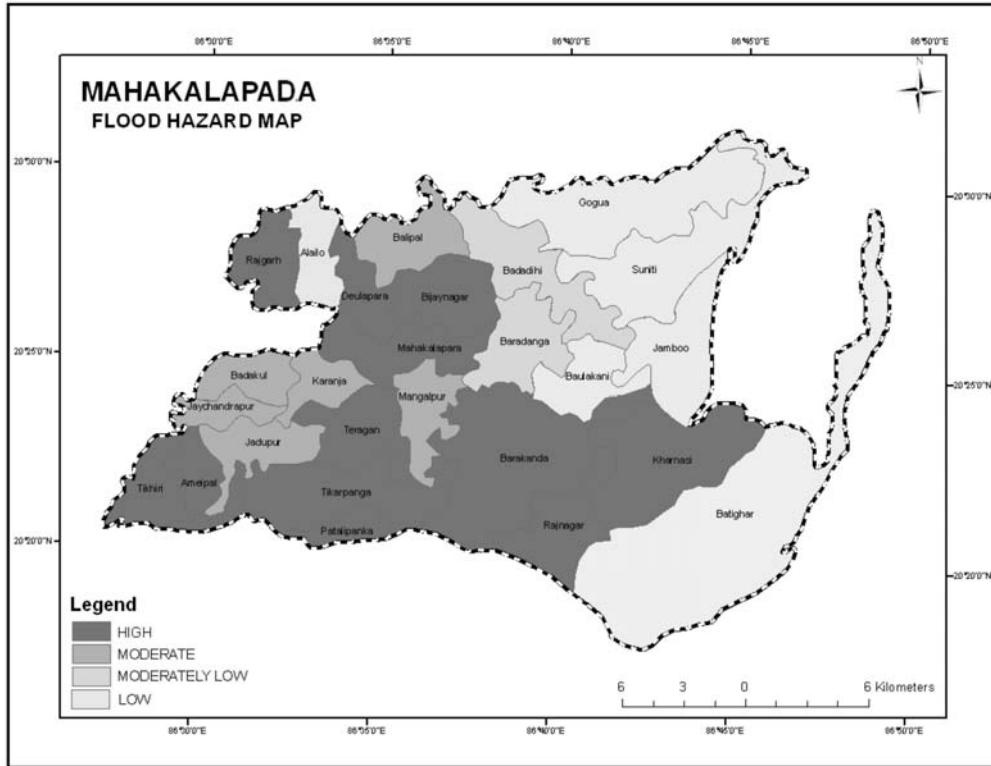


Fig 4. Flood hazard map of Mahakalapada

Economic vulnerability and risk are found to be high for most of the GPs. Threats to livelihood is a serious concern in the area. The environmental and health vulnerability assessment showed high risk prevailing in most of the GPs. Low economic development, lack of awareness about sanitation, lack of safe shelter for livestock are the factors responsible. Societal vulnerability and risk are found to be moderately high to moderately low for many areas. The priority concern is found to be lack of mental preparedness. Relief and rescue vulnerability and risk are found to be heterogeneously distributed. Operational vulnerability of roads is the priority concern for this category.

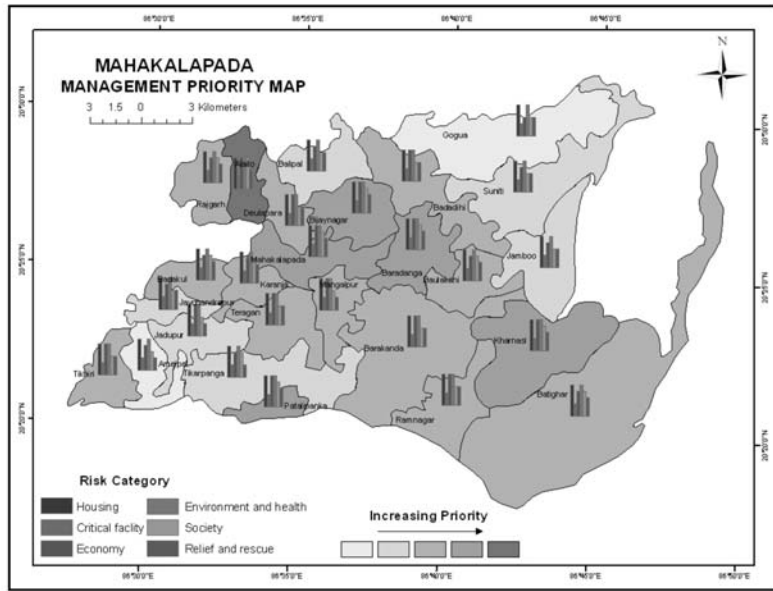


Fig 5. Management priority map based on vulnerability score and priority rank

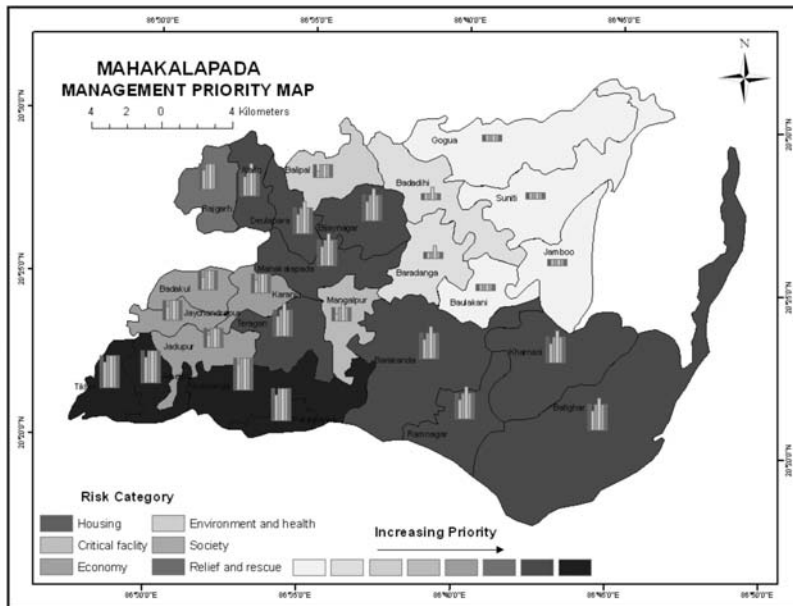


Fig 6. Management priority map based on risk score and priority rank

On the basis of location quotients Alailo, Baradanga, Bijaynagar, Kharnasi, Mahakalapada and Patalipanka GPs are found to be over represented in terms of fair value of vulnerability (Fig. 5). Ameipal, Batighar, Baulakani, Bijaynagar, Deulapada, Tikhiri, Ramnagar, Rajgarh are found to be over represented in terms of risk (Fig. 6). Hence these areas should be given first priority in mitigation programs. It is found that at block level, environment and health are at highest risk and critical facilities are at lowest risk. Similarly environment, health and housing facility have highest vulnerability (Fig. 7).

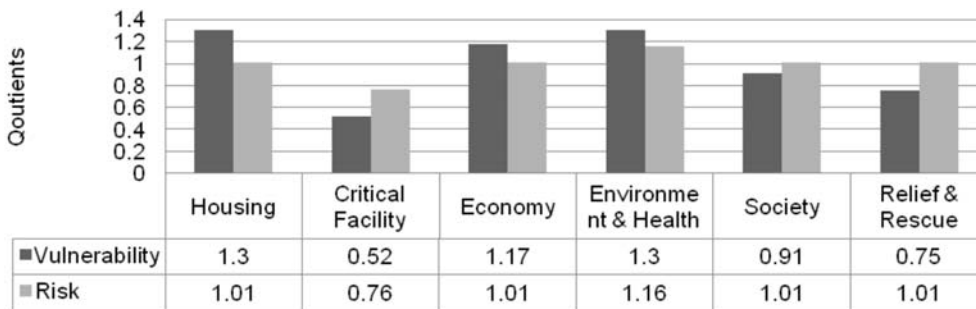


Fig 7. Priority Quotient at block level for combined vulnerability and risk

Product moment correlation coefficient (r) between combined vulnerability and risk scores is + 0.34, which confirms the absence of perfect positive correlation between variables. Hence it is inferred that there is absence of unfair amount of interplay between variables. This shows that the ranking system used in the study is efficient. The rank correlation coefficient (ρ) between risk elements is found to be ranging from 0.8 to 1. This shows serious symbiotic relations between these elements which demands integrated and holistic disaster resilient development policies for the block.

Conclusion

The application of a GIS and spatial modelling for natural hazard risk management is an emerging science. Providing a spatial context for risk is critically important for risk reduction. The maps and database created on vulnerability and risk can provide valuable and timely information for effective disaster management practice. Integration of priority ranks in geospatial data gives readily representable and cognizable information to disaster managers which would otherwise require tedious mathematical processes. These data can further be manipulated through spatial and attribution query

in GIS environment to help the spatial decision making process for ready response to disaster. A further future development of the proposed approach can include detailed study of individual categories of risk and their minute interrelationships using advanced spatial and attribution query methods in GIS environment. The approach may also be used for developing the decision support system for flood management.

References:

1. Aalst, M. K. (2009) *The impacts of climate change on the risk of natural disasters*, World Bank Institute.
2. Building material and technology promotion council, Government of India (1997) *Vulnerability Atlas of India*. New Delhi.
3. *Census of India* (2001).
4. Dhar, O.N. & Nandargi, S. (2003) *Hydrometeorological aspects of flood in India*. Natural Hazards, 28.
5. Hall, J. W., Evansb, E. P., Edmund, C., Sayersd, P. B., Thornee, C. R., Saulf, A. J. (2003) *Quantified scenarios analysis of drivers and impacts of changing flood risk in England and Wales: 2030-2100*. Global Environmental Change Part B: Environmental Hazards, (5), 51-65.
6. Islam, M.M. & Sado, K. (2004) *Development of flood hazard maps of Bangladesh using NOAA AVHRR images with GIS*. Hydrological science journal, 45 (3).
7. Kerlinger, F.N. (1986) *Foundations of Behavioural Research*. Holt, Rinehart, and Winston.
8. Menon, N.V.C. & Sahay, R. (2006) *Geoinformatics for disaster risk management*. GIS Development: Asia Pacific, 10 (10).
9. Ministry of Public Safety and Solicitor General; Provincial Emergency Program (2004) *Hazard, risk and vulnerability assessment toolkit*. British Columbia, Canada.
10. United Nations (1991) *Mitigating natural disasters: Phenomena, effects and options*.
11. National Institute of Disaster Management (2009) *National Policy on Disaster Management*. New Delhi.
12. National Oceanic and Atmospheric Administration (1999) *Risk and vulnerability assessment tool*. USA.
13. Oswald, T., Sinclair, A. (2005) *Values and floodplain management: Case studies from the Red River Basin, Canada*. Global Environmental Change Part B: Environmental Hazards, 6 (1), 9-22.
14. Ross, S. (1987) *Hazard Geography*. Longman, U. K.
15. Sanyal, J. & Lu, X. X. (2003) *Application of GIS in flood hazard mapping: A case study of Gangetic West Bengal, India*. National University of Singapore.
16. Satapathy, A. (2007) *Community vulnerability assessment and risk analysis for flood disaster in a coastal development block of Orissa, India*. M.Phil. dissertation, Utkal University, Bhubaneswar, India.

Use of Multi-Source Data Sets for Land Use/Land Cover Classification in a Hilly Terrain for Landslide Study

D. P. Kanungo and S. Sarkar

Abstract

The land use/land cover (LULC) information of an area is essential for monitoring and management of natural resources. It is an important input for many geological, hydrological, ecological and agricultural models. In this study, the IRS-1C LISS-III data have been used as the primary data source along with NDVI (Normalized Difference Vegetation Index) and DEM (Digital Elevation Model) images as additional data layers to improve the LULC classification accuracy in a hilly terrain. Image classification is performed using most widely used Maximum Likelihood Classifier (MLC). The IRS-1C PAN image is used as the reference data for generating training and testing datasets. The preparation of reference data is ably supported with field data as well as information from topographic maps. The results show a reasonable improves in the accuracy of classification on incorporation of NDVI and DEM as ancillary data. The LULC map thus prepared is useful as one of the input data layers for landslide hazard study. High spatial resolution IRS-1CPAN and PAN-sharpened LISS-III images were used to prepare a landslide distribution map which was verified from field surveys. Landslide density is found to be maximum in barren lands, followed by agriculture land, built-up land, tea plantation area, and forest cover. The relation between LULC and landslide density thus obtained was later used as an input for landslide susceptibility mapping.

Key word: Land use, Land cover, image classification, multi-source, landslide

Geotechnical Engineering Division, CSIR-Central Building Research Institute,
Roorkee 247 667, India
debi.kanungo@gmail.com, shantanu_cbri@yahoo.co.in

Introduction

The land use/land cover (LULC) information of an area is essential for proper planning, management and monitoring of natural resources. It is an important input for many geological, hydrological, ecological and agricultural models. LULC map generally shows distribution of forest cover, water bodies and types of land use practices. Many studies (e.g., Coppin and Richards, 1990; Selby, 1993; Mehrotra *et al.*, 1996) have revealed a clear relationship between vegetation cover and slope instability.

Remote sensing images help in gathering quality LULC information at local, regional and global scales because of its synoptic view, map like format and repetitive coverage (Csaplovics, 1998; Foody, 2002). Further, in mountainous regions like the Himalayas, particularly in the inaccessible areas due to high altitudes and ruggedness in the terrain, remote sensing images are quite useful for mapping. Due to changes in topographical and environmental conditions, spectral characteristics also change from region to region (Arora and Mathur, 2001). Therefore, the approach for LULC classification that incorporates ancillary data from other sources may be more effective than that is based solely upon multi-spectral data from one sensor. The topographic maps are useful in generating the DEM, which along with its attributes, such as slope and aspect; provide the basis for multi-source classification (Strahler *et al.*, 1978; Jones *et al.*, 1988; Frank, 1988; Janssen *et al.*, 1990; Saha *et al.*, 2005). Furthermore, the derivatives of multispectral images like Principal Components Analysis (PCA) and Normalised Difference Vegetation Index (NDVI) may also be useful to improve the LULC classification from remote sensing data in mountainous regions (Eiumnoh and Shrestha, 2000; Saha *et al.*, 2005). In mountainous terrain, such as Himalayas, shadow is the major problem in achieving the accurate land use land cover classification from remote sensing data. The use of NDVI image as an additional layer for classification has been recommended to overcome this problem, since the band ratio derivatives may help in nullifying the topographic effect to some extent (Holben and Justice, 1981; Apan, 1997). However, NDVI alone may not be able to eliminate the shadow effect completely. Later, Eiumnoh and Shrestha (2000) and Saha *et al.* (2005) incorporated both NDVI and DEM images as additional layers in the classification process and found a significant improvement in the classification accuracy.

This study focuses on Darjeeling hill which lies between latitudes 26°56'N and 27°8'N and longitudes 88°10'E and 88°25'E and covers an area of about 254 km² (Figure 1). The main habitat areas are Darjeeling, Ghum, Sonada, and Sukhiapokhri. The maximum elevation of 2,584 m occurs at the Tiger hill. The area is dominated by slopes ranging between 15° and 35° while steep slopes (i.e., >35°) occupy a smaller area. The annual

rainfall in the region varies from a low of 3,000 mm to a high of 6,000 mm. The major land use practice in the study area is tea plantation and agriculture mostly developed around the habitat areas.

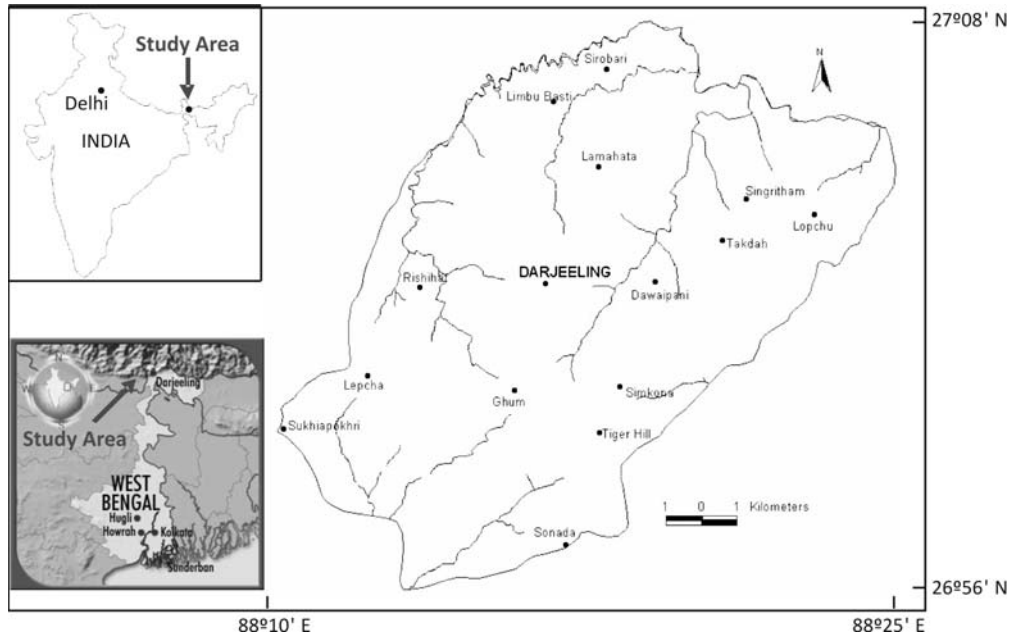


Fig 1. Study area

In this study, the IRS-1C LISS-III data (22nd March, 2000) with a spatial resolution of 23.5m has been used as the primary data source along with NDVI and DEM images as additional data layers to implement multi-source LULC classification process. A separability analysis using transformed divergence is performed to examine the significance of various spectral bands in the classification process. Most widely used Maximum Likelihood Classifier (MLC) is used to perform the classification. A very small portion covered by the cloud and its shadow in the original LISS-III image has been masked and then used as the primary data to perform LULC classification. The PAN image (3rd April, 2000) with a spatial resolution of 5.8m is used as the reference data for generating training and testing datasets. This is in accordance with other studies on LULC classification of remote sensing data, where finer resolution data have also been used as reference data (Fisher and Pathirana, 1990; Foody and Arora, 1996; Shalan *et al.*,

2003; Saha *et al.*, 2005). The preparation of reference data is ably supported with field data as well as information from topographic maps. The LULC map thus produced was used for landslide hazard study. High spatial resolution IRS-1C-PAN and PAN-sharpened LISS-III images were used to produce a landslide distribution map which was verified from field surveys. A total of 101 landslides showing areas occupied by sliding activity were identified. The landslide distribution in different categories of land use land cover in the area was also analyzed.

Methodology

A multi-source image classification involves a number of steps which include generation of ancillary data layers (NDVI and DEM), image classification and accuracy assessment.

Geometric registration of images

The digital images acquired from remote sensing satellites are fraught with geometric distortions, which render them unusable, as these may not be directly correlated to ground locations (Gupta, 2003). Geo-referencing involves the process of assigning map coordinate information to the image data so that the geometric integrity of the map in the image is achieved.

In this study, the geo-referencing of remote sensing data (IRS-1C LISS-III and IRS-1D PAN Images) has been performed using ERDAS Imagine software. In the first step, the Survey of India topographic maps have been geo-referenced to geographic coordinate system. These maps have been later used as reference maps for geo-referencing of satellite images.

The IRS-1C LISS-III image has been geo-referenced with the topographic maps by taking input GCPs from the LISS-III image and reference GCPs from topographic maps. A total of 35 well distributed GCPs have been considered for registration and an RMS control point error of 0.83 pixels is obtained. Also, the registration is checked with another set of independent 11 GCPs, which yielded an RMS error of 0.96. It is found that the RMS errors obtained using 1st order polynomial model for geometric correction is within the acceptable limit of one pixel. The nearest neighbor resampling method has been adopted to produce the geo-referenced LISS-III image (Figure 2), as this preserves the original brightness values in the output image.

Co-registration of IRS-1D PAN with IRS-1C LISS-III image is essential in view of the fact that the PAN image is used for selecting training and testing data samples for multispectral (LISS-III) image classification. Therefore, the PAN image has been registered with LISS-III image by taking input GCPs from the PAN image and reference

GCPs from LISS-III image. In this co-registration process, a set of 50 well distributed GCPs produced an RMS control point error of 0.71 pixels and 15 check GCPs yielded an RMS error of 0.68 pixels. The 1st order polynomial model with nearest-neighbor resampling method is used for this purpose. The registered PAN image thus obtained is shown in Figure 3.

The optical remote sensing images invariably contain the effect of selective atmospheric scattering and absorption of the solar radiation. In the visible - near infrared region of the electromagnetic spectrum, scattering is the most dominant process leading to path radiance. This has an additive role and affects the brightness values (Jensen, 1996). The remote sensing data, therefore, need to be corrected. Although, there are many techniques to perform this correction, the most widely used, the 'dark object subtraction' technique (Chavez, 1988) has been adopted to correct the atmospheric scattering. The minimum DN values for green, red, near infrared (NIR) and shortwave infrared (SWIR) bands were extracted and were expected to be due to path radiance. These values were subtracted from DN values of pixels in the respective bands to generate a path radiance corrected image. The corrected LISS-III and PAN images formed the data sources for preparation of land use land cover map.

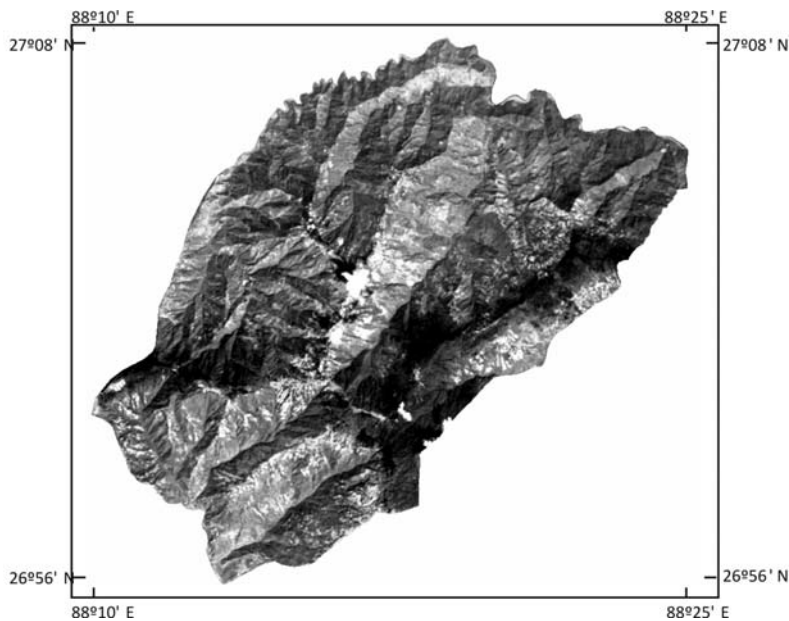


Fig 2. IRS-1C LISS-III False Colour Composite (NIR=R, Red=G, Green=B)

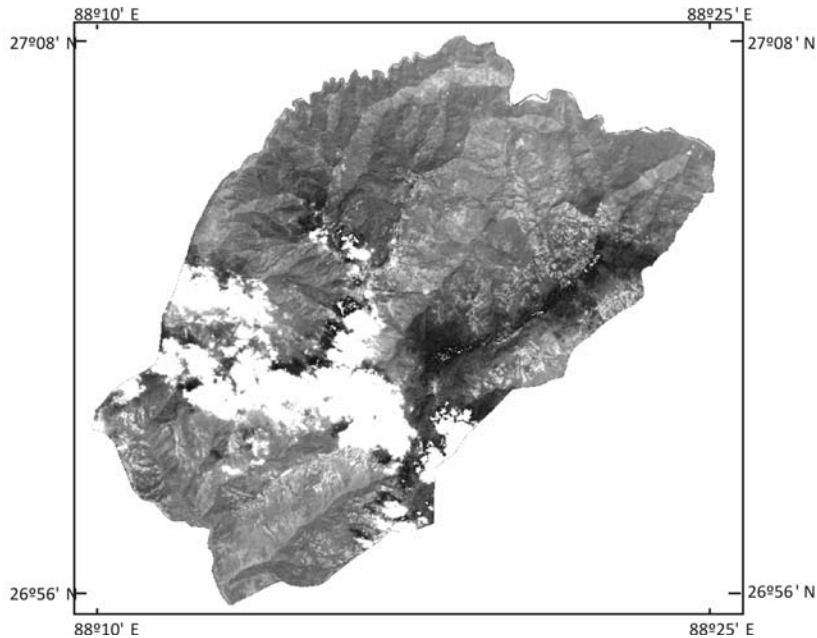


Fig 3. IRS-1D PAN image of the area (A large portion of this image is covered by clouds)

Ancillary Data generation

NDVI layer

During field surveys, different types of vegetation were observed in the study area. Hence, NDVI has been used as an ancillary data layer in the classification process to enhance the separability among various vegetation classes, and also to reduce the effect of shadow due to topography. The NDVI can be stated as,

$$\text{NDVI} = (\text{NIR band} - \text{Red band}) / (\text{NIR band} + \text{Red band}) \quad (1)$$

The DN values of pixels of the NDVI image thus produced range from 0.00 to 0.83 with higher values indicating increasing biomass. The positive values represent various types of vegetation classes. Near zero values indicate non-vegetation classes, such as water, river sand and barren land.

DEM layer

DEM represents the spatial variation of elevation over an area. It is an important basic

component in LSZ studies. In this study, DEM has been used as an input layer to multi-source classification of remote sensing data for land use land cover map preparation to minimize the error in classification due to topographic variations.

The DEM has been prepared using the conventional and most prevalent method by considering the contours from Survey of India topographic maps. The contours at 10m and 20m intervals on 1:25,000 scale topographic maps and 40m interval on 1:50,000 scale maps respectively have been used to generate the DEM using the triangulated irregular network (TIN) method. A DEM at spatial resolution corresponding to pixel size of 25m × 25m has been generated to match the nominal spatial resolution of LISS-III image.

Image Classification

Image classification process is based on several steps, a) selection of LULC classification scheme, b) formation of training dataset, c) separability analysis, d) Maximum Likelihood Classification (MLC) and e) accuracy assessment. The methodology of multi-source image classification for LULC is given in figure 4.

Selection of LULC classification scheme

A classification scheme defines the LULC classes to be considered to prepare land use land cover map from remote sensing image data. The number of LULC classes are sometimes chosen according to the requirements of the specific project for a particular application (Arora and Mathur, 2001; Saha *et al.*, 2005). In this study, the LULC classes are chosen keeping in view its application for landslide studies. During field visits, eight classes were identified in the study area. These classes are dense forest, sparse forest, tea plantation, agriculture, barren, built up, water bodies and river sand. Detailed description of all these classes along with their interpretative characteristics on the FCC of LISS-III image and PAN image is given in Table 1. This information is used to identify the training and testing areas on the image for carrying out supervised classification and accuracy assessment.

Formation of training dataset

The success of image classification highly depends on the quality of training dataset which in turn depends on the capability of image interpretation and knowledge on the LULC patterns of the study area. In this study, the number of training pixels for each class (Table 2) was defined in accordance with the proportion of the area covered by the respective classes on the ground. Similar to other studies, the fine spatial resolution PAN

image and Survey of India topographic maps were used as reference data for ground truths to demarcate the training pixels on the LISS-III image. All the eight LULC classes were visually interpreted on the PAN image based on their characteristics. The PAN image derived information and ground truth data from field survey were used to demarcate training areas on LISS-III image for all the classes. Majority of training areas were normally distributed, which is a basic requirement of the maximum likelihood classifier used in this study.

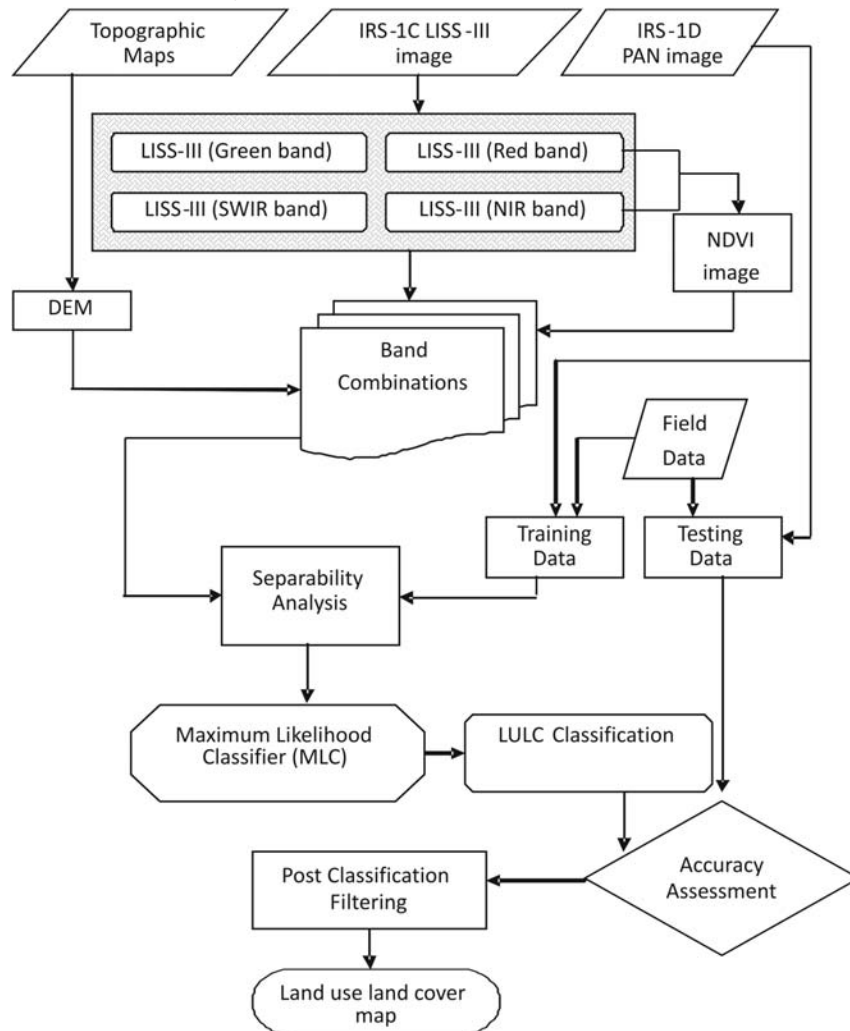


Fig 4. Methodology for multi-source LULC classification

Table 1. Characteristics of LULC classes

Land use land cover class	Description	Interpretation on LISS-III colour infrared composite	Interpretation on PAN image
Dense forest	Tall dense trees	Dark red with rough texture	Dark tone with rough texture
Sparse forest	Scanty tall trees and low vegetation density with exposed ground surface	Dull red to pinkish	Light tone with dark patches
Tea plantation	Tea plants with moderate vegetation density	Pink and smooth appearance	Light tone with smooth patches
Agriculture	Crops on hill terraces as step cultivation	Dull red and smooth appearance	Step like arrangement of fields and bright tone with smooth texture
Barren land	Exposed rocks/soils without vegetation	Yellowish	Very bright tone
Built up area	Towns and villages; block like appearance	Bluish	Typical blocky appearance with light tone
Water bodies	Rivers and lakes	Cyanish blue to blue according to the depth of water and sediment content	Dark tone
River sand	River sediments on the bank	Cyanish	Bright tone

Table 2. Number of training pixels for LULC classes used in image classification

Land use land cover class	Number of training pixels
Dense forest	1129
Sparse forest	622
Tea plantation	1127
Agriculture	639
Barren land	204
Built up area	288
Water bodies	193
River sand	273

Separability analysis

A separability analysis was performed with multi-source data layers using the training dataset of all the eight LULC classes to observe the spectral discrimination between these classes. In this study, a combination of six data layers comprising of Green, Red, Near Infrared (NIR) and Shortwave Infrared (SWIR) bands of multispectral LISS-III image, NDVI and DEM data layers were used as the input dataset for multi-source classification. Separability is a statistical measure devised on the basis of spectral distances computed for a combination of bands. From a number of separability measures, the Transformed Divergence (TD) measure (Janssen *et al.*, 1990) has been adopted in this study. The TD values range from 0 to 2000. A value close to 2000 indicates the best separability between the classes. The values between 1800 and 2000 are generally considered adequate to proceed for classification. As the present study intends for a multi-source classification, the average TD values of various band combinations including the ancillary data were computed. The band combinations with four bands of LISS-III image, NDVI and DEM resulted in the highest average TD value of 1977 as compared to those for the combination of only four spectral bands of LISS-III image and another combination of four spectral bands of LISS-III image and NDVI. The lowest TD value of 1723 is obtained for the signatures of barren land and agriculture. This is on expected lines as the agriculture lands without cultivation appear to be barren lands. Hence, a low separability between these two classes is observed. This analysis indicates that LISS III image together with NDVI and DEM has produced the best separability amongst various pairs of LULC classes. All the three combinations were used to perform LULC classification.

Maximum Likelihood Classification (MLC)

Over the years a number of classifiers have been developed and tested for remote sensing image classification. Each of these classifiers has its own merits and demerits in terms of efficiency and accuracy. The maximum likelihood classifier (MLC) was found to be the most accurate and most widely used for image classification, when the data distribution assumptions are met. The MLC is based on the decision rule that pixels of unknown class membership are allocated to those classes with which they have the highest likelihood of membership (Foody *et al.*, 1992). The details on this classifier may be found in Richards and Jia (1999). In this study, the MLC has been used to produce land use land cover maps, as it takes the variability of classes into account via covariance matrix.

Accuracy Assessment of LULC Classification

A testing dataset has been prepared with the help of reference data (PAN image and field data). The class allocation of each pixel in the classified image is compared with the corresponding class allocation on reference data to determine the classification accuracy. The pixels of agreement and disagreement are compiled in the form of an error matrix where the rows and columns represent the number of LULC classes and the elements of the matrix represent the number of pixels in the testing (reference) dataset. A number of accuracy measures, such as overall accuracy, user's accuracy and producer's accuracy can be estimated from the error matrix (Congalton, 1991). The overall accuracy indicates the accuracy of classification as a whole, whereas user's and producer's accuracy measures indicate the accuracy of individual LULC classes.

In the present study, field data on LULC classes and finer resolution PAN image have been used as reference data to prepare testing dataset for accuracy assessment. The testing pixels for each class have been randomly selected. These pixels are distributed all over the study area and are larger than 75 to 100 pixels per class as recommended by Congalton (1991) for accuracy assessment purposes. For comparison, the same testing dataset was used to determine the overall and producer's accuracy from different LULC classifications.

Results and Discussions

The objective of this study is to perform a multi-source classification including spectral and ancillary data to produce an accurate LULC map for its use in landslide study.

LULC Classification

The overall classification accuracy of 91.7% has been obtained in case of the dataset

using a combination of four spectral bands of LISS III image, NDVI and DEM. The overall accuracy corresponding to other two combinations (four spectral bands of LISS III image; four spectral bands of LISS III image and NDVI) are 88.1% and 89.4% respectively. Hence, it is clearly observed that on inclusion of NDVI and DEM data layers with the spectral data of LISS III, the overall accuracy for LULC classification is increased.

The accuracy of individual LULC classes was assessed based on producer's accuracy for all the three combinations (Table. 3). A glance at producer's accuracy values shows that the accuracy of all the LULC classes has increased gradually when NDVI and DEM data layers are included one by one in the classification process. This highlights that the misclassifications between the classes have been reduced.

It is observed in case of 6 data layer combination (LISS III, NDVI & DEM) producing highest overall classification accuracy that all the individual LULC classes except barren lands, built-up areas and water bodies have shown more than 90% producer's accuracy. The class barren land has been misclassified to some extent with the agriculture and tea plantation classes whereas the class built-up area has been misclassified with the classes tea plantation, agriculture, barren land and sparse forest. The class water body has been considerably misclassified with the class river sand.

Table 3. Producer's accuracy of individual LULC classes derived from accuracy assessment of classifications using different combinations

LULC classes	Producer's accuracy (%)		
	LISS III (4 spectral bands)	LISS III + NDVI	LISS III + NDVI+DEM
Dense forest	98.5	98.3	98.6%
Sparse forest	93.5	94.8	97.2%
Tea plantation	96.6	98.3	99.2%
Agriculture	82.6	89.5	95.9%
Barren land	81.2	79.0	82.3%
Built-up area	75.4	76.7	78.1%
Water body	86.3	87.5	89.2%
River sand	90.4	91.5	93.4%

The LULC classified image with highest accuracy contained some stray pixels over the whole image. To generate a smooth image by removing these stray pixels, a 3 × 3 pixels majority filter has been applied which assigns the most dominant class to the central pixel. Subsequently, the LULC information of the masked portion in the original

LISS III image has been replaced by the information collected from the topographic maps and some field data. The land use land cover layer thus prepared is shown in Figure 5. It can be observed that the northeastern, southeastern and southwestern parts of the area are dominated by thick forests. Tea plantation and sparse forests are the major land use land cover categories, which are distributed all over the area. The area-wise distribution of different LULC categories has been derived and is listed in Table 4. It is observed that the most frequent categories of LULC are tea plantation and sparse forest, followed by thick forest, agriculture land, barren land, habitation, the least being water bodies and river sand.

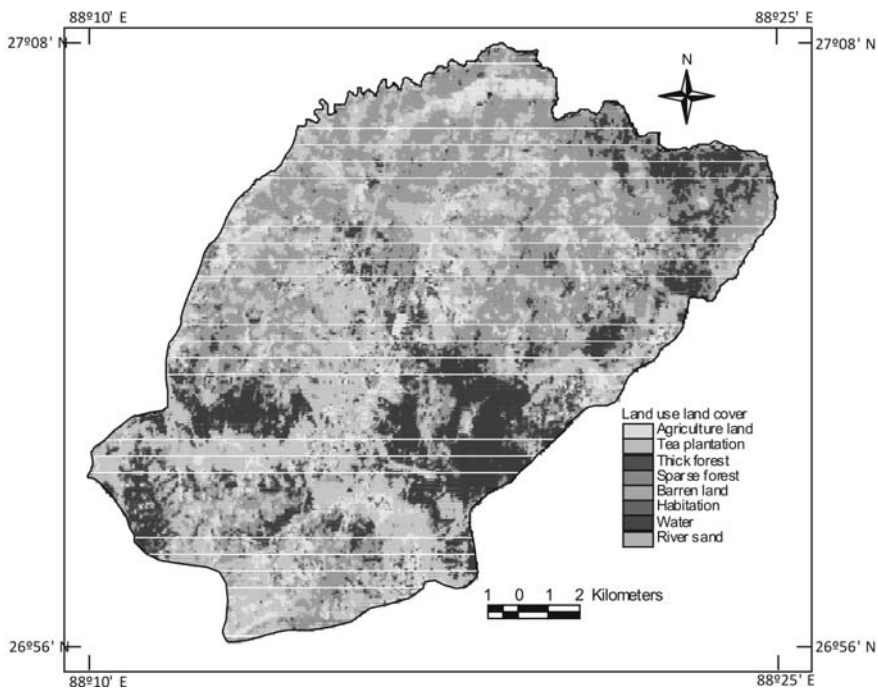


Fig 5. Land use/land cover map of the area

Landslide scenario in different LULC classes

Mapping of existing landslides is essential to understand the relationships between the landslide distribution and the causative factors, specifically land use land cover factor in this case. As, it is just not possible to map each and every landslide via field surveys in such a rugged terrain, a comprehensive mapping of landslide was undertaken through remote sensing image interpretation, aided by field verifications.

The identification of landslides on remote sensing image is based on the spectral characteristics, shape, contrast and the morphological expression. In general, there is a distinct spectral contrast between landslides and the background area. High spatial resolution IRS-1C-PAN and PAN-sharpened LISS-III images have been used for landslide identification, recognition and mapping. On the PAN image, landslides appear as features of very light tones due to rock debris without any vegetation on the slope. After enhancing the contrast of the PAN image, landslides occurring in barren areas could also be identified. A few old landslides were identified on the basis of their shape, landform and drainage. Feature extraction and interpretation is highly effective by using PAN-sharpened multi-spectral image products (Welch and Ehler, 1987; EOSAT, 1994; Sabins, 1996; Sharma *et al.*, 1996; Saraf, 2000; Prakash, *et al.*, 2001; Sanjeevi *et al.*, 2001; Shanmugam and Sanjeevi, 2001; Gupta, 2003). On the PAN-sharpened LISS-III image, the landslides appear as bright-white features (due to high reflectance) that are easily distinguished from other features. Further, landslides are also characterized by fan shape, sharp lines of break in topography and sometimes due to local drainage anomaly. Often, the toe part of the slide gives rise to a debris flow channel.

Many of the landslides identified on both PAN and PAN-sharpened LISS-III images have also been verified in the field. A total of 101 landslides of varying dimensions (180 m² to 27400 m²) were identified from remote sensing images and field surveys. Majority of landslides have an area-wise extent of 500 m² - 2000 m². Most of the observed landslides are rock slides. However, in some cases, complex types of failure are also present.

The spatial distribution of landslides in different LULC categories has been obtained (Table 4). It is observed that barren land and agriculture categories have maximum landslide densities in comparison to other categories as should be the case and water bodies and river sand categories are devoid of landslides.

Table 4. Distribution of existing landslides in different LULC categories

LULC categories	Area of LULC categories (km ²)	Percent area (%) (a)	Landslide area per category (km ²)	Percent Landslide area per category (%) (b)	Landslide Density (b/a)
Agriculture	22.3	8.8	0.053	25.0	2.84
Tea Plantation	89.1	35.0	0.052	24.6	0.703
Dense Forest	45.4	17.8	0.024	11.3	0.635
Sparse Forest	81.1	31.9	0.041	19.3	0.605
Barren Land	8.9	3.5	0.036	17.0	4.857
Habitation	6.5	2.6	0.006	2.8	1.077
Water	0.6	0.2	0.000	0.0	0.000
River Sand	0.6	0.2	0.000	0.0	0.000

Conclusions

In hilly regions like the Himalayas, particularly in the inaccessible areas due to high altitudes and ruggedness in the terrain, remote sensing images are the only available source for land use land cover mapping and monitoring. The factors influencing classification accuracy of various LULC classes in hilly areas using remote sensing data may be attributed to the presence of cloud cover, shadow, steep slopes, low sun angle and differential vegetation cover. Therefore, the approach for land use land cover classification that incorporates ancillary data from other sources has been more effective than that is based solely upon multi-spectral data from one sensor. The present study showed a reasonable improve in accuracy of LULC classification on incorporation of DEM and NDVI layers with IRS-LISS-III image. An overall classification accuracy of 91.7% and producer's accuracies for the majority of LULC classes of the order of above 90% were obtained in this case. It is also observed that the use of DEM and NDVI layers in the classification process could address the problem of misclassifications incurred due to the effect of shadow in the image and also due to the similarity in spectral characteristics of some classes such as barren lands and built-up areas in hilly regions. Hence, this study highlights the efficacy of multi-source classification to increase the accuracy of LULC classification in hilly regions like the Himalayas. However, the availability of multi-season LISS-III images would have probably provided better results.

Further, the spatial distribution of landslides in different LULC categories showed

that barren lands have the maximum landslide density, followed by agriculture land, built-up land, tea plantation area and forest cover. These results reflect the real field conditions in hilly terrains. The relationship thus obtained was later used as an input for landslide susceptibility mapping.

Acknowledgement

The authors are thankful to the Director, CSIR-Central Building Research Institute, Roorkee for granting permission to publish this paper. We are also thankful to the reviewers whose comments and suggestions helped to improve the quality of this paper.

References

1. Apan, A. A., (1997) Land Cover Mapping for Tropical Forest Rehabilitation Planning using Remotely-Sensed Data, *International Journal of Remote Sensing*, 18(5), 1029-1049.
2. Arora, M.K. and Mathur, S., (2001) Multi-source Classification using Artificial Neural Network in a Rugged Terrain, *GeoCarto International*, 16(3), 37-44.
3. Chavez, P. S. Jr., (1988) An Improved Dark Object Subtraction Technique for Atmospheric Correction of Multispectral Data, *Remote Sensing of Environment*, 24, 459-479.
4. Congalton, R. G., (1991) A review of assessing the accuracy of classifications of remotely sensed data, *Remote Sensing & Environment*, 37, 35-46.
5. Coppin, N. and Richards, I., (1990) Use of Vegetation in Civil Engineering, *Butterworths*, London.
6. Csaplovics, E., (1998) High Resolution Space Imagery for Regional Environmental Monitoring - Status quo and Future Trends, *International Archives of Photogrammetry and Remote Sensing*, 32(7), 211-216.
7. Eiumnoh, A. and Shrestha, P., (2000) Application of DEM Data to Landsat Image Classification: Evaluation in a Tropical Wet-Dry Landscape of Thailand, *Photogrammetric Engineering & Remote Sensing*, 66(3), 297-304.
8. EOSAT, (1994) Merge Process Enhances Value of Data Sets, *EOSAT Notes*, 9, 5.
9. Fisher, P. F. and Pathirana, S., (1990) The Evaluation of Fuzzy Membership of Land Cover Classes in the Suburban Zone, *Remote Sensing of Environment*, 34(2), 121-132.
10. Foody, G. M., (2002) Status of Land Cover Classification Accuracy Assessment, *Remote Sensing of Environment*, 80, 185-201.
11. Foody, G. M. and Arora, M. K., (1996) Incorporating Mixed Pixels in the Training, Allocation and Testing Stages of Supervised Classifications, *Pattern Recognition Letters*, 17, 1389-1398.
12. Foody, G. M., Campbell, N. A., Trodd, N. M. and Wood, T. E., (1992) Derivation and Applications of Probabilistic Measures of Class Membership from Maximum Likelihood Classification, *Photogrammetric Engineering & Remote Sensing*, 58, 1335-1341.
13. Frank, T. D., (1988) Mapping Dominant Vegetation Communities in the Colorado Rocky Mountain Front Range with LANDSAT Thematic Mapper and Digital Terrain Data, *Photogrammetric Engineering & Remote Sensing*, 54(12), 1727-1734.
14. Gupta, R.P., (2003) Remote Sensing Geology, 2nd Edition, *Springer-Verlag*, Berlin Heidelberg, Germany, 655p.
15. Holben, B. and Justice, C., (1981) An Examination of Spectral Band Ratioing to Reduce the Topographic Effect on Remotely Sensed Data, *International Journal of Remote Sensing*, 2(2), 115-133.
16. Janssen, L. E. Jaarsma, J. and Linder, E. van der., (1990) Integrating Topographic Data with Remote Sensing for Land-Cover Classification, *Photogrammetric Engineering & Remote Sensing*, 48(1), 123-130.
17. Jensen, J. R., (1996) Introductory Digital Image Processing: A Remote Sensing Perspective, 2nd Edition, *Prentice-Hall*, New Jersey, US, 318p.
18. Jones, A. R., Settle, J. J. and Wyatt, B. K., (1988) Use of Digital Terrain Data in the Interpretation of SPOT-1 HRV Multispectral Imagery, *International Journal of Remote Sensing*, 9(4), 669-682.
19. Mehrotra, G. S., Sarkar, S., Kanungo, D. P., Mahadevaiah, K., (1996) Terrain Analysis and Spatial Assessment of Landslide Hazards in parts of Sikkim Himalaya, *Geological Society of India*, 47, 491-498.
20. Prakash, A., Fielding, E. J., Gens, R., Genderen, J. L. van and Evans, D. L., (2001) Data Fusion for Investigating Land Subsidence and Coalfire Hazards in a Coal Mining Area, *International Journal of Remote Sensing*, 22(6), 921-932.
21. Richards, J. A. and Jia, X., (1999) Remote Sensing Digital Image Analysis: An Introduction, 3rd Edition, *Springer-Verlag*, Heidelberg, Germany, 363p.
22. Sabins, F. E., (1996) Remote Sensing Principles and Interpretations, *W. H. Freeman & Co.*, New York, US, 494p.
23. Saha, A. K., Arora, M. K., Csaplovics, E. and Gupta, R. P., (2005) Land Cover Classification Using IRS LISS III Image and DEM in a Rugged Terrain: A Case Study in Himalayas, *Geocarto International*, 20(2), 33-40.
24. Sanjeevi, S., Vani, K. and Lakshmi, K., (2001) Comparison of Conventional and Wavelet Transform Techniques for Fusion of IRS-1C LISS-III and PAN Images. In: Proceedings of ACRS 2001 - 22nd Asian Conference on Remote Sensing, 5-9 November, Singapore, 1, 140-145.
25. Saraf, A. K., (2000) IRS-1C-PAN Depicts Chamoli Earthquake Induced Landslides in Garhwal Himalayas, India, *International Journal of Remote Sensing*, 21(12), 2345-2352.
26. Selby, M., (1993) Hillslope Materials and Processes. *Oxford University Press*, Oxford.
27. Shalan, M. A., Arora, M. K. and Ghosh, S. K., (2003) An Evaluation of Fuzzy Classifications from IRS 1C LISS III Imagery: a Case Study, *International Journal of Remote Sensing*, 24(15), 3179-3186.
28. Shanmugam, P. and Sanjeevi, S., (2001) Analysis and Evaluation of Fusion Techniques using IRS-1C LISS-3 and PAN Data for Monitoring

- Coastal Wetlands of Vedaranniyam, Tamil Nadu. In: *Proceedings of the National Symposium on Advances in Remote Sensing Technology with special emphasis on High Resolution Imagery & Annual Convention of Indian Society of Remote Sensing (ISRS)*, 11-13 December, Ahmedabad, India.
29. Sharma, P. K., Chopra, R., Verma, V. K. And Thomas, A., (1996) Flood Management using Remote Sensing Technology: The Punjab (India) Experience, *International Journal of Remote Sensing*, 17(17), 3511-3521.
 30. Strahler, A. H., Logan, T. L. And Bryant, N. A., (1978) Improving Forest Cover Classification Accuracy from Landsat by Incorporating Topographic Information. In: *Proceedings of 12th Symposium Remote Sensing Environment*, Ann Arbor, Michigan, US, 2, 927-942.
 31. Welch, R. and Ehlers, M., (1987) Merging Multi resolution SPOT HRV and Landsat TM Data, *Photogrammetric Engineering & Remote Sensing*, 53(3), 301-303.



Application of GIS and Remote Sensing in Disaster Vulnerability Modeling and Management: A Representation in Coastal Kerala

Manjush Koshy¹, Aneesh Anandadas² and Jayalekshmi A.B.³

Abstract:

Advent of high resolution satellite imaging technologies has improved the efficiency and accuracy of geoinformation applications in disaster management. The use of geospatial tools and technologies is still to be explored in disaster management scenario. The Indonesian Tsunami of December 26, 2004 brought up importance of advanced crisis informatics capabilities for natural hazards management. This paper highlights the multilevel application of disaster informatics in local geographic scales using geospatial data. Appropriate tracking of evacuation routes and modes of evacuation are developed in a matrix of geospatial components. Vulnerability of lowland areas and inland water bodies that are connected to sea through the coastal fresh water tidal creeks are priority mapped. Supported by GIS softwares, thematic layers are integrated, queried and geographically analyzed to derive supportive information on hazard proneness of the coastal settlements in the area. Interpreted data is used to produce maps for assessing vulnerability of areas, rescue routes and shelters. A shortest evacuation route finder application is developed in Map Objects and VB.NET that is capable of assisting the first responders to help public in reaching the nearest evacuation shelter quickly. The paper also highlights the need of implementation of Public Participatory Geographic Information System (PPGIS) for community preparedness and mitigation activities at local level using Open Source Geographic Information System (OSGIS).

-
1. Disaster Informatics Coordinator, Centre for Advanced Remote sensing and Environmental Studies
 2. Research Associate, Ashoka Trust for Research in Ecology and the Environment
 3. Project Fellow, GML, Centre for Earth Science Studies

Introduction

Use of geospatial technologies in disaster management applications is evident from the multi-tier decision making process and participation during a disaster. The significance of the spatial components in disaster vulnerability modeling is emphasized from the hallucination capabilities of Geoinformation technologies. In a recent document published by the United Nations Development Programme (UNDP) in the Americas, a disaster is defined as 'a social crisis situation occurring when a physical phenomenon of natural, socio-natural or anthropogenic origin negatively impacts vulnerable populations causing intense, serious and widespread disruption of the normal functioning of the affected social unit'.(Wattegama, 2007). Natural disasters have their greatest impact at local level, especially on the lives of common people. As most of the populated areas in the world are situated near coasts around the world, vulnerability of such coastal settlements to disasters like storm surge and tsunami is a matter of great concern. Disaster management can be defined as the discipline and profession of applying science, technology, planning and management to deal with extreme events, that can injure or kill large numbers of people, cause extensive damage to property, and widespread distribution to society (Kreps, 1991). In developing countries, Disaster Management is limited to post-disaster recovery, rehabilitation and reconstruction. Developed countries concentrate towards disaster planning and preparedness measures which considerably reduce the overburden on post disaster activities, and also saves valuable lives. Impact of disasters on the society can be reduced by preparing communities to be more disaster resilient (Poland, 2010).

GIS is a valid tool in Disaster Management activities like Preparedness, Mitigation, Recovery, and Disaster Response (figure 1.). Most of the data requirements for disaster management are of a spatial nature and can be located on a map. GIS can be used effectively to achieve this objective. Using a geospatially linked information, it is possible to pinpoint hazard trends and start to evaluate the consequences of potential emergencies or disasters. When hazards are viewed with other map data, such as buildings, residential areas, rivers and waterways, streets, pipelines, power lines, storage facilities, forests, etc., disaster management officials can formulate vulnerability indices. More importantly, human life and other values (property, habitat, wildlife, etc.) at risk from emergencies can be quickly identified and targeted for protective action (Russ 2000). After potentially vulnerable locations are identified, risk is assessed and mitigation needs can be addressed. This process involves analysing the developments in the immediate aftermath of a disaster, evaluating the

damage and determining what facilities are required to be reinforced for construction or relocation purposes. By utilizing a geographically referenced information system, agencies involved in response can share information through databases on computer-generated maps in one location. Most disasters do not allow time to gather these resources. Geospatial tools thus provide a mechanism to centralize and visually display critical information during an emergency. This would facilitate scientists and disaster managers in creating models that would simulate trends observed in the past, present and also assist with projections for the future (Wattegama, 2007).

Crisis Informatics is an emerging field showcasing the application of information communication technology (ICT) in Disaster Management. Crisis informatics concerns with the extended social arena of disaster response which includes preparation, warning, response and recovery. Utilizing modern techniques of geo-informatics such as, Remote Sensing, GIS and GPS actions can be solicited in more systematic and precise way to respond to disasters, mitigate their effect and to make a better preparedness plans. High resolution satellite image is imperative for disaster management as it provides a cost effective solution for remote area coverage needed to support emergency preparedness efforts. Satellite image taken after a catastrophe reveals the secondary hazardous areas like low lands and creek connected water bodies near to the coast line, existing vegetation states, new access roads and vulnerable areas, settlements at risk, shelter proximity and alternative evacuation routes the settlements that need immediate attention can be located and emergency personnel can be re directed to that area. Pre disaster and post disaster images can be used for change detection and damage assessment effectively and quickly. It provides vital information to disaster managers for strategic planning.

This paper is an attempt to demonstrate the application of geospatial tools and technologies in vulnerability mapping of natural hazards including the spatial analysis of the landscapes in terms of its geographical settings and the patterns of human inhabitations. Capabilities of remote sensing and GIS as modeling tools enhances the interpretation of geographical trends and spatial patterns of risks of a natural disaster like storm surge or tsunami in a coastal scenario.

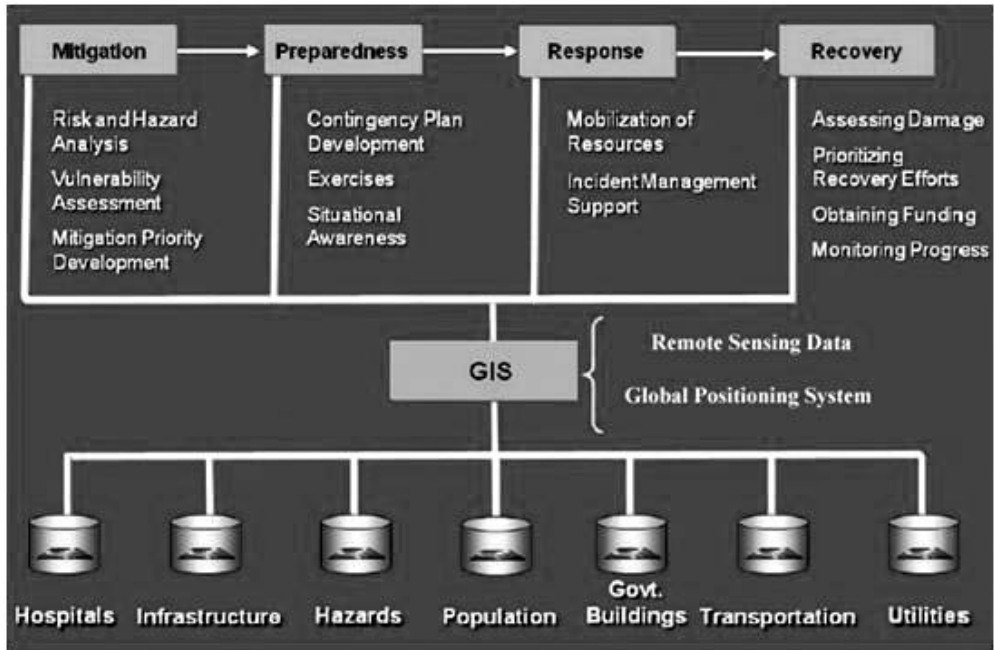


Figure 1. GIS in Disaster Management

Source: ESRI White paper May 2000

Study Area

Study area is a coastal district with vast networks of backwaters, lagoons and tertiary geological plains situated in the south western corner of Indian Peninsula. Alleppey is the smallest district in Kerala considering the area but it has the highest density of population (1492 /Sq.Km). The district has a coastline of 82 Kms (Panchayat Level Statistics 2006, Alleppey). The Alleppey municipality is full of manmade canals and bridges. The coastal wards in Alleppey municipality were selected to demonstrate the application of Geospatial technologies in disaster management. The study area lies between 9°27'46" and 9°31'19" north latitude, 76°18'41" and 76°20'05" east longitudes. It is bounded on the north by Aryad South panchayat, east by Aryad South and Punnapra North panchayats, south by Punnapra North panchayat and on the west by Arabian Sea. The Alleppey municipality at present consists of 50 wards of which 8 are coastal wards. In the 8 wards there are a total of 6150 houses which contain 29,573 people. For conducting vulnerability study of the settlements in a coastal district with very high

population density, a small area of Alleppey Municipal town with comparatively high risk with its proximity to seafront and continuous inland water body network and a lake was selected on the basis of its socio environmental settings.

Methodology

To demonstrate the application of geomatics in disaster management, a study was conducted which focuses along the coastal belt of Alleppey municipality in central Kerala. Coastal areas in Kerala are highly populated and vulnerable to maritime and climatic disasters. In this area coastal plain is undulated with sandy beach ridges and low lying swales. Inland micro wetlands which run along the plains are opened to coastline to discharge into sea. High density of population, important utilities and public installations along the coastal stretch warrants mitigative measures against natural calamities like tsunami and storm surge. With the help of QuickBird images of 0.6m resolution, high quality geospatial inventorying and mapping of disaster vulnerability of the coastal settlements is attempted. Depiction of geographical trend and spatial pattern of natural disasters like storm surge and tsunami is modulated in a geographically referenced frame work. Vulnerability mapping and risk assessment of the area includes identification of coastal locations in terms of its nature and human settlements. Appropriate tracking of evacuation routes and modes of evacuation is done in a spatial context. Locations for safe rehabilitation of the evacuated people are spatially represented. Vulnerability of lowlands and inland water bodies that are connected by creeks that are tidally active proximal to the coast line are mapped. Thematic mapping of the area from satellite data is done with perspective of disaster preparedness and response planning. The tsunami of Dec 26 2004 has already revealed its grip on the coastal dwellings of the municipality. The main concern in developing a disaster preparedness and response mapping system includes the identification of each and every settlement at risk and assigning them varying vulnerability weighthatges depending upon their proximity to the coast line, proximity to a creek or lowland area. Quick Bird images of resolution 0.6meter were used to extract the settlements, roads, water bodies, lowlands and vegetation. The Quick Bird imagery is geo-referenced using the GPS values from field observation and this geo coded image is used as the base data. Other data collected from the local bodies like cadastral maps, resource maps etc. were also georeferenced with respect to the base data using image processing software. Related non spatial databases are integrated into a common frame work. According to feature geometry, shape files are generated in GIS platform. Thematic layers are extracted from the image and location of individual households, roads, land use and the individual parcels are extracted from the Cadastral maps.

Thematic layers and cadastral datasets are integrated and geographically analyzed to derive meaningful data on vulnerability of the coastal settlements. The secondary hazard area like lowlands and creek connected water bodies near coast line are also mapped. The land use and land cover of the area was digitized using satellite image.

Using this digital database, Coastal Regulation Zone (CRZ) is demarcated; the 200m and 500m regulation lines were drawn uniformly along the coast from the High Tide Line (HTL). The Coastal Regulation Zone (CRZ) was delineated by creating a buffer of 200m from the High Tide Line (HTL) which is the No Development Zone (NDZ) and another buffer of 500m was created from the HTL as per the government of India CRZ standards. The settlements in CRZ zones were identified from image and digitized in GIS. The risk zone mapping includes identification of the settlements with high hazard vulnerability near coast line including Coastal Regulation Zones (CRZ).

The second part includes marking of evacuation routes and modes of evacuation in terms of the geographical context, air lift and supply capabilities by means of helicopters need to be used in areas that are not directly accessible after the catastrophe, two Indian Air Force using emergency landing helipads- the Police Ground and the SD college ground were identified with reference to the coast and town of Alleppey which can be used in rapid response activities operating from remote. The next is mapping locations where evacuated people can be safely kept, which include open spaces, public and community assets with sufficient capacity, situating at a safer distance from vulnerable coastline. The LEO XIII School, SDV School and the ST. Michel School were identified.

Techniques to measure vulnerability have varied according to the discipline assessing the vulnerability and "what" is "vulnerable to what". Depending on the perspective of the analysis, there can be social vulnerability (Carmen *et al.* 2003), which addresses the capacity of human populations to respond to an event.

A coastal disaster vulnerability mapping of settlements for tsunami hazard is attempted against risk of the area. Study area was divided into grids of 12.5m interval and based on these grids, different vulnerability ranks were assigned to these grids depending on criteria like presence or absence of settlements in a grid, road connectivity to a grid, coastal proximity of the grids and proximity to inland water bodies. Different index values were set to sum up the vulnerability index of the area. These ranked grids were intersected into the centroids of the grids and based on the Inverse Distance Weighted interpolation technique using the 3D Analyst extension of ArcGIS a 3D raster model is developed in GIS (figure 2).

It can be done by the assumption that grids containing features which are not settlements or any other human or living establishments can be omitted as zero

vulnerable and the 12.5 m grids containing adjacent or contiguous settlement patterns can be further included in a comparatively larger vulnerability rank. The priority will be given more to the settlements which are within 200m from the shoreline and other criterion which increases the vulnerability value is the proximity to creeks and low lying areas (figure 3). Further for this beach profile, only roads are the obstructions to tidal intrusions with reference to the local level field experience. The grids which intersect the roads and settlements in the West side will be given priority more than those which intersect grids in the East. The concentration of raster colors representing high vulnerability can be mapped as the areas which need preference in the time of information, orientation and rescue. The strategy implemented to address coastal disasters vulnerability of the settlements in the region aim to attend to emergencies rather than plan for prevention. This study will help non geospatial groups in multi dimensional visualization of vulnerability while participating and responding in a disaster scenario.

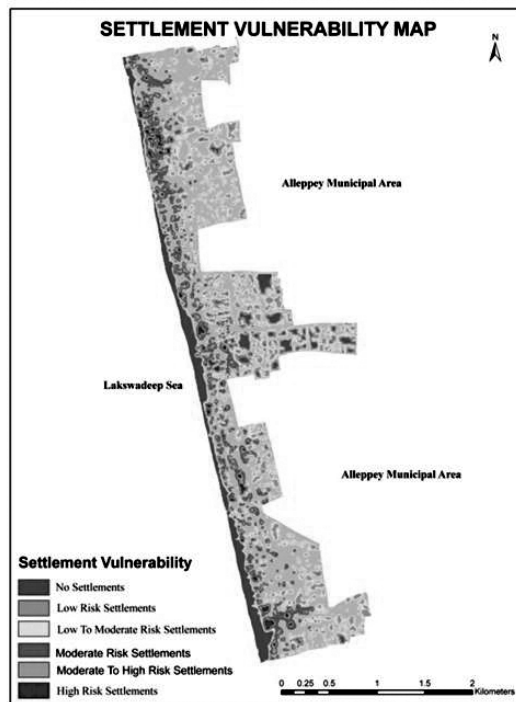


Figure 2. Settlement vulnerability map



Figure 3. Settlement vulnerability mapping using QuickBird image of 0.6m spatial resolution.

Using GIS software platform, thematic layers are integrated, queried and geographically analyzed to derive conclusive information on vulnerability of the coastal settlements in the study area. The entire road network of the municipality was digitized from quick birb imagery and was projected into UTM 43N, WGS84 coordinate system. Resultant data set was used to develop a decision support system (figure 4) using Map Objects and VB.NET which could be used by the emergency responders that provides information on the route events and shortest route to the settlement areas at risk, alternative rescue routes to the nearest evacuation shelters are associated with complete spatial control. Finding the shortest route is exceedingly important especially during a crisis situation. This system will help the first responders like police, fire force, emergency medical personnel and the local authorities during an emergency response as they might be unaware of the roads in an area. Spatially referenced accurate information allows the command and response units to work more efficiently and coordinate regional disaster response more effectively with the spatial location known and with a proper plan figured out, people will still have a chance to stand to the disaster.

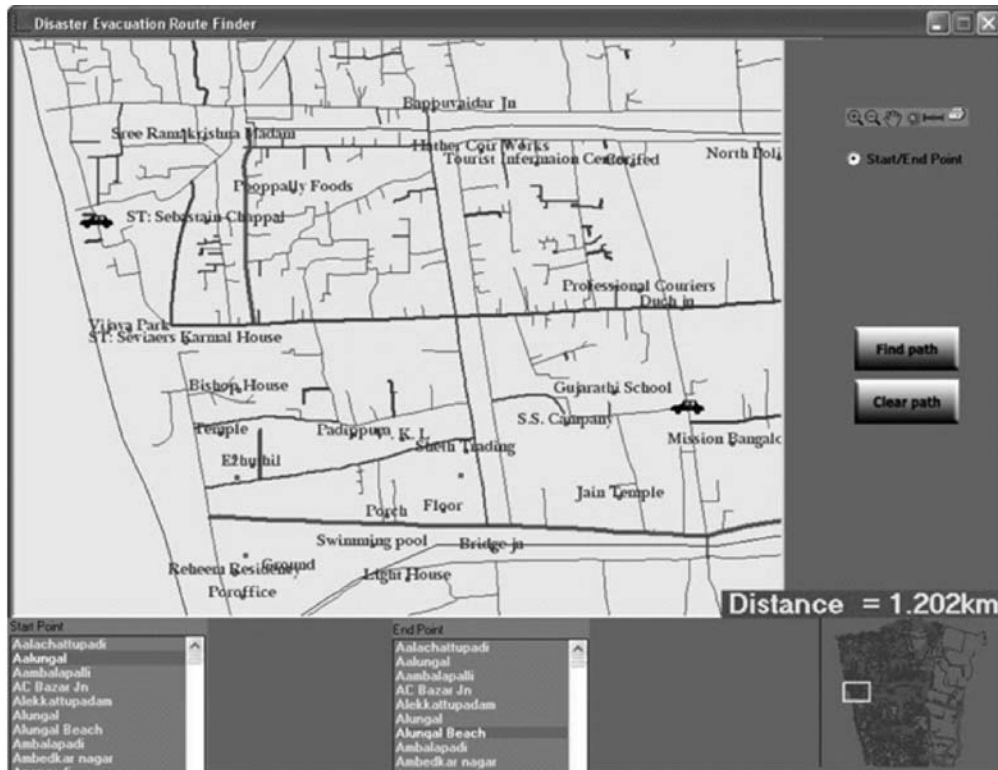


Figure 4. Shortest evacuation route finder

Results and Discussions

In many countries like India, risk analysis is limited to hazard mapping, showing areas where different levels of hazard can be expected. The available risk information is usually at too limited in spatial and temporal resolution to provide useful information on increasingly complex and dynamic risk patterns. Even where risk analysis takes into account vulnerability, this is normally restricted to the physical aspects. In most countries it is extremely rare to find risk analysis to take account of the social, economic, institutional and cultural aspects of vulnerability (Srivastava *et al.* 2004).

During the preparedness and response phases, GIS can accurately support better response planning in areas such as determining evacuation routes or locating vulnerable infrastructure and vital lifelines, etc. It also supports logistical planning to be able to provide relief supplies by displaying previously available information on roads, bridges, airports, railway and port conditions and limitations. Apart from this, activities

such as evacuee camp planning can also be done using GIS. It can also provide answers to some of the questions important to disaster management, such as the exact location of the fire stations if a five-minute response time is expected or the number and locations of paramedic units required in a specific emergency. Based on the information provided by GIS, it is also possible to estimate what quantity of food supplies, bed space, clothes and medicine will be required at each shelter based on the number of expected evacuees.

Further this paper also discusses the need for implementation of Geographic Information System (GIS) at the local level through qualified local body officials by the use of Open Source Geographic Information System (OSGIS).

Open Source GIS promotes the use of geo-information for community participation in disaster mitigation. Quantum GIS (QGIS) is free GIS software (figure 5) that supports Linux, Windows and Mac operating systems. Ward leaders could be trained in using QGIS software, the objective is to bridge the gap between several levels of local administration and common people through an extensive knowledge workshop that ensured public participation for preparedness activities by defining roles and responsibilities of community leaders and task forces which include assigning 10 houses for a team leader who in turn will be monitored by the area leader who will be reporting directly to the ward official and training task forces and above all simulation of a crisis situation to evaluate both preparedness and post disaster response effectiveness, using evacuation route print outs generated by QGIS for mock drills. Also response initiatives like relief coordination, search and rescue and first aid training should also be discussed. The local knowledge on disasters is highly important; OSGIS helps in taking technology to the common people. It suggests a way to mobilize available human and technical resources in order to strengthen a good partnership between local communities and local officials. More efforts should be made towards capacity building of local people by use of available resources. It will help in developing their own knowledge base, and to develop methodologies like public participatory GIS, that promotes activities for reducing risks in a sustainable way thereby increases disaster resilience of the community by making people think spatially there by helping them better understand the area they live in and the risk they are exposed to.

The ward leaders could be trained in using Quantum GIS (QGIS) software. The objective was to bridge the gap between several levels of local administration and common people through an extensive knowledge workshop that ensured public participation for preparedness activities. Greater efforts should be made to strengthen the capacity of local people for developing their own knowledge base, and to develop

methodologies like Public Participatory Geographic Information System (PPGIS), that promote activities for reducing risks in a sustainable way which results in community capacity building.

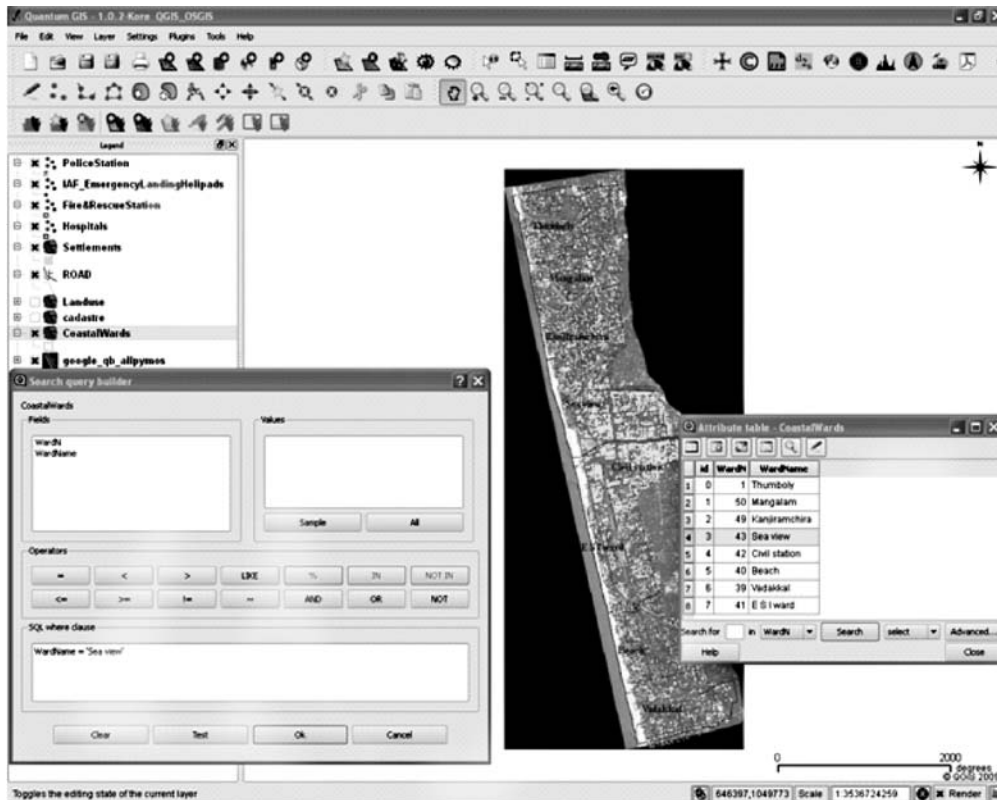


Figure 5. Use of OSGIS for Public Participatory Preparedness Initiatives

Conclusion

This study gives an idea on the advantage of using high resolution satellite imagery in disaster management; the 0.6 m resolution QuickBird imagery is extremely valuable as a means of providing local level and large scale mapping capability in disaster management. The present study delineates the purpose of an assessment of the area during a coastal disaster like storm surges or tsunami, with special preference given to early evacuation routing and community preparedness and an information system developed in GIS platform. The ultimate aim of this study is to achieve the task-specific

delivery of geographic information to those in the field who are actually facing or responding to a disaster. The quality and timeliness of response services during a disaster can be improved using this system. Use of OSGIS is a cost effective method for local level community preparedness and public participatory geographic information sharing, it can be used for organizing mock drills and community preparedness plans, GIS makes people think and act spatially. Accurate information allows the command and response units to work more efficiently and coordinate regional disaster response more effectively with the spatial location known and with a proper plan figured out, people will still have a chance to stand to the hazard. Disaster management plans are to be integrated within the mainstream planning and development activities of local authorities and GIS needs to be deliberately infused into these activities for a better disaster resilient society. The local authorities can develop a crisis informatics unit by implementing this methodology and can make this system available to other local bodies and by equipping these units with the best technology and crisis informatics available, a high standard of State disaster response team could be developed in a responsible manner.

References

1. Kreps GA (1991) Organizing for Emergency Management. International City Management Association, Washington Conference.
2. Russ Johnson, 2000. GIS Technology for Disasters and Emergency Management. An ESRI White Paper.
3. Carmen Lacambra S, Iris Moller and Tom Spencer, 2003. The Need for an Ecosystem-Inclusive Vulnerability Index for Coastal Areas in Colombia.
4. Sanjay K Srivastava, VS Hegde and V Jayaraman, 2004. Community Centric Approach of Geo-informatics for Disaster Risk Reduction, GIS Development.
5. Chanuka Wattedgama, 2007. ICT for Disaster Management (UNDP-APDIP).
6. Poland, C.D. Commentary on Building Disaster Resilient Communities. Journal of Disaster Research Vol.5 (2) 2010.

Accuracy Aspects in the use of GPS Technology for Geoinformation System

S. K. Katiyar

Abstract

In the process of rescue operations and assessment of damage to a specific location during natural and man-made disasters; maps play an important role. The developing countries like India have seen the rapid urbanization and unplanned growth of cities and this requires fast updating of various type maps related to land use. In various applications an up-to-date map is essential and modern mapping tools like remote sensing satellite images and Global Positioning System (GPS) are proving reliable and fast techniques in the development, management and analysis of Geo information system.

This research paper investigates the accuracy of hand-held L1 frequency GPS receivers (Magellan Sport track and Leica GS5). Different linear and aerial features in the study area have been digitized using hand-held GPS receivers. Accuracy of the above digitized features were determined by comparing the corresponding feature dimensions extracted from Indian Remote Sensing satellite (IRS-P6) LISS-IV sensor images and Leica make Total Station based measurements. The investigation results have shown that even a single frequency hand-held GPS in the stand-alone mode could provide planimetric accuracy in the range of 3 to 6 m. This makes the GPS a very quick and reliable tool for surveying tasks related to medium scale plannimetric map database in the development of Geo information System.

Introduction

Maps have an important role in the development and planning process and these are basic components of Geo information System. In the construction of any small or big

Associate Professor, Civil Engineering Department, Maulana Azad National Institute of Technology Bhopal (M.P.) - 462051 Email- skatiyar7@rediffmail.com

project, information about the topography and land use of the site is very essential and this requires an up-to-date base map of that area (Clavet, 1993). Because of rapid urbanization in the developing countries like India, maps require frequent updating. In the many regions of the world, the large-scale topographic maps do not exist and it is necessary to carry out surveying field work for specific application (Cook and Pinder, 1996; Kardoulas *et al.*, 1996). The map data capture using conventional methods takes longer time and some alternative quick and reliable method is desirable (Katiyar, 2003).

Modern surveying equipments such as robotic total station, electronic distance measurements (EDMs) and digital and laser levels have replaced traditional surveying equipments. The main advantage of these equipments is the automation of map making process, using computer interface and high accuracy. The developments in space technology and electronic industry have given the new dimensions to the map data collection methods. The high-resolution remotely sensed imagery are playing a major role in the mapping and cartography. In order to use the remote sensing satellite images as base map, its geo referencing is essential and this process requires attaching of precise coordinates of some selected landmarks.

The most significant development of the twentieth century for the navigators was the development of the Global Positioning System (GPS) by the U.S. Department of Defence (DOD) and known as NAVSTAR (Navigation System with Time and Ranging). Civilian users quickly realized the potential for survey positioning and began using these experimental satellites to perform surveys, in spite of inconvenience as viewing times and uncertainty of signal availability (Satish Gopi, 2005). GPS can provide an alternative to the ground control survey methods for the poorly mapped areas, which could not be mapped using conventional methods and during natural calamities. Differential mode of GPS known as DGPS has the capability of providing very precise position of any point up to centimeter level accuracy (Hofmann-Wellenhof *et. al*, 1993). GPS has increased tremendously the application potentials of the remotely sensed images (Thapa and Bossler, 1992; Katiyar, 2003).

GPS technology has got diversified applications not only in mapping but also in precise time determination, vehicle tracking, navigation etc. After termination of selective availability (SA) of GPS signals, the hand-held GPS accuracy has improved considerably and various possibilities for the cost-effective use of GPS technology have emerged. The GPS technology could prove to be very useful in the infrastructure development and utility mapping. In the age of information and space technology, GPS could provide variety of mapping data inputs in a very short time with the desired level of accuracy, which could be directly used in the software for the map plotting and

developing the Geo information System database. This research paper focuses for developing an understanding on the accuracy aspects of GPS technology, in preparing the geo information database in a cost-effective manner.

GPS Principle

The GPS receivers calculate position of the station occupied on the basis of well-known resection principle of surveying (Schofield, 2001). If the three-dimensional position of three control stations are known, and their distances (R1, R2 and R3) to an unknown station are given, then it is possible to calculate the three-dimensional position of the unknown station as shown in figure-1. In GPS control stations are satellites whose positions in the orbit are precisely known. Positioning and navigation is done by GPS receivers with the help of time-coded transmission from satellites (Katiyar *et al.*, 2002). The three-dimensional position of the ground station carrying an accurate clock can be determined if three satellites are visible simultaneously. However the clock used by receiver on the ground is normally less accurate (Kaplan, 1996). Because of non-synchronization of two clocks, the calculated distance to a satellite is not exact and is therefore called pseudo-range (R) given by following relation

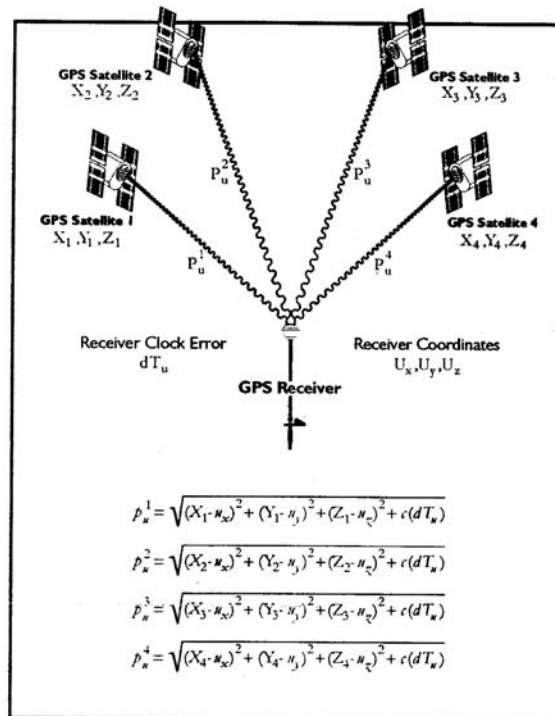


Fig1. Global Positioning System Principle (Sickle, 2001)

$$R = C(T_t - T_r) + \frac{C \cdot A}{F^2} + T$$

Where,

C - speed of light

T_t - GPS signal transmission time

T_r - GPS signal receiving time

A - constant relating to the electron density of ionosphere

F - GPS signal frequency

T - Excess path length due to troposphere

The clock bias is a systematic error which can be determined if information from a fourth satellite can also be obtained. After knowing P_1 (three-dimensional position) and RI (pseudo-ranges) from four satellites, we can uniquely solve for four unknowns which are position (X,Y, Z) of ground station and clock bias which will yield true clock time for the receiver. In the navigation mode, Doppler principle is used for the determination of instantaneous velocity of GPS receiver.

In general, GPS receivers can be divided in to two broad categories, single frequency and dual frequency receivers. The dual frequency receivers are costly, while the single frequency receivers are very cheap (costing around Rs. 15,000/-). The GPS receivers provide observations in two different modes stand alone and differential mode (DGPS) as shown in figure-2. After the termination of the selective availability (SA) of the GPS signals the accuracy of GPS measurements even in the stand-alone mode, using single frequency receivers has increased considerably (Katiyar et. al, 2002; Sateesh Gopi, 2005).

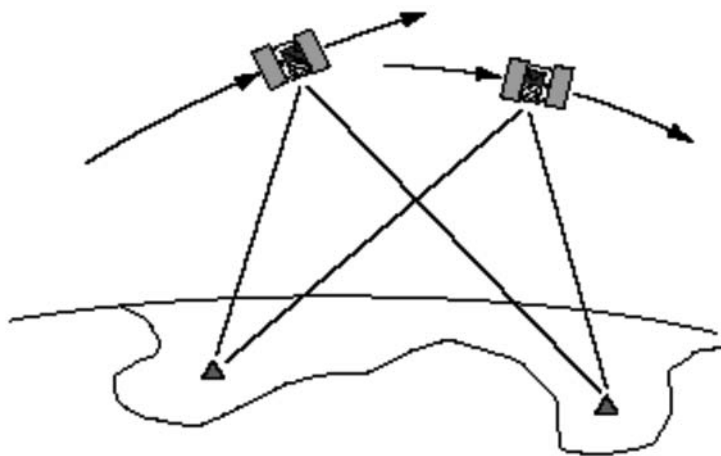


Fig 2. DGPS observation technique (Leica, 2000)

Error Sources in GPS Measurements

There are several sources of error that degrade the GPS positioning accuracy (Hofmann-Wellenhof, 1993; Kaplan, 1996; Leica, 2000). The main error sources are summarized here

Ionospheric and Atmospheric Delays

The GPS satellite signal is slowed down as it passes through the ionosphere. This action is similar to light refraction through a glass block. At night there is very little ionospheric influence and signal quality is better as compared to day time. The ionospheric errors are mitigated by using DGPS measurements.

Satellite and Receiver Clock Errors

The GPS satellite clocks are very accurate (about 3 nano seconds), but sometimes they may drift slightly. This drift in time will cause small errors, and affects the positional accuracy. Any drift in timing is corrected from GPS satellite control stations. The GPS receivers are fitted with quartz clocks, hence its time measurements are less precise and result the receiver clock errors.

Multipath Errors

Interference caused by reflected GPS signals arriving at the receiver, typically as a result of nearby structures or other reflective surfaces as shown in figure-3 is known as multipath error. Signals traveling longer paths produce higher (erroneous) pseudorange estimates and consequently positional errors.

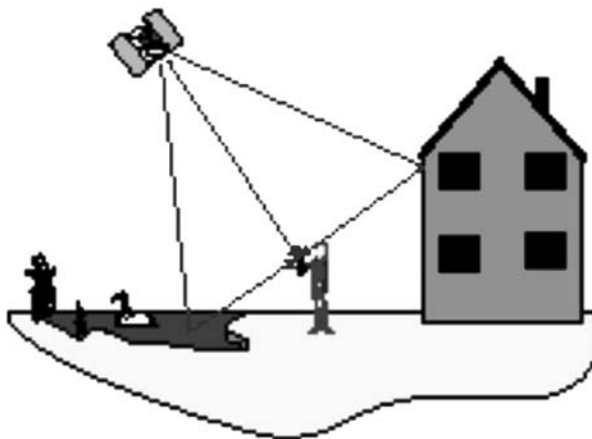


Fig 3. Multi-path errors in GPS observations (Leica, 2000)

Dilution of Precision (DOP)

The dilution of precision (DOP) is a measure of the strength of satellite geometry or a description of the geometrical contribution to the uncertainty in a position fix. This number is somewhat similar to the strength of figure in the triangulation survey (Schofield, 2001).

Selective Availability (SA)

The U.S. Department of Defence (DOD) employs a method of GPS signal degradation that limits the precision with which the C/A code may be used in navigation and positioning. This technique is called Selective Availability. The DOD can presumably control this distortion by algorithms (describing this distortion), which are available in military type receivers. The SA has been put off since May 2000.

Datum Transformations

The old series of topographic maps prepared by Survey of India (SOI) uses Everest ellipsoid, while GPS system uses WGS-84 ellipsoid. The parameters of these two ellipsoids are appreciably different and given in the (table-1). If proper attention is not given on these aspects, then a large amount of error will be introduced in the GPS observed coordinates.

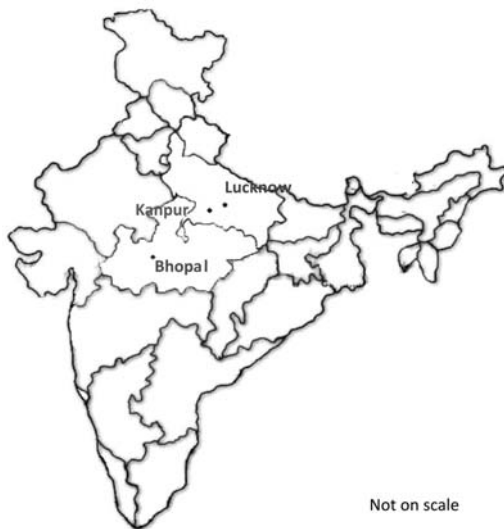


Fig 4. Study area location map

Investigations

This research work presents investigations pertaining to the accuracy of a hand-held GPS receivers of Leica (GS5) and Magellan (Sport track) make in autonomous mode, by making observations at well-distributed stations in the cities Kanpur, Lucknow & Bhopal (figure-4). The investigations of this work were carried out on two different aspects, the accuracy of coordinates observed with a hand-held GPS receiver and difference of Indian datum and corresponding WGS-84 datum coordinates of various study area control points.



Fig 4(b). False color composite of Bhopal city and nearby area generated from IRS-1D, satellite LISS-III sensor imagery



Fig 4(c). False color composite of Kanpur city and nearby area generated from IRS-1D, satellite LISS-III sensor imagery



Fig 4(d). False color composite of Lucknow city and nearby area generated from IRS-1D, satellite LISS-III sensor imagery



Fig 4(e). GCP's marked on the IRS-1D, satellite PAN sensor imagery of Bhopal city

Eight different stations were established at IIT Kanpur campus and various date and time observation were recorded for a period of about one month, in order to establish the average coordinates of the stations. The standard deviation of the measured planimetric coordinates and heights for these stations are shown in figure-5. These distances were measured with the help of Total Station instrument as well as on the geo referenced IRS-P6 satellite images of LISS-IV sensor. The discrepancy between observed distances using hand-held GPS and Total Station measured are shown in the figure-6.

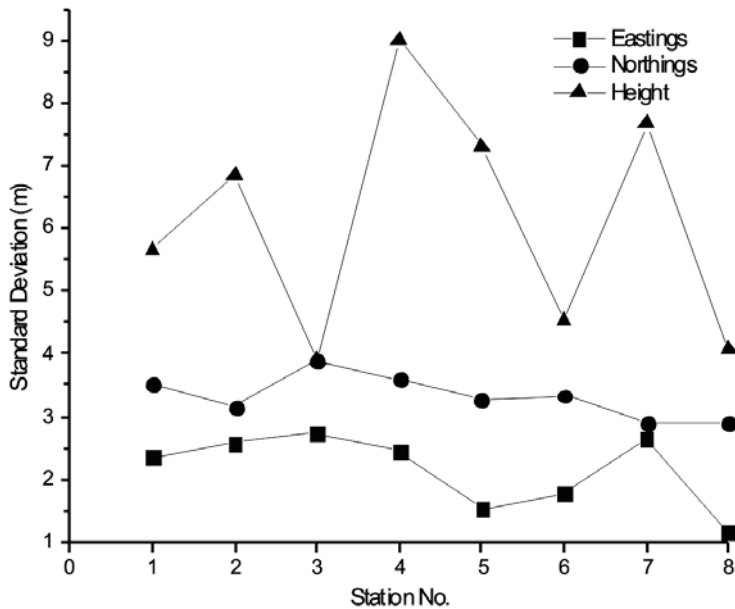


Fig 5. Standard deviation of GPS observed coordinates: eastings, northings and height above ellipsoid (H) at different stations.

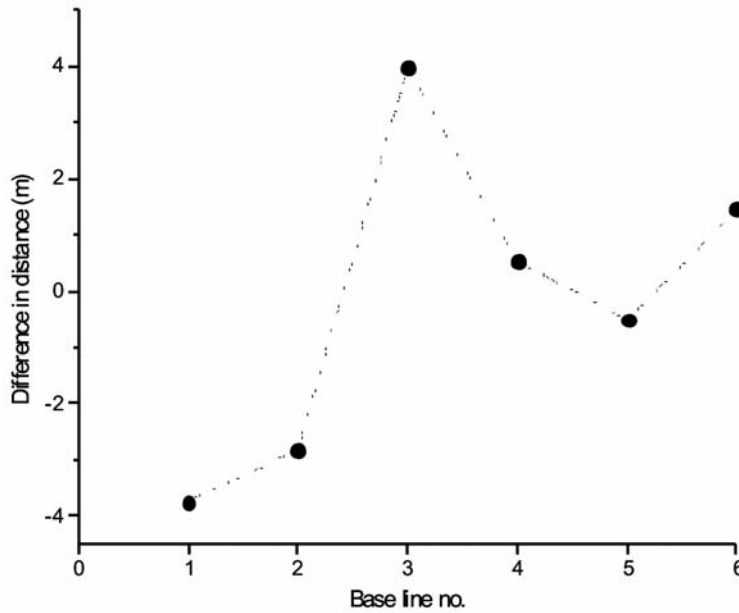


Fig 6. Difference in GPS measured and total station measured distances between different stations

For the analysis of offset between Indian and WGS-84 datum coordinates different GCPs like road and railway line intersections were selected and their coordinates were measured. These WGS-84 ellipsoid GPS observed coordinates were also compared with the corresponding Indian datum coordinates read on the 1:50,000 scale Survey of India topo sheets for the Bhopal, Lucknow and Kanpur cities and difference between these two values for 15 numbers of stations are shown in the table-2.

Table 1. WGS 84 and Everest (India 1956) ellipsoid parameters (NIMA, 2000)

Details of parameter	WGS-84 ellipsoid	Everest ellipsoid
Semi-major axis (a)	6378137.0 m	6377301.243 m
Flattening (f)	1/298.257223563	1/300.8017
Angular velocity of Earth (ω)	$7292115.0 \times 10^{-11}$ radian/s	Not available
Earth gravitational constant (GM)	$3986004.418 \times 10^8 \text{ m}^3/\text{s}^2 \pm 0.1 \times 10^8 \text{ m}^3/\text{s}^2$	Not available

Table 2. Difference between WGS-84 datum and map derived Indian datum planimetric coordinates for the study sites

GCP No.	Bhopal 1:50,000 scale map		Kanpur 1:50,000 scale map		Kanpur 1:25,000 scale map		Lucknow 1:50,000 scale map		Lucknow 1:25,000 scale map	
	$\Delta\phi$ (s)	$\Delta\lambda$ (s)	$\Delta\phi$ (s)	$\Delta\lambda$ (s)	$\Delta\phi$ (s)	$\Delta\lambda$ (s)	$\Delta\phi$ (s)	$\Delta\lambda$ (s)	$\Delta\phi$ (s)	$\Delta\lambda$ (s)
1	-3.54	3.76	-1.41	5.06	-1.31	6.05	-1.26	7.34	-1.54	7.97
2	-2.76	4.03	-2.37	5.87	-1.21	6.58	-0.54	6.61	-0.74	5.11
3	-0.99	5.66	-0.92	7.59	1.67	7.18	-0.50	7.44	-1.09	5.57
4	0.53	3.32	-0.06	6.06	-1.60	7.97	-1.28	7.19	-1.69	5.15
5	-1.67	3.62	-3.93	5.99	-0.90	6.17	-0.57	8.29	-1.33	6.01
6	-0.86	4.54	-3.07	5.88	-0.06	6.11	-1.14	6.90	-0.72	5.14
7	-1.61	3.95	-0.06	6.87	-0.41	4.35	0.04	7.41	-0.32	5.55
8	-0.53	2.49	-0.34	6.14	0.16	6.90	-0.20	7.22	-0.25	5.73
9	-0.49	2.54	-0.68	6.39	-0.98	6.01	-1.07	8.51	-1.63	6.27
10	-0.53	4.64	-1.19	6.41	-0.46	5.16	0.52	6.30	-0.57	4.76
11	-1.27	2.90	-0.15	6.39	-0.74	5.11	0.22	6.99	-0.38	4.88
12	-2.36	3.72	-1.42	6.03	-1.69	6.71	-0.73	7.50	-0.53	5.40
13	-1.23	3.43	-1.36	8.03	-0.12	6.96	-0.57	6.01	-0.09	5.96
14	-1.18	4.01	0.55	6.07	1.13	6.94	-1.77	5.99	-1.98	4.85
15	-1.07	4.55	-1.47	5.37	-1.58	6.79	-0.77	6.93	-1.23	5.98

$\Delta\phi$ Latitude difference

$\Delta\lambda$ Longitude difference

s Seconds

Conclusions

Based on the investigations of present research work, following conclusions are drawn:

- Map derived GCP coordinates should not be used for the geometric correction of modern age high-resolution images from IRS-1C/1D, IRS-P6 or any other high-resolution sensor. The GCP coordinates collected from hand-held GPS receiver would suffice the sub-pixel accuracy requirements even for IRS sensor PAN images.

- Averaging of a number of repeated GPS observations at the same station using hand-held GPS receiver can provide the accuracy in the range of 3 to 6 meters and this is appropriate for so many applications in the development of Geoinformation system database.
- In the use of GPS data, the non-availability of transformation parameters between WGS-84 and Indian datum is a big problem at least for civilian users.

References

1. Clavet, D., Lassere, M. and Pouliot, J., 1993, GPS control for 1:50,000 - scale topographic mapping from satellite images. *Photogrammetric Engineering and Remote Sensing*, Vol. 59, No. 1, pp. 107-111.
2. Cook, A. E. and Pinder III, J. E., 1996, Relative accuracy of rectifications using coordinates determined from maps and the global positioning system. *Photogrammetric Engineering and Remote Sensing*, Vol. 62, No. 1, pp. 73-77.
3. Hofmann-Wellenhof, B., Lichtenegger, H. and Collins, J., 1993, *Global positioning system: Theory and practice*. III edition, Springer-Verlag Wien, New York.
4. Kaplan, E. D. (ed.) 1996, *Understanding GPS- Principles and applications*, 1 edition, Artech House, London.
5. Kardoulas, N. G., Bird, A. C. and Lawan, A. I., 1996, Geometric correction of SPOT and Landsat imagery: A comparison of map- and GPS-derived control points. *Photogrammetric Engineering & Remote Sensing*, Vol. 62, No. 10, pp. 1173-1177.
6. Katiyar, S.K., 2003, geometric correction of IRS-1C/D satellite imagery. *Ph.D. thesis*, Deptt. Of Civil Engineering, I.I.T. Kanpur.
7. Katiyar, S.K., Dikshit, O. and Kumar, K., 2003, GPS autonomous mode for satellite imagery geocoding: Benefits of low-cost hand-held GPS, *GIM International*, Vol. 17, No. 6, pp. 29-31.
8. Katiyar, S.K., Dikshit, O. and Kumar, K., 2002, GPS for the geometric correction of remotely sensed imagery: Possibilities after termination of SA., *Proceedings of The Asian GPS Conference*, CSDMS, New Delhi, 24-25 October, 2002., pp.57-62.
9. Leica, 2000, GPS operation manual. Leica Geosystems, Switzerland.
10. NIMA, 2000, World Geodetic System 1984; its definition and relationships with local geodetic datums, National Imagery and Mapping Agency Technical Report 8350.2, 3rd edition, US Department of Defense Washington DC. (For WGS-84 parameters and ellipsoid offsets)
11. Sateesh Gopi, 2005, *Global Positioning System: Principles and Applications*, Tata McGraw-Hill Publishing Company Limited New Delhi.
12. Schofield, W., 2001, *Engineering Surveying: Theory and Examination Problems for Students*, 5th edition, Butterworth Heinemann, Oxford.
13. Sickle, Jan Van, 2001, *GPS for Land Surveyors*, 2nd edition, Ann Arbor Press, Chelsea, Michigan.
14. Thapa, K. and Bossler, J., 1992, Accuracy of spatial data used in geographic information systems. *Photogrammetric Engineering and Remote Sensing*, Vol. 58, No. 6, pp. 835-841.

GIS-based slope stability evaluation of a landslide complex – case study from Paglajhora, Darjeeling Himalaya, India

Saibal Ghosh*, Niroj K. Sarkar
and Chinmoy Paul

Abstract

Detailed mapping (1:5000 or larger) along with finer-resolution (1 m X 1 m pixel) deterministic stability assessment are pre-requisites to understand the behaviour of any active and complex landslide. Geological mapping of the affected slope is the first step towards any such stability assessment which provides fundamental inputs about slope parameters such as morphometry, type and nature of slope forming material (both rock and overburden), geometry of probable failure surface, past landslide movements, their failure modes/mechanisms, hydrological situation, anthropogenic interferences and land cover, etc. Through detailed geological mapping of above said parameters, probable causal mechanisms involved during the temporal evolution of the slope are ascertained. These thematic maps and related information are used by the planners/geotechnical engineers to understand the slides and design appropriate protective structures in consultation with geologists.

This paper deals with the detailed geological mapping of a large and complex landslide carried out in Darjeeling Himalaya (Paglajhora) revealing various critical slope parameters and relevant geological characteristics, which were subsequently used for the evaluation of the slide and applied as a vital input for the GIS-based stability assessment of the slide complex. Pixel-wise factor of safety (F_s) under three hypothetical saturation conditions were calculated using slope parameters from map and determined shear parameters of representative insitu slope-material. The above stability model confirmed substantial portion of stable slopes ($F_s > 1.7$) under dry condition becoming unstable ($F_s < 1.0$) under various increasing saturation conditions. Under dry condition, only 25% of slope was potentially unstable, which increased up to 51% and 65%, respectively, under

Engineering Geology Division, Geological Survey of India, Kolkata, India, DK-6, Sector - II, Salt Lake, Kolkata - 700091
(Corresponding author: Saibal Ghosh* mail_id: ghosh@itc.nl)

intermediate and total saturation conditions. This stability modeling could be more effective with use of measured depth-to-failure surface, pore-water condition, and larger spatial variability of the determined shear parameters.

Introduction

Deterministic slope stability models are primarily based on determination of physically-based shear parameters of potentially-failing material and developing an insitu hydrological model for subsequently using both the determined physical and hydrological parameters for the calculation of slope instability indicators such as Factor of Safety or F_s (van Asch, 1992). The F_s value is a quantitative measure representing the ratios between resisting force and the sliding forces. The same is used as a metric to classify topographic slope as per their inherent instability. Application of this model for a large landslide complex needs to apply the same in a spatially-distributed manner and preferably be determined in a GIS platform, which always remained to be a challenge to the researchers, since, 2-D or 3-D deterministic techniques using compatible hydrological models are always mathematical complex and has an inherent limitation to use in 2-D GIS environment. One of the simplest ways to execute this application within a GIS is to prepare boundary conditions for a one-dimensional infinite slope model, where by considering some basic assumptions, F_s values at each unit of study or grid-cell can be determined. The above stability calculation can also be carried out outside the GIS, but reproducing the results of such distributed deterministic stability models again onto a map sometimes are problematic due to incompatibility in the data formats of the two systems (Terlien *et al.*, 1995). Therefore, it is always preferable that for distributed deterministic analysis, we attempt to employ the entire stability calculation inside the GIS system through incorporating mapped features representing topography (slope), material properties from geological attributes and from spatially-distributed thematic layers representing physically-determined different shear parameters.

In this paper, a GIS-based method is presented where detailed-scale geological and topographic mapping of a large landslide complex in Darjeeling Himalaya was used as the primary source information of various input parameters for a spatially-distributed deterministic slope stability model. For this, the simple one-dimensional infinite slope model was applied and predictive F_s maps under three hypothetical ground saturation scenarios were generated. Scenario-based deterministic stability analysis performed using the above method quantitatively delineated how the extents of instability increase with increase in ground saturation. Application of this model also revealed the inherent

limitations of the model and recommends further for incorporation of more site-specific physically-determined hydrologic and shear parameters as model variables to improve the performance of stability calculation.

Study area, topography and geology

Paglajhora slide complex, located south of Kurseong town in between 35 Km and 41 Km stretches of National Highway -55 (NH-55) has been reported to be an active subsidence and slide zone since more than the last five decades (Fig. 1). This slide complex has severely affected the above-mentioned national highway (the road leading to Darjeeling town from Siliguri) in between Gayabari - Mahanadi (Lower Paglajhora) and Mahanadi - Giddapahar (Upper Paglajhora) sectors for a cumulative length of about 3 Km (cf. Fig. 2). The NH-55 passes through this slide complex both along lower level (*m.a.s.l.* 1130 m to 1190 m) and along upper level (*m.a.s.l.* 1280 m to E.L. 1335 m) (cf. Fig. 1).

Paglajhora slide is located within the upper catchment areas of Shiva nala (cf. Fig. 1), a southerly-flowing tributary Mahanadi river. The entire slide complex has numerous prominent and discontinuous active to dormant rock as well as debris scars, which has been activated during a number of landslide events spread over a temporal period of six decades. The slope is mainly drained by Paglajhora (a local name for the

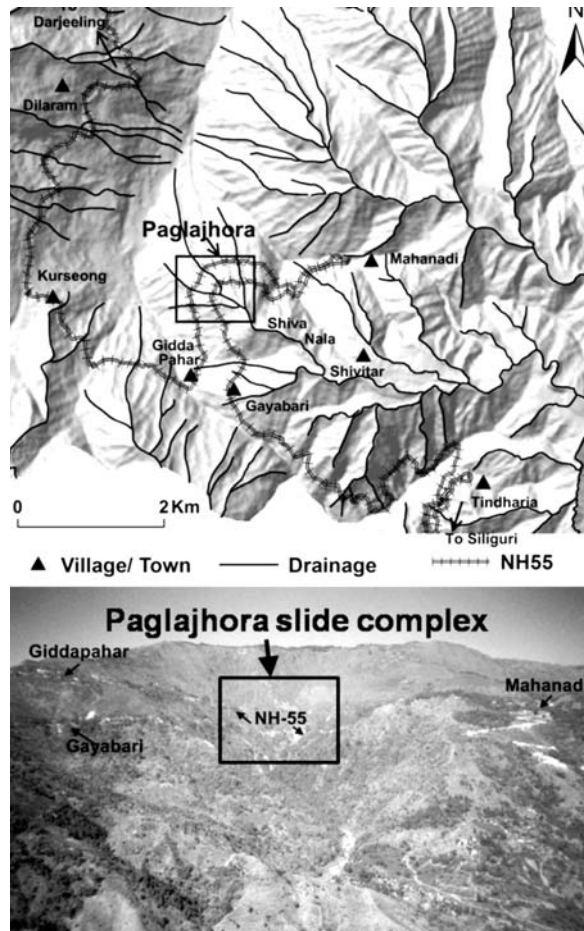


Fig 1. Location map and field photograph of Paglajhora slide complex.

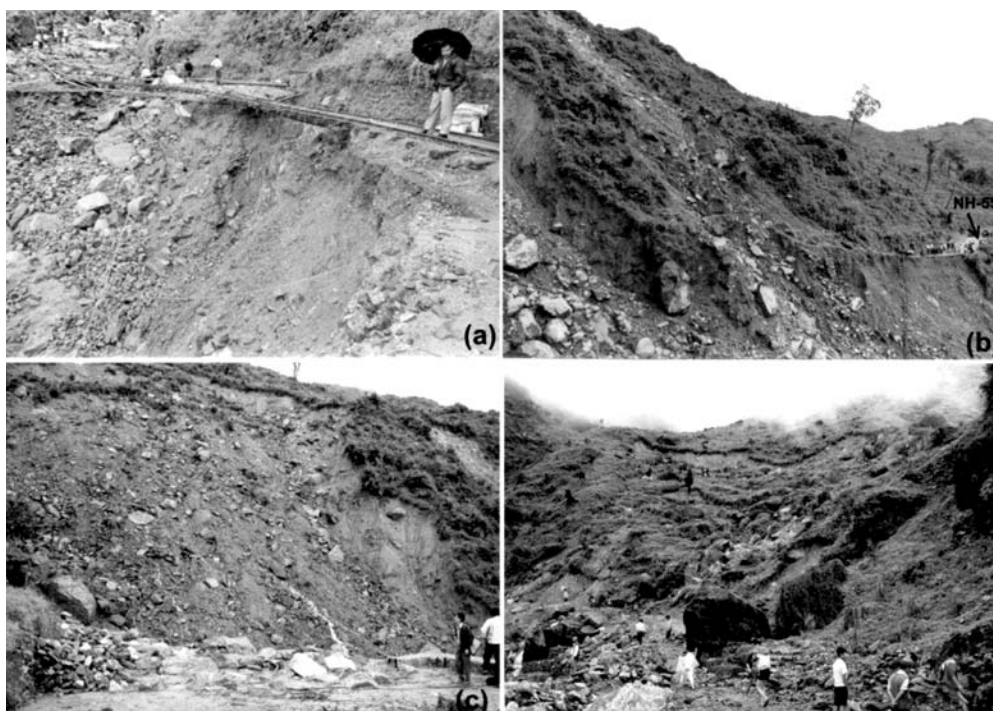


Fig 2. Field photographs of different fresh and active landslides within upper and lower sections of Paglajhora slide complex (examples are from 1998-landslide event): (a) & (b) Complete damage of rail-road bench of NH-55 in the Lower Paglajhora section, (c) A shallow translational debris slide in Upper Paglajhora section, and (d) Failure and subsidence of the left bank slope of Pagla nala (Lower Paglajhora Section)

main lower order tributary of Shiva nala) and other numerous SE-ly to southerly flowing tributaries of Shiva nala. Locally, the top part of the slide complex is moderately steep-to-steep and the middle part is gentle followed by moderately steep to steep lower part near the banks of Shiva nala. The NE part of the slide complex is bounded by a steep south-westerly sloping rocky spur (cf. Fig. 3 a). Similarly, towards SW, exposed rocky stratum marks its southern boundary. The area around Paglajhora slide is mainly traversed by exposures of fresh to weathered quartzo-feldspathic gneiss of Central Crystalline Gneissic Complex (CCGC) (cf. Fig. 3 a). Along the left bank of Pagla Jhora within the middle slope, highly sheared and weathered gneiss is exposed in the middle part of the slide. Towards south, a sheared and fractured phyllonitic rocks are exposed

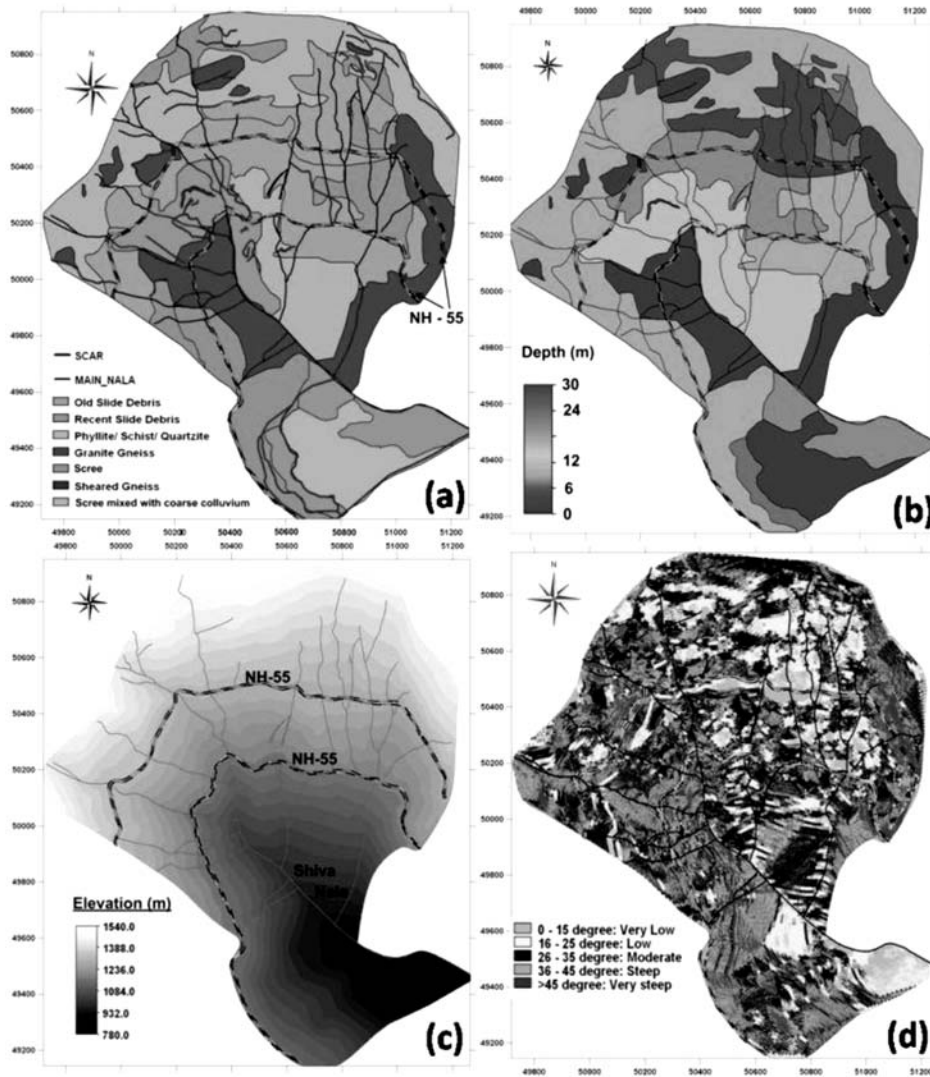


Fig 3. Different mapped themes of the Paglajhora slide complex: (a) Map showing distribution of different lithology (both bedrock and overburden), including other mapped elements such as active rock and debris scars and NH-55, (b) Interpreted depth to bedrock map, (c) 1 m X 1 m resolution DEM and (d) Classified slope map, prepared from DEM.

adjacent to highly-fissile schists and fractured quartzites of Daling Group are exposed. It is inferred that the Main Central Thrust (MCT) probably is passing along the basal part of sheared phyllonite that is along the southern-most boundary the main Paglajhora slide complex. At this location, within Paglajhora slide complex, a very active deep-seated retrogressive rock slide is present, which is locally called as "14 Mile Slide". Since the rockmass of this area is highly folded, wide variation in the attitudes of the pervasive planar fabric i.e. the foliation plane has been observed. In general, the foliation planes strikes N40°-70°E with dips 30°-50° NW (askew within the hill). But foliation planes having attitudes N55°-80°W/30°-40°NE has also been observed towards the eastern arm of the Paglajhora slide. Apart from foliation-parallel joint, the rockmass is traversed by at least 4 sets of continuous, rough planar steep joints are present. The joints are dipping towards WNW, SSE, NNE and East respectively.

Material and methods:

To document the geological and morphometric attributes of the Paglajhora landslide complex, different surface features were mapped in 2006 on detailed scale (1:2000) using Total Station Surveying Instrument (cf. Fig. 3). During detailed geological mapping, all such mappable elements on ground such as different rock outcrops with prominent structural orientation data, boundaries of different overburden materials, rock and debris scars and all the protection structures such as contour and stepped chute drains, protection wall and road were surveyed and documented. All these mapped elements were later used to generate different derived geofactors theme layers in a GIS for stability analysis (e.g. Fig. 3 b & d). During detailed scale geological mapping, for understanding the slope morphometry, spot elevations (in m) at closer interval were recorded from the entire mapped area of the slide complex, which, were later used to generate a digital elevation model (DEM) with 1 m x 1 m grid scale resolution (cf. Fig. 3 c) using open source GIS software ILWIS 3.x. This DEM was used to calculate further the slope (Fig. 3 d), aspect and relative relief rasters using open source GIS software ILWIS 3.x to understand the slope morphometry in detail of the entire slide complex.

In this research, an attempt has been made to create the quantitative slope stability or distributed F_s maps of Paglajhora slide complex using a simple one-dimensional slope stability model (the Infinite Slope model) under a raster-based GIS environment (cf. Terlien *et al.*, 1995; Soeters and van Westen, 1996). As input data, shear parameters of insitu samples (C & ϕ) from overburden material and data of detailed-scale (1:2000) geological map (e.g. lithology) and other interpretative parametric maps (e.g. depth) of Paglajhora Slide area were used simultaneously to generate a number of derived

thematic layers based on the distribution of different shear parameters of varying overburden material. The above derived thematic maps were later directly used in a GIS for calculation of F_s values for each grid-cell of the mapped area. In this research, the above raster-GIS-based deterministic slope stability analysis was carried out using open source GIS software ILWIS 3.x Software (cf. van Westen, 1993).

Deterministic slope stability analysis:

For preparation of the quantitative stability model, the degree of instability is determined quantitatively for each pixel by calculating the Factor of Safety (F_s), which is the ratio between the forces that make the slope fail and those that prevent the slope from by using the following the basic stability equation (cf. van Westen, 1993).

$$F_s = \frac{C + (\gamma - m\gamma_w)z \cos 2\beta \tan \phi'}{\gamma \sin \beta \cos \beta}$$

Where, C = Cohesion, γ = Unit weight of soil, $m = Z_w/Z$, Z_w = Height of the water table above failure plane, Z = Depth of failure plane below ground surface, β = topographic inclination ($^\circ$) and ϕ' = Effective angle of shearing resistance.

To apply the above one-dimensional slope instability model, it was assumed that most of the slides of Paglajhora areas are translational in nature (Fig. 2). The depths of probable failure surfaces are considered to be the depths to the bedrock, since the interface between overburden and bedrock are always found to be the most susceptible plane of least shearing resistance, along which, in general the translational slides occur frequently and depth to length ratios are in the range of low (≤ 0.2).

From the map data, an inferred overburden thickness map was prepared (cf. Fig. 3 b), which has empirically been considered as the depth of possible failure surfaces (Z) of different slope portions for the sake of this stability analysis. Thus, to have a broad quantitative empirical estimate for the above stability analysis, the above overburden thickness map has been used for the estimation/ assumption of depths of probable failure surfaces. In the above stability analysis, following three hydrological scenarios - dry, wet and completely saturated were assumed. For Dry, m (Z_w/Z) was assumed to be 0, for wet, m was considered 0.5 and for completely saturated scenario, it was assumed that the phreatic surface coincides with the natural soil line (NSL), and therefore, m (Z_w/Z) was considered 1. To incorporate the exposed rocky areas within the ambit of above slope stability analysis, the mapped bedrock areas are assumed to be filled up with a thin (0.2 m to 0.5 m) veneer of scree material. Using our map data, we selected 10

different insitu soil sample locations keeping in mind the lithological variability of overburden material mapped. The shear parameters of the collected insitu soil samples under different saturation conditions were tested using tri-axial shear test and corresponding variation in the C , γ & ϕ values under dry, wet and full saturations were estimated. Using these values, derived shear parameter maps (Fig. 4) are prepared, which represented spatially-distributed variability of shear parameters of soil samples for use in F_s calculation in each grid-cell.

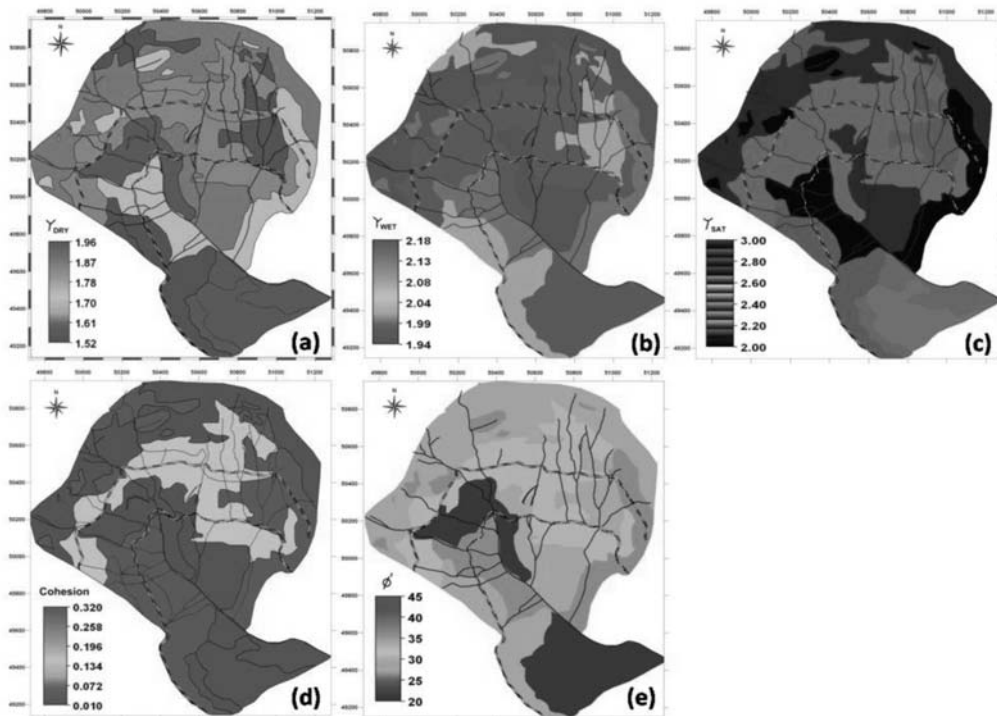


Fig 4. Map showing spatial distribution of different shear parameters of overburden material; The quantitative measure of different shear parameters were obtained from the tri-axial shear test of 10 representative soil samples from the different types of overburden material. (a) Unit weight (γ) in gm/ cc tested under dry situation, (b) Unit weight (γ) in gm/ cc tested under wet situation, (c) Unit weight (γ) in gm/ cc tested under completely saturated situation, (d) Cohesion and (e) Residual friction angle .

Results:

Detailed geological mapping and evaluation of Paglajhora slide complex:

Paglajhora slide complex represents an ensemble of numerous individual slide zones of varied dimensions, which are characterised by a number of well-developed prominent and discontinuous debris as well as rock scars (cf. scars in Fig. 3 a). Overall, the entire influence zone of this slide complex is wider in the upper part towards north and northwest and is narrow or constricted towards its toe in southeast. The detailed scale geological map of the slide complex shows that the maximum length along the slope of this slide complex is about 1.52 Km, whereas the maximum width comes about 1.55 km elevation-wise, the uppermost border of the Paglajhora slide complex is at *m.a.s.l.* 1540 m and the toe part goes down to *m.a.s.l.* 780 m located adjacent to the right bank of Shiva Nala. At the central or axial part of Paglajhora Slide complex, a distinct zone of depletion has been observed from spoon-shaped concave geometry, whereas the relatively gentler slope towards its flanks and the middle portion represents the zone of accumulation. The accumulation zone is filled up with a considerably thick (approximately 5-20 m) heterogeneous slide debris (cf. Fig. 3 a). Adjacent to the Paglajhora slide complex (towards its south), there exists a most prominent active rock slide, which is locally known as 14 Mile slide. This rock slide in the present form has been developed since the monsoon of 2002 due to the rapid retrogression of a smaller rock slide on a moderately steep slope within the last 7-8 years. Presently, the crown of the 14 Mile slide has reached up to the NH-55 road level and has damaged the road bench for a width of about 500m. The maximum width of this particular slide is ~ 520m and crown to toe slope length is ~ 703m. Elevation wise, the present crown is at *m.a.s.l.* 1125 m and toe reaches down to the right bank of Shiva Nala at *m.a.s.l.* 780 m.

Elevation wise, the entire influence areas of Paglajhora Slide can be divided into three separate morphometric domains - A, B and C. Domain-A represents part of the Paglajhora slide complex from the NH-55 road bench level up to its northern boundary towards upslope. In this domain, two distinct triangular debris cones or zone of accumulation have been delineated. Apart from the two accumulation zones, the rest is covered mainly with thin (<5 m thick) colluvium with/ without fresh debris and bare rock exposures. The zone of accumulation or debris cones is in general thick having tentative thickness of ~10-15m. These debris cones become thicker more towards down slope areas i.e. within Middle Paglajhora (Domain-B). Within the colluvium-covered areas, a number of prominent slide scars are identified and mapped, whereas, within debris-filled areas, discontinuous and prominent debris

scars are plenty. Within this domain, the slope-forming material is predominantly consisted of greater concentration of large-sized, angular gneissic boulders set in minor constituents of coarse grained sandy to pebbly matrix. Three prominent exposures of quartzo-feldspathic gneiss are present in Domain-A i.e. two along its two flanks and one at the west-central location, where a prominent rocky scar is observed near the NH-55 road bench. Apart from the above slide scars, in the upper Paglajhora NH-55 road bench, adjacent to Domain A, three prominent stretches of road sinking have been mapped, where the present road bench is found to have subsided/ sunk (maximum 0.5m) from its static level. These sinking zones at NH-55 road level spatially coincide with the zones of debris accumulation present in this area. Within this zone, wherever bedrock (quartzo-feldspathic gneiss) is exposed, the rock is fresh and competent in nature. The prominent foliation within bedrock strikes N35°E - S35°W with dips 25-35° NW i.e. askew to the hill mass. Along rock scar face, two sets of prominent valley-ward dipping (N25°E/ 80° SE and N60°E/ 75-80°SE) continuous joints are observed. Towards eastern boundary of the slide complex, a continuous rocky arm is observed right from Domain-A to Domain-B and C, wherein the scar face is marked by a well-developed westerly dipping joint plane (N40°-45°E/ 40°-50° NW). All the rock scars present in the uppermost levels of Domain-A clearly bears the signatures of several episodes of past rock sliding, which contributed the formation of thick debris heap down below.

Domain-B represents the middle Paglajhora region bounded by upper and lower Paglajhora NH-55 road benches. This zone is broadly bounded by the NH-55 road benches passing through this terrain at two different elevations. In Domain-B, from west to east, three prominent geotechnical zones are identified. Along the axial portion, through which, the main Pagla Jhora flows is found to be the most affected/ distressed part of Domain-B, where clear evidences of recent mass movements are noticed as evidenced by concentration of both arcuate and longitudinal slide scars and prominent zone of depletion. The lower Paglajhora road section marks the border of Domain-B, which registered the maximum rate of subsidence (maximum 5m) at three prominent stretches. Within this domain, along the right bank of Pagla Jhora, a linear rock scar is longitudinally exposed, which is represented by a highly sheared, shattered and fractured quartzo-feldspathic gneiss with prominent penetrative planar fabric dipping lowly 15-20° towards N40°W. Presence of this sheared rocky scar infers possible presence of a prominent shear sub-parallelly disposed to the trend of the main Paglajhora nala. Apart from this thin shear, the entire slope is covered with thick slide debris and slope wash deposits. The slope forming material is broadly

heterogeneous in nature and is represented by a coarse admixture of large to medium sized boulders of gneiss set in a micaceous sandy to silty matrix. In this zone, differential concentrations of finer as well as coarser matrix both in space and at different elevations are noted.

Domain-C represents the part of the slope below the lower Paglajhora NH-55 road bench down to the banks of Shiva Nala. Domain - C represents the inner lowermost part of the arcuate catchment slope of Shiva Nala. In this domain, slope adjacent to the right bank of Pagla Jhora and Shiva Nala is steep and mostly scree with/ without bedrock (quartzo-feldspathic gneiss) covered. Wherever, bedrock is exposed on slope, it is fresh and competent in nature. Along the left bank of Shiva Nala, the slope is moderate to steep and is mostly covered with scree, debris (both old and younger loose). Towards eastern flank, the slope becomes steeper and is characterised by a exposed bedrock, which has been observed right from Domain-A down to the left bank of Shiva nala. This rocky ledge marks the easternmost boundary of the entire Paglajhora Slide Complex.

The shape of whole mapped area is amphitheatre like within the upper catchment slope of Shiva Nala and is being drained towards SE by all its lower order tributaries. Amongst the three morphometric domains, the Domain - B is the most failure-prone and consists of a number recent debris scars, a prominent zone of depletion in the central part and accumulation of failed colluvium. Within this zone, the NH-55 road bench at two elevation levels is situated, which suffers maximum amount of subsidence.

GIS-based stability analysis:

Considering all the model assumptions, values of all the above-mentioned raster map data, the F_s maps for Dry, Wet and Completely Saturated are prepared after slicing F_s maps into the following three categories - Unstable ($F_s < 1.0$), Critical ($1.0 < F_s < 1.7$) and Stable ($F_s > 1.7$). The upper limit of F_s values within the critical category has been kept as 1.7 because, the F_s map database indicates that pixels having a maximum F_s values 1.7 under Dry scenario can also be unstable ($F_s = 0.9$) in completely saturated condition. Therefore, an intermediate threshold zones having F_s values between 1 and 1.7 is delineated, which was termed as "Critical". Under Dry condition, about 60% area is stable, 35% area is critical and 25% areas are unstable (cf. Fig. 5 a). Whereas, in wet situation, stable portion is reduced to 28% areas, about 50% areas become unstable and 22% areas become critical (cf. Fig. 5 b). Under completely saturated condition, only 5% stable areas area lost, but the amount of unstable slope increased substantially that is about 65% from the 50% in the wet condition (cf. Fig. 5 c).

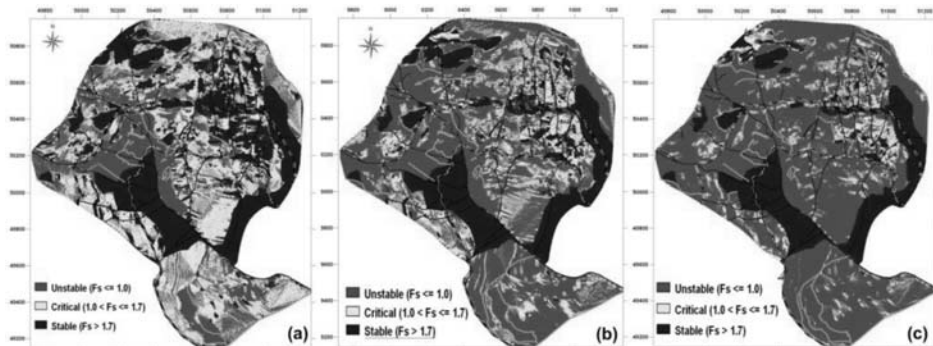


Fig 5. Spatially-distributed stability map (a) Dry condition, (b) Wet condition and (c) Completely saturated condition.

Conclusions and Discussion

The Paglajhora slide has broadly three domains. The uppermost domain contains mostly the rocky scars, whereas the middle and lower domains contain mainly discontinuous debris scars as evidenced from various types of scars spread within the accumulated thick colluvial material. Physiographically, the Paglajhora catchment is traversed by a number of prominent SE-ly flowing streams, maximum of which are having strong erosion potentiality, which favours continued slope instability in this area. Broadly, the primary causes of different types of slides in Paglajhora slide complex are enumerated below:

- Moderately steep to steep upper and lower slopes.
- Influence of a regional tectonic fabric (MCT), which is passing across the slide complex along its southern boundary.
- Presence of thick and fractured sheared gneiss along the axial part, sub-parallelly disposed to the course of Paglajhora.
- Accumulation of highly anisotropic and heterogeneous debris material of very low shearing strengths in the middle and lower part. On differential saturation, this slope-forming material easily loses its shearing strengths and fails selectively. This type of failures is very common in the middle and lower part of the slide.
- Arcuate physiographic configuration of the Paglajhora slide complex favour accumulation of surface and ground water mostly in the axial zone, where during monsoon pore water pressures becomes so high that failures are rarely

be avoided in this region. This can be evidenced by development of a deep zone of depletion in the axial part of the slide and major subsidence and lateral shifting of the road bench in the lower Paglajhora reach.

- A number of un-guided tributaries of Shiva Nala are present in the slope, which erodes and accentuates toe cutting of debris-filled slope at a number of places. These actions trigger the failures in debris-accumulated slope.
- Presence of flat areas in the Domain-B favours concentration of high recharge, which trickles downward up to Domain-C and also favours piping of finer material. This was evidenced from the size distribution of slope forming material from upper reaches to lower levels. At lower elevations, debris and slope wash material are found to be relatively finer than its counterparts in Domain-A and upper part of Domain-B. This piping action is more severe in the lower reaches i.e. in the lower part of Domain-B and in Domain - C. Because of the severe piping in the lower reaches, the lower Paglajhora road bench registers maximum amount of road sinking in comparison to its upper counterpart.

Spatially-distributed deterministic stability analysis indicated that substantial areas become unstable with increase in saturation condition. An estimation of about 25% areas as unstable in dry condition is perhaps the result of limitations of the assumption of the model to consider depth to bedrock as the depth to failure plane in all locations. Since in dry situation in Paglajhora slide complex, rarely any slope instability occurs. Furthermore, several other following limitations have also contributed the performance of the above deterministic model, which can substantially be improved if several model assumption and limitations are reduced.

- Lack of in-situ instrumental data (e.g. inclinometer etc.) designed to know the actual depth and pattern of slip surface.
- A simple one-dimensional translational slide has been assumed to attempt the infinite slope model for stability analysis, which may not always be true in all the domains of Paglajhora Slide Complex, especially the middle part, where, some rotational failures (with multiple failure planes) and/ or higher depth to length ratios of individual failures overestimated the F_s values.
- Lack of piezometric monitoring data to know the depth of actual phreatic surface. That is why, in the stability equation, proper estimation of pore water pressure could not be incorporated. In this context, availability of an insitu hydrological model would definitely add values to the predictive power of the

deterministic process.

- In general, the debris in Paglajhora is mostly heterogeneous and anisotropic in nature, thus assuming a part of the area in terms of compositional homogeneity for the sake of the model at times leads to erroneous results. But in the same time, it should also be noted that this problem can to some extent be lessened, if more number of representative insitu soil samples both spatially and depth-wise could be collected for laboratory analysis.

Therefore, as part of a future research, Paglajhora slide complex can be considered a suitable site for developing a 2-D and/ or 3-D failure susceptibility model incorporating 3-D hydrological model parameters incorporating piezometric data to understand better the behaviour of the complex instability processes of such a hydrostatically-induced large landslide complex.

Acknowledgements:

The authors express their sincere gratitude to the Deputy Director General, Geological Survey of India, Eastern Region, Kolkata for his valuable suggestions in improving the manuscript and allowing us to publish this research. The authors also acknowledge the contribution made by S/Shri Tapas Das and Tarun Saha, for assisting in the topographic survey of the area.

References

1. Soeters, R. and van Westen, C.J., 1996. Slope Instability. Recognition, analysis and zonation. In: A.K. Turner and R.L. Schuster (Editors), Landslide: Investigations and Mitigation. Special Report 247. Transportation Research Board. National Research Council. National Academy Press., Washington, D.C, pp. 129-177.
2. Terlien, M.T.J., van Westen, C.J. and Asch, T.W.v., 1995. Deterministic modelling in GIS-based landslide hazard assessment. In: A. Carrara and E. Guzzetti (Editors), Geographical Information Systems in Assessing Natural Hazards. Kluwer Academic Publishers, Netherlands, pp. 57-77.
3. van Asch, T.W.J., 1992. The role of water in landslide hazard analyses, 1st Symposio International sobre Sensores Remotes y Sistemas de Information Geographica para el estudio de Riesgos Naturales, 10-12 March, 1992, Bogota, Columbia, pp. 485-498.
4. van Westen, C.J., 1993. GISSIZ : training package for Geographic Information Systems in slope instability zonation : Part 1. theory. ITC Publication Number 15. ITC, Enschede, 245 pp.

VILLAGE INFORMATION SYSTEM (VIS)

Development of Village Economy through Space Technology

Kiran Jalem* and A.K. Singh**

Abstract

Paradox prominently persists in Jharkhand in terms of resource base and regional/socio-economic development and natural resource management. Peace and freedom, though, are not necessarily outcome of economic development, it is a must to have the affordability to the minimum level of basic needs like food, shelter, health, education, and decent living conditions in the marginalized/underdeveloped regions/societies.

Village Information System (VIS) is an interdisciplinary approach with Remote Sensing, GIS and GPS technologies conceptualized to bring about the development in such regions through creating/updating, disseminating information related to resources and aspects of development. VIS, a GIS based customized information system, aims to integrate various datasets at micro-level (village, panchayat & block). This project is being carried out for Namkum block of Ranchi district in Jharkhand on pilot basis which will later on be implemented to the entire state. The objectives include the Geospatial technology based thematic mapping on various natural resources viz. Geology, Geomorphology, Soils, Landuse/Landcover and Forest type & density as well as Socio-Economic profile consisting of amenities/infrastructure like healthcare, schools, roads, power, drinking water, etc., to help meet the above stated goals in the villages of Jharkhand.

The project also attempts to integrate and generate comprehensive information including Computerization of Land Records (Land Records Information System) to develop various development action plans which addresses issues like Land Utilization, Rural Development and Poverty Alleviation, Tribal Development, Natural Resource

* Asstt. Professor, Disaster Management Centre (DMC), Shri Krishna Institute of Public Administration (SKIPA), ATI Main Building, Meur's Road, Ranchi-834008.

** Director General, Shri Krishna Institute of Public Administration (SKIPA), ATI Main Building, Meur's Road, Ranchi-834008

Management & Utilization, Wasteland, Watershed Prioritization, Infrastructure Planning finally leading to the overall Regional Development. The information will be made available and accessible to the people ranging from the policy makers, administrators, plan executors, researcher and academicians, NGOs to the villagers and other people concerned.

This study is being carried out using Indian Remote Sensing Satellite data (LISS-III and LISS - IV) and Quick Bird Data of 2004-05, Census 1991 and 2001 Data and Primary Survey Data on Household, Village Information, Health Information and Education Information Survey.

Introduction

Paradox prominently persists in Jharkhand in terms of resource base and regional/socio-economic development and natural resource management. Peace and freedom, though, are not necessarily outcome of economic development, it is a must to have the affordability to the minimum level of basic needs like food, shelter, health, education, and decent living conditions in the marginalized/underdeveloped regions/societies. Jharkhand is one of the largest producers of mineral resources of the country spreading over majority of the districts with a paradox to be among the bottom lying states in terms of development till now. It has got the vast resources in flora and fauna or biodiversity too. In terms of human reserve the state is rich, which can be converted into quality human resources through proper efforts and intervention. The other endowments, like scenic beauty, all over the state with a vast potential for tourism are also unutilized or underutilized. The figures indicate that a considerable portion of the land is under agricultural wastelands that have to be beneficially utilized for rural development.

The state has also received the special development plans as hill and tribal region (as Chotanagpur Plateau prior to the Jharkhand State). Yet the development indicators indicate the poor results of the plan efforts. To uplift the State in terms of development, the development of rural areas is a prerequisite. Since the rural areas are regionally heterogeneous at micro-level, it is necessary to have local specific plans and programmes. For any kind of development plan or programme the most required aspect is availability of reliable real-time database/information at easy access to the policy/decision makers, administrators, executors and the people concerned. It may also motivate the participation of the villagers in local/village level decision making and development activities with understanding about their settlement locations, resources and environment or village ecology with an input of indigenous/local expertise or

technology. Therefore, it is necessary to design and develop a comprehensive and systematic database to attain the goal in sustainable manner. Therefore, this work is oriented towards creating and providing information on all resources related to land, water, forests, minerals, soils, agriculture and human and socio-economic development, infrastructure and facilities, etc. The integration of these sets of information would fill the data gaps to some extent in planning process and development efforts. This is an endeavour by geo-spatial technology like Remote Sensing, GIS, GPS, etc, and application projects for the development of the state.

The Need

Urban population is increasing in India at an alarming rate, but urban development trend is affected by shortage of resources and environmental problems. Hence optimum use of natural resources like water, which forms the part of basic amenities in urban settlement, is the need of the hour. Jharkhand state has blessed with abundance Natural resources like Minerals, Rivers, Forests etc, but its improper management is acting as a hindrance for development. Especially the capital "Ranchi" lacks either the proper assessment or development or Management of basic infrastructure facilities. The present condition of utility services in the state capital needs Preparation of Landuse map, Management & updation of other Utility services.

Development of any settlement rural or urban can be broadly categorized into 4 phases:

- Pre-planning phase
- Planning and implementation phase.
- Monitoring and Evaluation phase.
- Re-planning for existing and future development phase

Planning, Development and management at settlement, village or urban level, need information not only for the initial stage but on regular interval so that the whole process of planning can be systematized in terms of data sources, data collection, storage, processing, updating, retrieval and meaningful efficient use, which acts as the basic information required for the urban utility services.

This project "Village Information System" on completion will address to all the above issues and will help in Updation, Analysis, Development, Assessment, Management and Retrieval of data related to above mentioned urban utility services.

Village Information System (VIS) is an interdisciplinary approach with Remote Sensing, GIS and GPS technologies conceptualized to bring about the development in

such regions through creating/updating, disseminating information related to resources and aspects of development. VIS, a GIS based customized information system, aims to integrate various datasets at micro-level (village, panchayat & block). This project is being carried out for Namkum block of Ranchi district in Jharkhand on pilot basis which will later on be implemented to the entire state. The objectives include the Geospatial technology based thematic mapping on various natural resources viz. Geology, Geomorphology, Soils, Landuse/Landcover and Forest type & density as well as Socio-Economic profile consisting of amenities/infrastructure like healthcare, schools, roads, power, drinking water, etc., to help meet the above stated goals in the villages of Jharkhand.

The project also attempts to integrate and generate comprehensive information including Computerization of Land Records (Land Records Information System) to develop various development action plans which addresses issues like Land Utilization, Rural Development and Poverty Alleviation, Tribal Development, Natural Resource Management & Utilization, Wasteland, Watershed Prioritization, Infrastructure Planning finally leading to the overall Regional Development. The information will be made available and accessible to the people ranging from the policy makers, administrators, plan executors, researcher and academicians, NGOs to the villagers and other people concerned.

The other dimension of this project is to take the utility and fruits of this geospatial technology to the door steps of even the remote villagers through printed maps and also through the network accessible at Info-Kiosks or Village Resource/Information Centers (VRCs) connected by VSAT. In nutshell, it will be of immense help in proper and effective development intervention in the same paradigm of 'bottom up approach' in regional development.

Objectives

The main objectives of VIS are:

1. To generate and integrate information on various natural and human resources
2. Integration of thematic information in GIS environment to draw up area-specific and location-specific action plans like Land Resources Development Action Plan, Water Resources Development Action Plan, Watershed Prioritization, etc.
3. To disseminate these information to the policy makers, administrators, plan executors, villagers and people concerned

4. To customize user-based softwares for browsing and query
5. Training and transfer of technology to various users/ departments

Data Base

Spatial/Maps:

Since there are many aspects involved in VIS, different materials and methods have been used. The materials used for this project are Survey Of India toposheets, latest Remote Sensing Data (LISS-III, LISS-IV, IKONOS and Quickbird) of 2004-2005. Theme wise data sources have been given below:

Geology:

1. Quadrangle Geological Map of Geological Survey of India.
2. IRS P-6 LISS -IV data to modify the Litho Units

Geomorphology:

IRS P-6 LISS -IV data to interpret and delineate the geographic units (Valley Fill, Valley Slope, Plateau (Weathered & Dissected), Tors & Domes, Denudational Hills, etc.

Landuse/Landcover:

IRS LISS-III and LISS-IV

Soil:

IRS P-6 LISS -IV data to map Soil Series

Slope:

SOI Toposheet (1:50000)

Drainage:

IRS P6 LISS IV data

Forest Resource Assessment (FRA)

IRS P-6 LISS -IV

Computerization of Land Records (Land Information System or LIS)

1. Revenue or Khasra Maps collected from the Block or District Nazareth Office,
2. Quick Bird Satellite Data

Attribute Data

1. Census of India, 2001- Village Directory and /PCA
2. District and Block Offices (Document II, Anganbari Centers, BPL, etc)
3. Primary Survey based on questionnaire for Village Information, Education Information, Health Information, and Household Information

The other thematic, tabular and textual secondary and ancillary information have also been obtained supplemented by the field survey and ground truthing.

Methodology

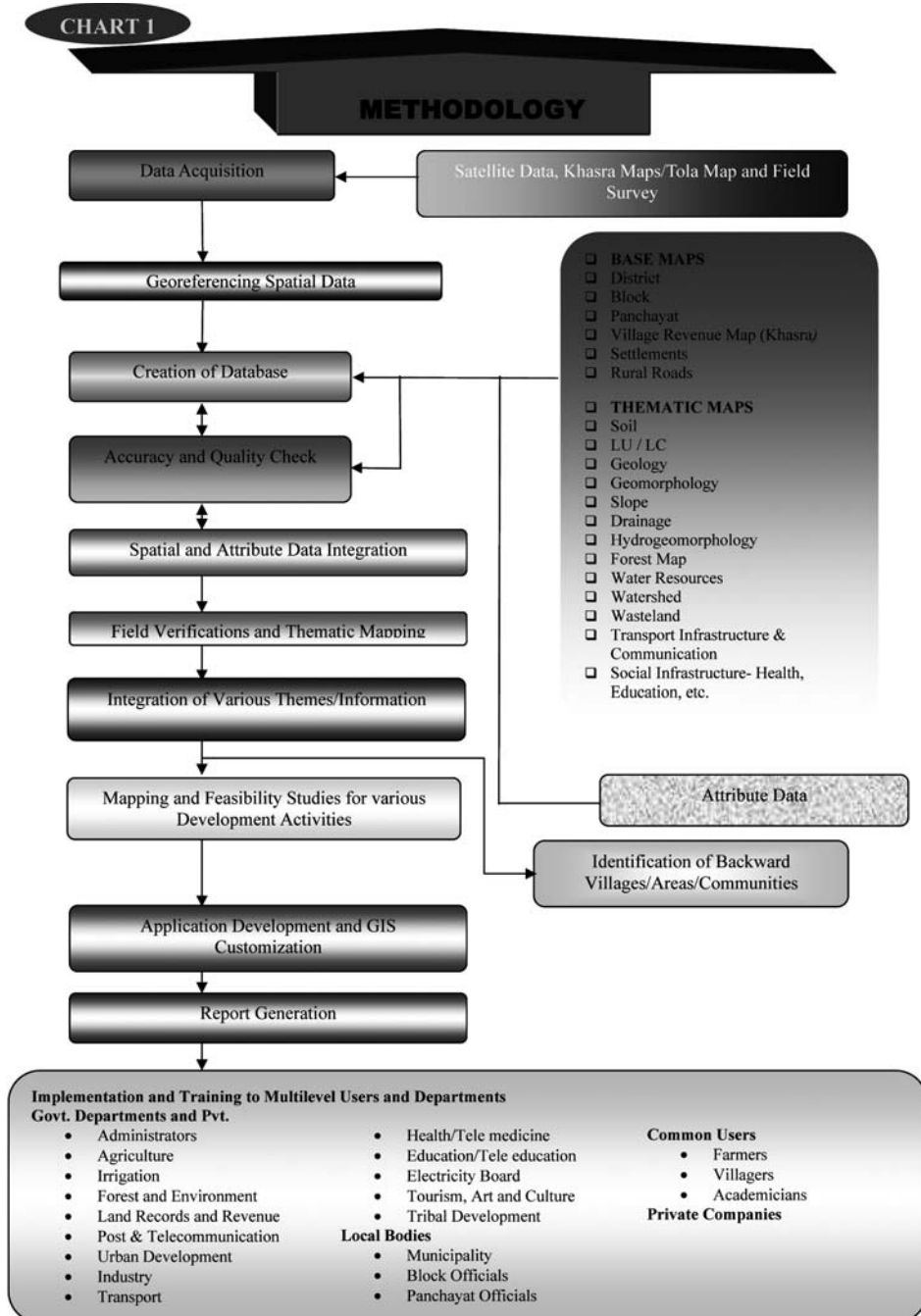
Different methods have been followed for generating different themes in this project. The methods are following (the methodology and approach have been shown in the flow charts given subsequently):

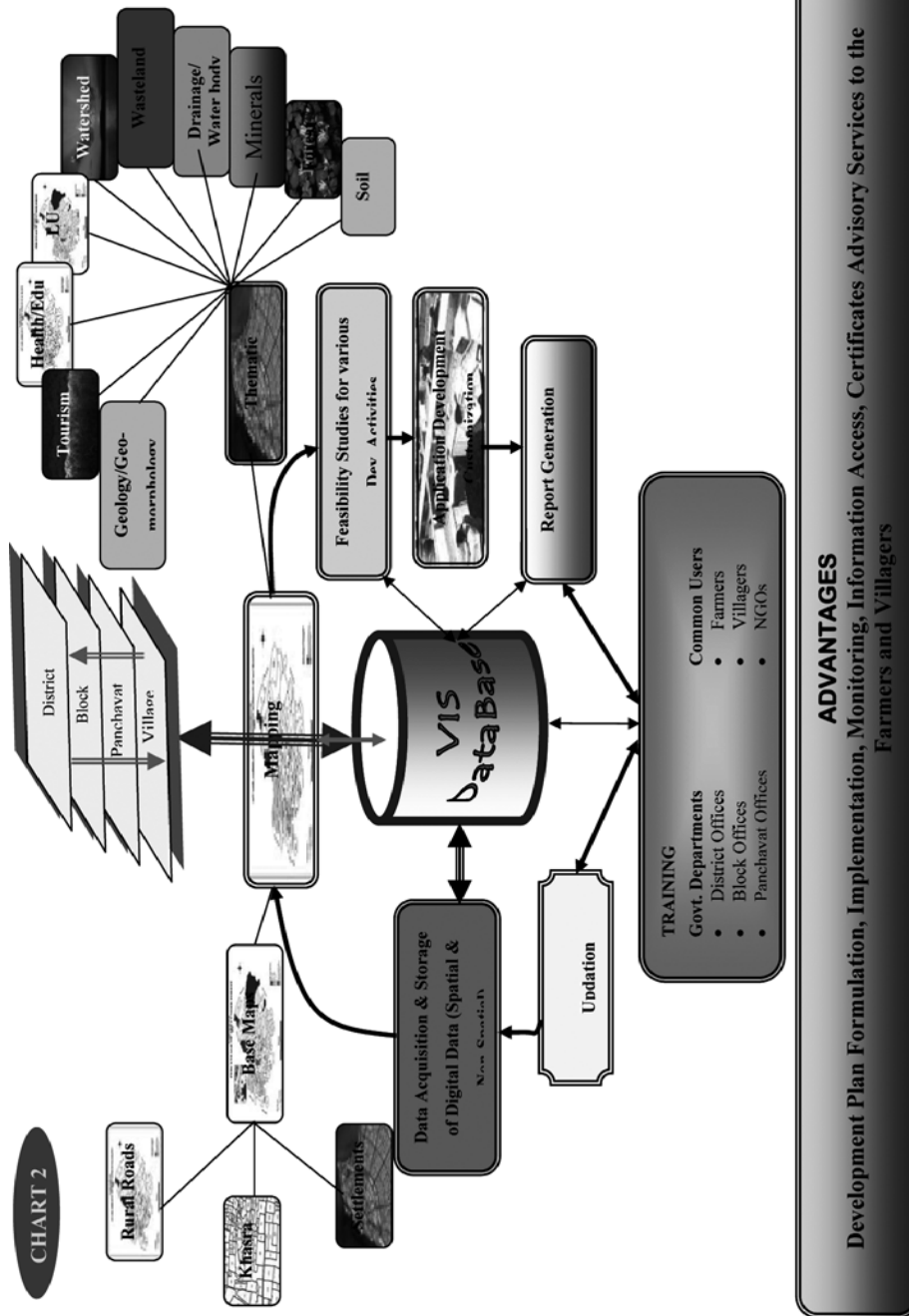
1. **Village Boundary Mapping:** Boundary map acquired from the Census of India and confirmed with the Block about the present boundary, since it falls partly in the urban area now. The paper maps were scanned, georeferenced, digitized, village-codes assigned and socio-economic data attached for thematic mapping.
2. **Landuse/Land Cover Mapping:** Landuse/Landcover mapping of Namkum Block was carried out using IRS LISS-III and LISS-IV Satellite Image. Visual interpretation techniques and adequate ground verifications was considered to identify various Landuse/Landcover classes. Major emphasis was given to delineate the landuse classes such as agricultural, fallow land (kharif, rabi, double cropping seasons), agricultural plantations, forest, wasteland, built-up land, quarrying sites and water bodies.
3. **Soil Mapping:** Soil resource mapping of Namkum Block on 1:25000 scale was carried out by using LISS-IV satellite data. Soil series were mapped occurring on different physiographic units. The detailed morphological, properties of the soil were studied in the field and physio-chemical analysis was carried out in the laboratory. The soil samples were classified as per the soil taxonomy.
4. **Geology:** Geological mapping of Namkum was done using Quadrangle Geological map of Geological Survey of India and litho units were modified/updated on the basis of IRS P-6 LISS-IV data and limited field checks.
5. **Geomorphology:** IRS P6 LIS-IV data supported with limited field checks were used for interpretation and delineation of geomorphic units of Namkum Block.

6. **Forest Mapping:** Forest type and Forest cover mapping of the Namkum Block was carried out by using LISS-IV data. Both Forest Type and Forest Cover were mapped using onscreen visual interpretation techniques. Sample plots were laid out in the forest for community ecosystem analysis with adequate field checks.
7. **Slope:** Maps were prepared based on contour spacing of consecutive elevation.
8. **Drainage:** Drainage were demarcated based on Survey Of India Toposheets and updated by IRS P6 LISS IV data and limited field checks.
Socio-Economic Profile: Village wise socio-economic thematic maps have been prepared based on data availability from the Census of India (2001) that includes Social Composition, Sex Ratio, Literacy Workers Classification, where as Health Facilities, Educational Facilities, Safe-Drinking Water Facilities, Post and Telegraph Facilities, Power Supply, etc. were collected from the primary survey on village information, health information, educational information and household information. A detailed village level primary survey is carried out to collect the latest socio-economic data for household, village, school and health related information. In addition, latest information regarding hand-pumps by their working conditions from the Public Health Engineering Department and school information from Jharkhand Education Project Council (JEPC) have also been collected and mapped.
9. **Water Resource Development Plan:** Water Resource Development Action Plan has been prepared on the basis of integration of information on geology, geomorphology, hydrological characteristics, surface water availability, drainage, land use and current status of ground water exploitation keeping in view of both immediate and long term needs of water in the area.
10. **Land Resources Development Action Plan:** Land Resources Development Action Plans has been prepared based on the integration of land use, geomorphology, soils, ground water, rainfall, socio-economic data and irrigation facilities available in Namkum area.

VILLAGE INFORMATION SYSTEM (VIS)
Development of Village Economy through Space Technology

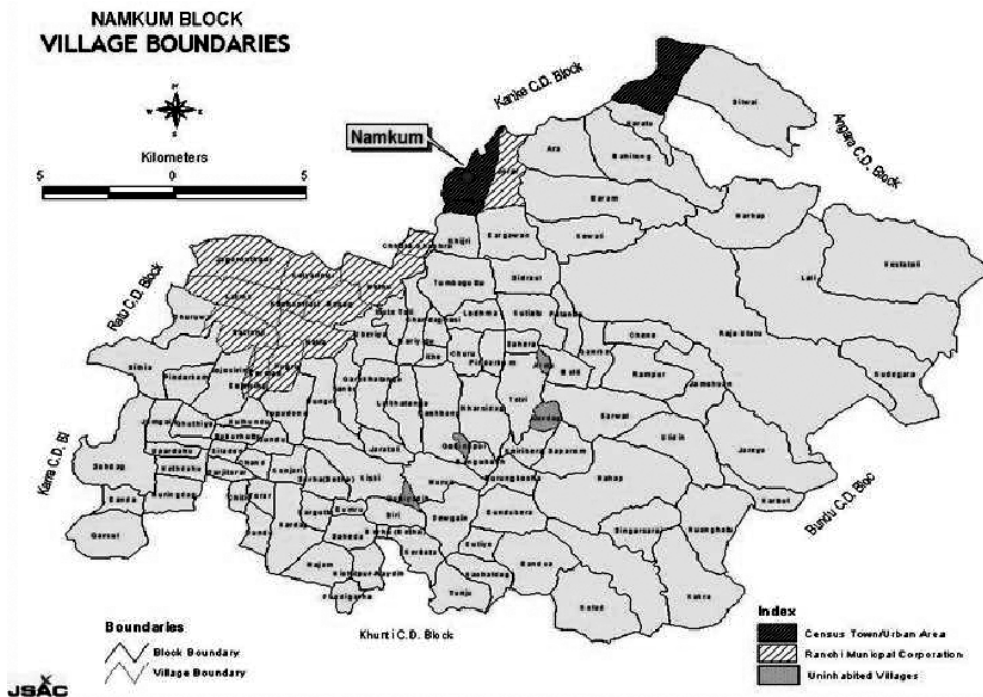
CHART 1





The Pilot Area: Namkum Block (Ranchi District, Jharkhand)

Namkum Block of Ranchi has been taken as a pilot block. It is roughly located between 85o13'33" N and 85o14'4" N and 23o10'0" E and 85o23'31" E. It falls partially under the Ranchi city. Part of Namkum village has developed as an urban centre along with Tati, a Census Town (CT). The Ranchi Municipal Corporation boundary has also been now extended. The Namkum Block has been surrounded by the Kanke block in the north, Angara in the north, north-east, Ratu in the west north-west, Karra in the west, Khunti in the south Bundu in the south south-east and Sonahatu in the east. The average annual rainfall is 1293 mm.



A large part in the block is under the cantonment area. It has also got a number of industrial units varying from small to large notable among them is Usha Martin, Vaxpol India, High Tension Insulator Factory, Daewoo Motors, along with the Software Technology Park of India, etc.

The Census of India, 2001 suggests that there are 21156 households with a population of 114397 in the Namkum block out of which only 9.2 per cent population resides in the urban area (table 1). The Scheduled Tribes (ST) are the largest constituents of the total population in the block with 63.2 per cent share followed by the Others (31.8 per cent) and the Scheduled Castes (SC) with only 5.0 per cent share. The main community, ST, is primarily rural as only 7.6 per cent resides in the

urban localities. The sex-ratio is little above the national average for all (940), which is better in the rural areas (951).

There is diversity in the economic activities blending the modern traditional and conventional occupations with the modern hi-tech white and blue collar jobs. For example half of the population is engaged with the agricultural and allied primary activities and half of the population

is involved with the secondary sector like household industry and manufacturing industry other than household industry, construction and building, and tertiary sector like trade and commerce, transport and communications and other services.

A sizable population is engaged as main workers in the block (65.8 per cent). Out of the total main workers little above half of the population has the occupation related to agriculture, where 46.2 per cent are cultivators and 4.7 per cent are still agricultural labours. In both cases, percentage of females goes higher than males indicating their positions in the society. The data also shows the significant percentage of female workers

Table 2: Socio-Economic Profile of Namkum Block, Part II

Indicators		Total	Rural	Urban
Main Workers	Total	65.8	64.3	87.8
	Male	75.2	73.7	90.6
	Female	49.5	49.2	65.1
Cultivators	Total	46.2	49.9	6.8
	Male	40.4	44.7	4.6
	Female	61.7	62.5	31.4
Agricultural Labour	Total	4.7	5.0	0.7
	Male	4.2	4.6	0.5
	Female	6.0	6.1	3.6
Household Industry	Total	3.2	3.2	2.3
	Male	2.6	2.7	1.8
	Female	4.7	4.6	8.2
Others	Total	45.9	41.8	90.1
	Male	52.8	48.0	93.1
	Female	27.6	26.8	56.7
Non-Primary Sector	Total	49.1	45.1	92.5
	Male	55.4	50.7	94.9
	Female	32.2	31.4	64.9
Non-Workers	Total	63.0	61.8	74.4
	Male	54.3	53.9	58.1
	Female	72.2	70.2	93.8

Source: Census of India, 2001

as the agricultural labourers. Surprisingly household industry registers only 3.2 per cent workers in the block. Diversifications has taken place in the block as 45.9 per cent main workers are engaged in Other activities (incl. construction, trade and commerce and other services) and 49.1 per cent workers are engaged in the non-primary sectors. Thus, still half of the workers are engaged in the agricultural and allied activities constituting the primary sector in the block.

There are significant variations across the villages of Namkum block in the above indicators. As a block partially falling in the Ranchi Urban Area, there is much contrast over the space. Even the population density is widely variable in the block.

Project Team

The following team has been involved in the project right from the project formulation to the database creation, survey, database integration, thematic mapping and the preparation of action plan maps and application development:

- JSAC, Dept. of IT, Govt. of Jharkhand - Scientific Team

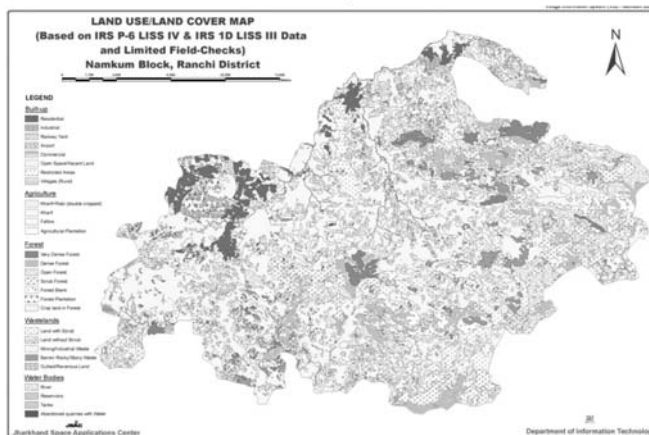
Outcome And Discussion

The following maps and data have been generated under this project:

Village Boundary, DEM, Roads and Railways, Soil, Landuse and Landcover, Slope, Drainage, Geology, Geomorphology, Watershed, Wasteland, Forest, Land Information System (LIS) or computerization and updation of land records, Demographic information like social composition, sex ratio, literacy, occupational structure,

educational facilities, health facilities, communication facilities, safe drinking water facilities, electricity connections, Action Plan Maps like Water Resource Development Action Plan and Land Resource Development Action Plan. More maps, reports and data integration are also in progress especially based on the data collected through primary survey. Important

Map 1.

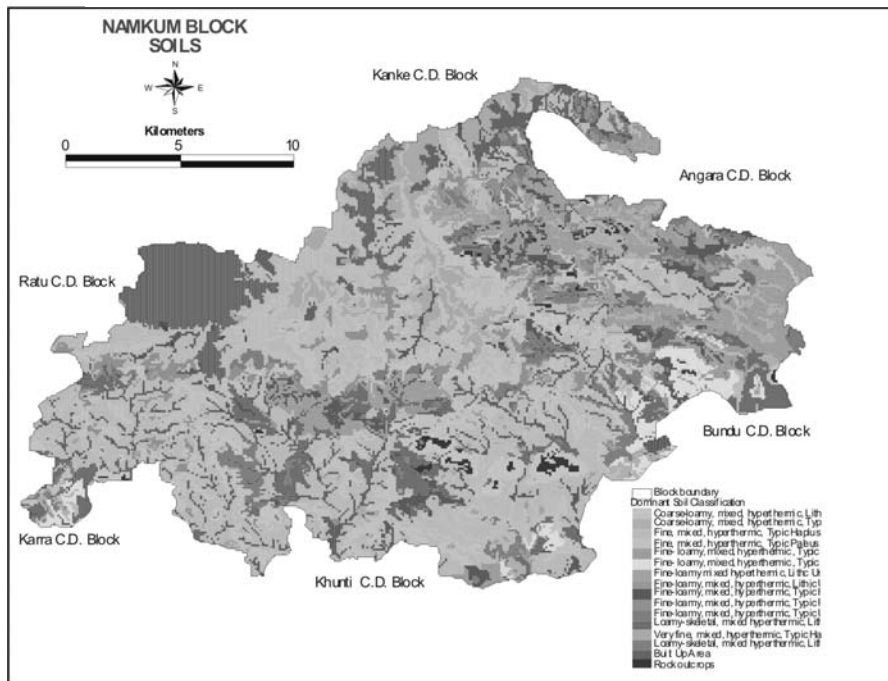


among them is the mapping of tolas with houses, roads, amenities, and service centres based on the layout sketch from the field survey and the quick bird satellite data. Subsequently this will be integrated with the household level information for each individual. Similarly other features like road, school, health centre, wells, handpumps will also be integrated with the associated data collected from the field work and the respective departments.

Landuse/Landcover: Landuse/landcover (Map 1) is an essential component of VIS, which will be used as a basic unit in conjunction with other natural resources as well as socio-economic data for Land and Water Resource Development Action Plan.

Soil: The soil database (Map 2) is created and interpreted as per the user needs like Soil Irrigability Classification, Soil Site Suitability for different crops, Soil Fertility Status, Soil Erosion Status, and Land Capability Classification. This information is used for preparing the detailed Land Resource Development Plan on sustainable basis.

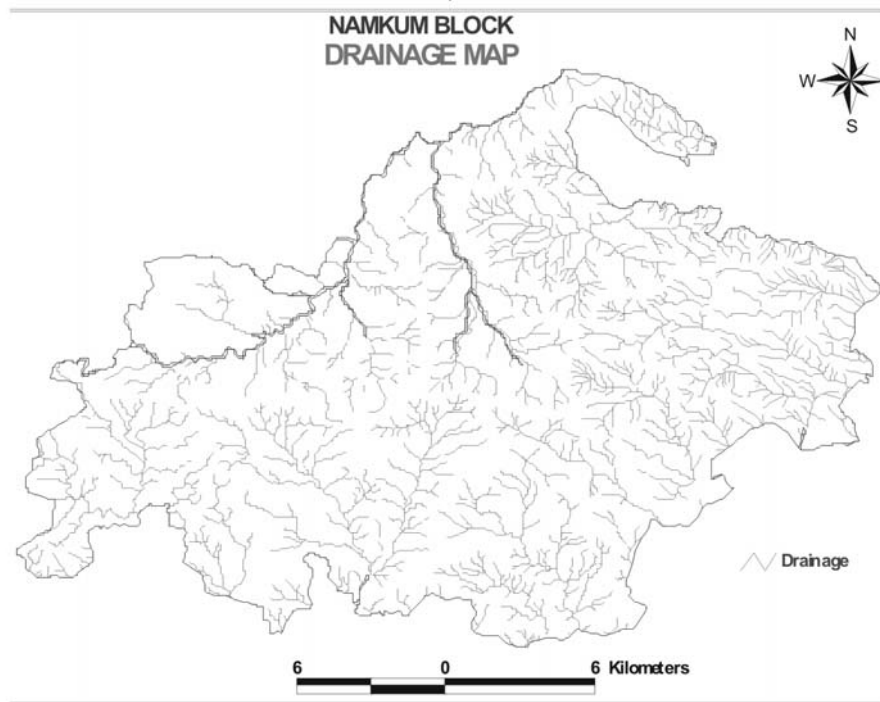
Map 2.



Geology: It is observed that the area is predominantly composed of granite Gneiss and Granite rocks. Various geological units/features were mapped and integrated with

geomorphology/ hydrology of the region to finalize Ground Water Prospects zones there by contributing as one of the major components in preparation of Land & Water Resources Development Action Plan.

Map 3.



Geomorphology: Geomorphologically, area has been classified into Valley Fill, Valley Slope, Plateau (weathered and dissected), Tors & Domes, Denudational Hills, etc. These geomorphic units were used as the base ground water zonation for Water Resource Development Action Plan.

Forest: The resultant maps showing Dense Forest Blanks, Open Forest, Scrub Forest, etc. being used for deriving Land Resources Development Action Plan.

Drainage: The Subarnarekha is the main river passing through the block, which originates south of village Nagri, 15 km west and south- west of Ranchi town. It contains treacherous quick sand, which is dangerous to cross. The name means streak of gold and gold is found in its bed in minute quantities. The other important drainages of the block

are Sapahi Nadi, Raru Nadi, Kocha Nadi and Kanchi Nadi. Mostly, perennial rivers are effluent in nature in which ground water seeps continuously. The drainage map of Namkum block has been shown in Map 3.

Fig 1.

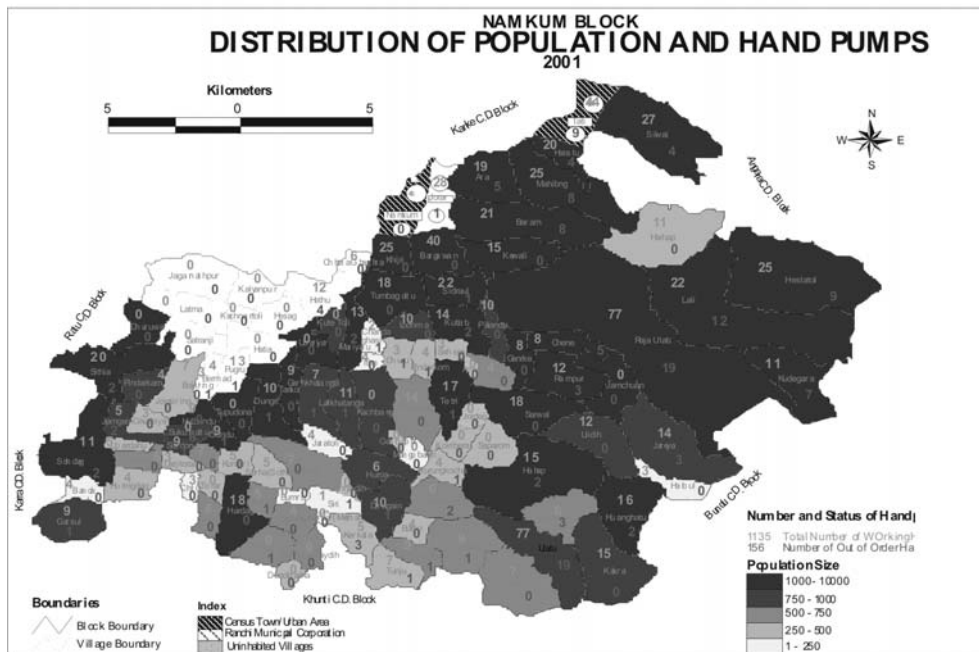


Slope: The study area is basically part of Chhotanagpur plateau but locally characterized by flat to undulating terrain with some high rising hills in North- West and Southern part of the block. The general slope of the terrain is towards south and southeast. The altitude from mean sea level varies from 360 m in valley portions to as high as 750 m on hill tops.

Computerisation of Land Records (Land Information System or LIS): It has been a great effort to mechanize the maintenance and updation of land related information and better land management, land base and land use planning, agriculture planning, infrastructure planning (roads, drainages, canals etc.), planning developmental schemes to eradicate rural poverty and improve village income, minimization of land disputes, etc. Map showing village boundaries shown in Figure 1.

Socio-Economic Data Survey for the Effective Planning: Any kind of plan or programme aims directly or indirectly to the well-being of society. And the information

Map 4.

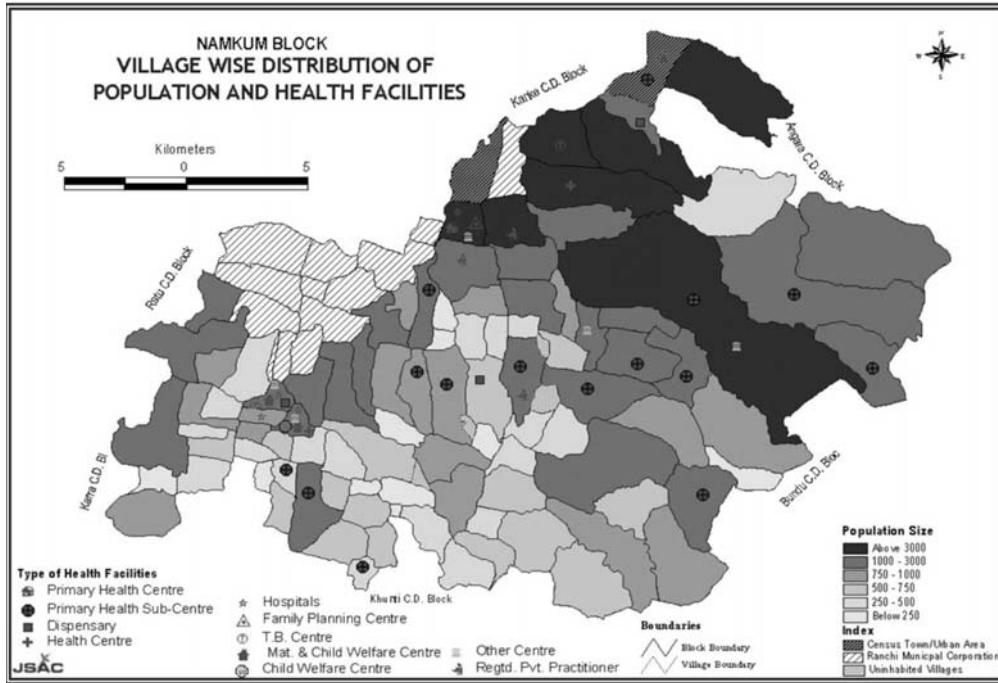


HOME

GIS

NEXT

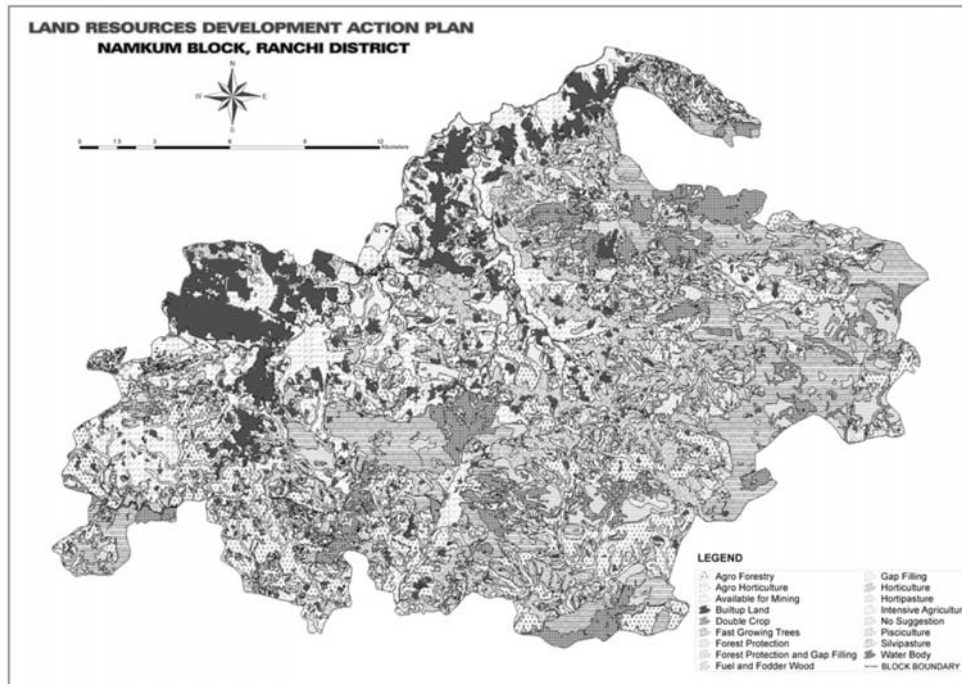
Map 5.



is a must for better and meaningful planning. Moreover, socio-economic background is also an inevitable component in policy making. One of the major activities and achievements is the latest data collection on tola wise village information, health information, educational information and household information for entire Namkum Block. The survey covers 327 tolas in 93 revenue villages covering 20,861 households and 108,489 populations. It covers the 27 government health centres and nine private health centres and clinics, and 136 government and private educational institutions in the rural areas of Namkum block. It gives useful information regarding the infrastructure, amenities and facilities in the tolas and villages, unserved areas, community wise housing condition, poverty, literacy and educational levels, economic infrastructure and activities, safe drinking water, etc. The analysis and translation in map is in progress (Map 4 & 5).

Water Resource Development Plan: The map (Map 6) shows different geomorphic units and its ground water prospects based on field survey, well data and existing literature. Different water harvesting structures like check dams, desilting of tanks,

Map 7.



Limitations And Future Scope

Limitations

1. Data Unavailability
2. Data Inaccessibility
3. Resources

Future Scope

1. It will have complete coverage of Individuals, Households, Tolas, Villages, Blocks, Districts and State in the process of balanced regional development and well-being. VIS will help in leading to the real development, decentralization, self-governance and ensured public participation towards the destination of Gram-Swaraj. Through VIS, every remotest area in the state will be covered.
2. The household level information will be integrated with household map drawn with the help of Quickbird data and layout maps of tolas. Similarly information regarding tolas/villages, health and educational centres will be integrated with the collected attribute data.

3. The project is expected to help in e-governance in the State.
4. The information technology will be at the doorstep of every villager of Jharkhand with very simplified visual understanding. The information generated under this project will be of immense help for the planners and bureaucrats as well.
5. The priority villages (relatively backward) will be identified on the basis of certain parameters condensed in a single Village Development Index (VDI) to bring into the mainstream of development.
6. The VIS will benefit the government departments (administrative, agriculture, irrigation, forest & environment, land records and revenue, post & telecommunication, urban development, industry, transport, health, education, electricity board, tourism, art and culture, tribal development), local bodies (municipality, block officials, panchayat officials), common users (farmers, villagers and academicians), NGOs and private companies.
7. It will be available on the Internet/Public domain for universal accessibility through customized software to disseminate all the information on intra and internet.

Conclusions

Thus the VIS has made attempts towards providing information on various development and management scenarios to decision-makers and the public for the integrated balanced and sustainable development of resources at the Village, Panchayat, Block, District and the State Level. The project attempts to generate and integrate comprehensive information on priority areas like Land Utilization, Tribal Development, Natural Resource Management and Utilization, Wasteland, Rural Development, Infrastructure and Amenities, Poverty Alleviation, Overall Development, e-Governance and other aspects to meet the goal of overall development of the State through grassroot. It has been an inter-disciplinary approach to generate and integrate necessary information for the multi-dimensional development in the Block and State.

References

1. AISLUS. 1970. Soil Survey Manual, IARI, New Delhi., pp
2. Application of GIS for Land use /cover change and analysis in a mountainous terrain S Ghosh, A C Sen, U, Rana K-S-Rao, IC Saxena, Journal of Indian Society of Remote Sensing, vol, 24:3, 193
3. Avery, T.E. 1977. *Interpretation of Aerial Photographs*, Third Edition, Burgess Publishing Company, Minneapolis.
4. Botkin, D.B., Estes, J.E., Mcdonald, R.M. and Wilson, M.V., 1984. Studying the Earth's vegetation from the space. *Bioscience*, 34: 508.
5. Brahmabhatt, V. S., Dalwadi, G. B., Chhabra, S. B., Ray, S. S. , and Dadhwal, V. K. 2000. Land use/ land cover change mapping in Mahi Canal command area, Gujrat, using multitemportal satellite data. *Journal of Indian Society of Remote Sensing*, 28, pp. 221-232.
6. Brahmabhatt 2000, Landuse, land cover change mapping in Mahi canal command tree Gujarat using multi-temporal satellite data , *Journal of Indian Society of Remote Sensing*, vol 28, 4, pp 221-232
7. BS Bisht, BP Kothari, 2001, Land-cover change analysis of Garua-Ganga watershed using GIS RS techniques, *Journal of Indian*

- Society of Remote Sensing, vol, 29:3, pp 137-42
8. Champion, H.G. and Seth S. K., 1968. *A revised Survey of the Forest Types of India*, Manager of Publication, Government of India, New Delhi, p 404.
 9. Daniel, D. and Shenan, I. 1987. A preliminary assessment of Landsat TM imagery for mapping vegetation and sediment distribution in Walsh estuary. *International Journal of Remote Sensing* 8(7): 1101-1108.
 10. Eswaran, H. J (1989). Soil Taxonomy and agrotechnology transfer.p 9-28. In: Soils for development (Ed. Van Cleemput et al. Proceedings Symp., 25st anniversary of ITC for PG Soil Scientists, Stqate Univ., Ghent (Belgium). ITC Ghent, Publ. Series 1. p. 107.
 11. Eswaran, H., Kimble, J., Cook, T. and Mausbach M (1987). World Benchmark Soils Project of SMSS. Soil survey and land evaluation 7: 111-122.
 12. FAO (1993). Agroecological assessments for national planning: the example of Kenya, FAO Soils Bulletin 67, Rome 1993.
 13. Ghose, S., Sen, K. K., Rana U., Rao, K S. and Saxena K. G. 1996. Application of GIS for land use / land cover change analysis in a mountainous terrain. *Journal of Indian Society of Remote Sensing*, 24, (3) pp. 193-202.
 14. Hall, R.J., Dams, R.V and Lyseng, L.N., 1991. Forest cut cover mapping from SPOT satellite data. *International Journal of Remote Sensing* 12(11): 2193-2204.
 15. Jakson, M. L. (1967). *Soil Chemical Analysis*. Prentice Hall, New York
 16. Jakson, M. L. (1973). *Soil Chemical Analysis*. Prentice Hall, New York.
 17. Klingbiel, A.A. and Montogomery, P.H. 1961. Land Capability Classification. Agric. Handbook, 210 SCA, USDA, Washington D.C.
 18. Kuchler, A.W., 1988. The classification of vegetation. In *vegetation mapping*. eds, A.W. Kuchler and I.S. Zonneveld, Kluwer Academic Publishers, London.
 19. Land use land cover Mapping and change detection in parts of Eastern Ghats of /-Tamilnadu using Remote Sensing, GIS, *Journal of Indian Society of RemoteSensing*, vol 31:4,pp251-260
 20. Land use / Land cover change analysis change in Mumbai - Navi Mumbai cities and its effects on the drainage basin & -catchments using GIS, *Journal of Indian Society of Remote Sensing*, vol : 26 1 & 2, ppl-6
 21. Lillesand, T.M. and R.W. Kiefer. 1987. *Remote Sensing and Image Interpretation*. Second Edition. John Wiley & Sons, New York.
 22. Loksha, N., Gopalkrishna, G. S., Honne Gowada H.and Gupta A. K. 2005. Delineation of ground water potential zones in a hard rock terrain Mysore district, Karnataka using IRS data and GIS techniques. *Journal of Indian Society of Remote Sensing*, 33, (3) pp. 405-412.
 23. Londhe, S.L. 1998. Study of spectral reflectance properties in specially associated red and black soils of Saptadhara Watershed, Nagpur district. M.Sc. (Agric.) Thesis (Unpub.)
 24. Minakshi, Churasia & Sharma P K , 1994, Land use land cover mapping and change detection using satellite data, A Case study of Ludhiana district Punjab, *Journal of Indian Society of Remote Sensing*, vol, 21 & 22, pp 115- 1 22
 25. Prasad, N., Goyal, S.P., Roy, P.S. and Singh, S., 1994. Changes in wild ass (*Equushemionus khur*) habitat conditions in Little Runn of Kutch, Gujarat from a remote sensing perspective. *International Journal of Remote Sensing*, 15 (10): 3155-3164.
 26. R.K. Jaiswal, A. Saxena, Sanmitra Mukherjeepp 123:128 Approach of RS techniques for Landuse and Land Cover
 27. Robinson, A.H., R.D. Sale, and J.L. Morrison. 1978. *Elements of Cartography*, Fourth Edition. John Wiley & Sons, New York.
 28. Roy, P.S. (1999). Forests resource assessment, prospects and issues, *GIS Development*, 3(5).
 29. Roy, P.S., Saxena, K.G., Pant, D.N. and Kotwal, P.C. 1986. Analysis of vegetation using remote sensing in Kanha National Park. *Proceedings Seminar-cum-workshop on Wildlife Habitat Evolution Using Remote Sensing Techniques*, 22-23 oct. 1986, Dehradun, p 6-12.
 30. Saxena, R.K., Verma, K.S., Chary, G.R., Srivastava Rajeev and Barthwal, A.K. 2000. IRS 1C data application inwatershed characterization and management. *International Journal of Remote Sensing*, 21, pp. 3197-3208.
 31. Sehgal, J. L. Saxena, R. K. and Vadivelu, S. (1989) *Field Manual- Soil Resource Mapping of different states in India*. Tech. Bull., 13, NBSS Publ.
 32. Talukdar, G.T. 2002. *Geospatial Modeling of Land Dynamic Processes in Shifting Cultivation Induced Landscapes of Meghalaya*. D.Phil thesis, University of Pune.
 33. Tisdale, S. L. Nelson W. L., Beaton J. D. and Havlin J. L. (1993). *Soil fertility and fertilizers*, fifth edition, Prentice Hall Publ. 634 pp
 34. Tucker, C.J., Gatlin, J.A. and Schneider, S.R., 1984. Monitoring vegetation in the Nile Delta with NOAA-6 and NOAA-7 AVHRR imagery. *Photogrammetric Engineering and Remote Sensing*, 50: 647-651.
 35. Walsh, S.J., 1980. Coniferous tree species mapping using Landsat data. *Remote Sensing of Environment* 9: 11-26.
 36. William, D.L. and Nelson, R.E 1986. Use of remotely sensed data for assessing forest stand conditions in Eastern United States. *IEEE Trans. Geosci. Remote Sensing* E-24: 130-138.



Remote Sensing Based Hazard Assessment of Glacial Lakes – A Case Study from Kumaon Himalaya, India

K. Babu Govindha Raj

Abstract

The climate change of the 20th century had a pronounced effect on glacier environments of Himalaya. The formation of moraine dammed glacial lakes and outburst flood from glacial lakes (GLOF) is major concern in countries such as Bhutan, China (Tibet), India, Nepal and Pakistan. Indian Himalaya possesses about 30 dangerous lakes out of 549 glacial lakes. The hazardous lakes, however, are situated in remote areas and very difficult to monitor through ground surveys due to rugged terrain and extreme climatic conditions. Study using temporal satellite data on one of the glacial lake in Kumaon Himalaya showing the glacial lake grown to an extent of 0.078 Km² areas in 2005. Empirical relations showing the lake can generate a discharge vary from 10.3 m³/sec to 118.2 m³/sec.

Keywords: Glacial lake; Kumaon Himalaya; GLOF; Satellite Data; Remote Sensing

Introduction

Global climatic change during the 20th century had a significant role in modifying the high mountainous glacial environment. Many glaciers retreated rapidly resulting in the formation of a large number of glacial lakes bounded by moraine dams. Warmer climates of past 100 to 150 years have resulted in widespread glacial retreat and formation of moraine-dammed lakes in many mountain ranges (Clague and Evans 1994). Eventually, either the volume of water becomes too great for the moraine to support or an event such as a large ice block detachment occurs and the moraine is

breached. Sudden discharge of large volumes of water along with debris from these lakes causes glacial lake outburst floods (GLOFs) in downstream areas. This results in destruction of valuable natural resources such as forests, farms, and expensive mountain infrastructures and human lives. Such flash floods are a common problem in countries such as Bhutan, India, Nepal and Pakistan.

During August 2000, in Tibetan Plateau, GLOF occurred and destroyed more than 10,000 houses and 98 bridges and financial losses were about 75 million US dollars (Shen 2004) . In 2008, GLOF from Gulkin glacier, Karakoram Himalayas also damaged many properties (Richardson and Quincey 2009). The GLOF event in Nepal during 1981 damaged the Friendship Bridge of the China-Nepal Highway and destroyed the Koshi power station in Nepal and caused serious economic losses (Bajracharya *et al.* 2006). Most of the glacial lakes in the Himalayan region are known to have formed within the last 5 decades, and a number of GLOF events have been reported in this region and many of which have trans-boundary impacts (Table 1).

Table 1. List of some of the Recorded GLOF events in Himalayan Region (Source: [3] and [4])

No	Year	Lake	River Basin/Area	Country affected	Cause of GLOF
1	September 1964	Gelhaipuco	PumQu / Arun	China and Nepal	Glacier surge
2	September 1977	Nare	Dudh Koshi	Nepal	Moraine collapse
3	June 1980	Nagma Pokhari	Tamor	Nepal	Moraine collapse
4	July 1981	Zhangzangbo	Boqu / Sun Koshi	China and Nepal	Glacier surge
5	August 1985	Dig Tsho	Dudh Koshi	Nepal	Ice avalanche
6	October 1994	Lugge-Tsho	Pho Chu	Bhutan	Moraine collapse
7	September 1998	Sabai Tsho	Khumbu Himal	Nepal	Not known
8	2008	Ghulkin Glacier lake	Karakoram	Pakistan	Moraine collapse

The hazardous lakes, however, are situated in remote areas and very difficult to monitor through ground surveys due to rugged terrain, inaccessibility and extreme

climatic conditions. Most glacial lakes in Indian Himalayan region have not yet been identified or studied completely because of their remote locations (Richardson and Reynolds 2000). Remote sensing is found to be one of the best techniques for identifying such glacial lakes and offers strong advantages for first and qualitative hazard assessments of glacier lakes.

A first level inventory of glacial lakes and their characteristics were done by the International Centre for Integrated Mountain Development (ICIMOD), Nepal for Himalaya (Bajracharya *et al.* 2006). A compiled list of some of the glacial lakes in Indian Himalaya is given in Table 2.

Table 2. List of some of the glacial lakes in Indian Himalaya, (Source: [4] and *[13])

River Basin/ State	Glacial Lakes		
	Number	Area (sq Km)	Potential GLOF
Himachal Pradesh	156	385.22	16
Uttarkhand	127	2.49	0
Tista River	266	20.20	14
Sikkim*	6	7.6	Not available
Chandra basin*	01	1.04	01

Study Area

The moraine dammed glacial lake (30° 26' 45.53" N, 80° 23' 18.74" E) situated at an elevation of 5000 m at the snout of the glacier (no name exists) in the Lassar Yankti river basin of NE part of Pithoragarh district, Uttarakhand, India (Figure 1). The glacier is a simple mountain basin glacier orientating NE-SW having well developed lateral and terminal moraines.

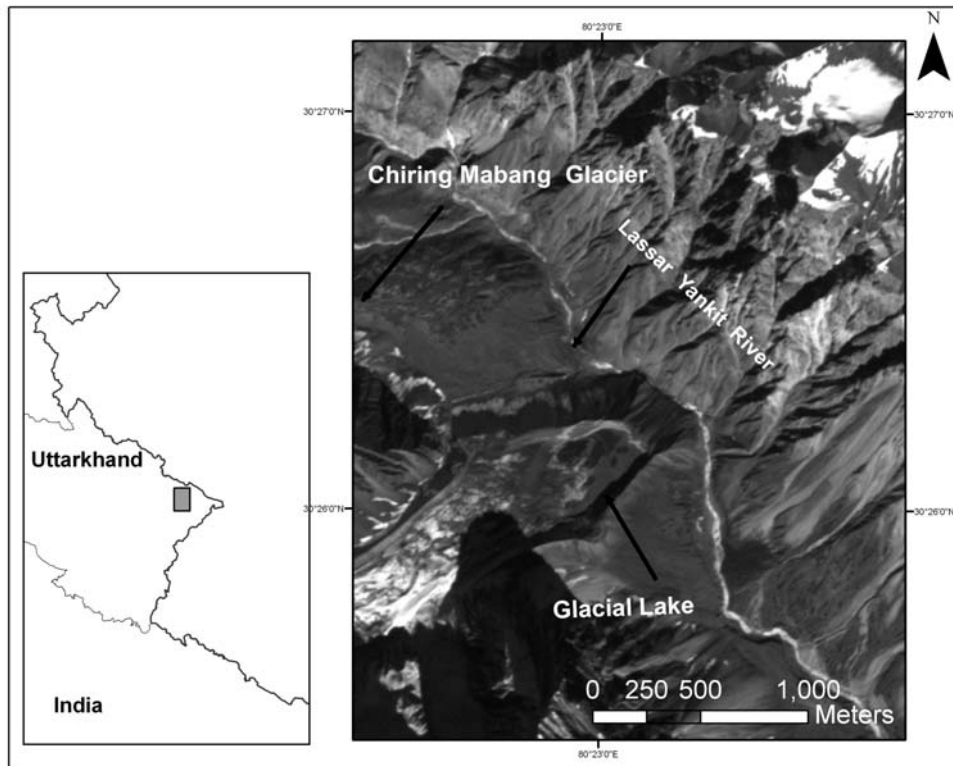


Fig 1. Lassar Yankti river basin of NE part of Pithorgarh district, Uttarakhand, India

Data Used

Landsat MSS and TM and Resourcesat-1 LISS III satellite data were used in this study. Apart from satellite data, Garhwal Himalaya OST map (1955) on scale 1:1, 50,000 (provided by Swiss Foundation for Alpine Research) and ASTER DEM were also used. Table 3 shows details of the data used in the present study.

Table 3. Details of Satellite data used in the present study.

Satellite	Sensor	Spatial Resolution (meters)	Acquisition Date / Remarks
Landsat -2	MSS	57	15-11-1976
Landsat -5	TM	30	15-11-1990
IRS P6	LISS III	23.5	18-11-2005
TERRA	ASTER	~20 (vertical)	ASTER GDEM

Methodology

For this study, Garhwal Himalaya OST map prepared in 1955 was used as the base data. The glacier extent was mapped from the Georeferenced OST map. The lake is not shown on the OST map. Therefore, it can be assumed that the lake is formed after 1955. The first occurrence of the lake is marked in the Landsat MSS data of 1976. The glacier boundary and lake areal extent mapped from the MSS data. From 1955 the glacier receded about 177 meters and the lake formed in the cavity created by the retreating glacier. The length measurements were carried out along the centre line of the glacier. In 1976, the lake is having an aerial extent of 0.03 km² and the lake is attached to the glacier terminus bounded by the lateral moraines and terminal moraines.

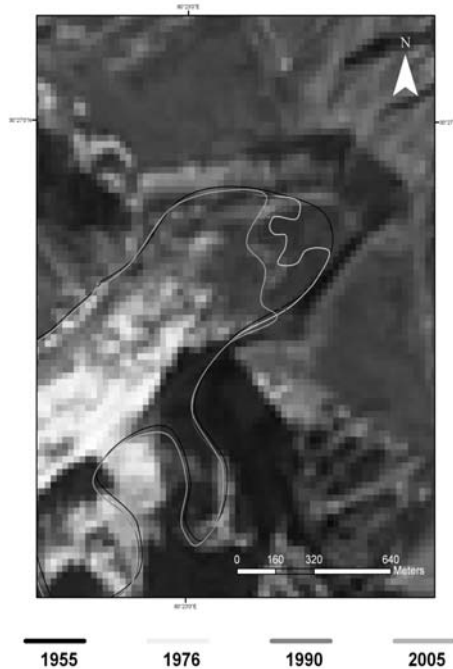
In 1990 the glacier boundary and areal extent of lake mapped from Landsat TM data.

The glacier retreated 18 meters and the lake grown by 0.013 Km² from the earlier extent of 1976. The latest extent measured in 2005 shows the glacier receded 128 meters and the lake has grown to an extent of 0.029 km² from 1990 (Figure 2).

The depth measurements of the lake carried out from ASTER DEM. The difference in height of the bounding lateral moraines and center part of the lake is considered for calculating the depth of the lake. For further analysis the depth of the lake is taken as 25 m. The areal extent of the lake is measured as 0.078 km² in year 2005. The volume of lake is estimated as the product of area and depth and calculated volume is 1.97 million m³.

The magnitude of a flood caused by the breach of moraine dam is relevant for further hazard analyses. The empirical equations used for estimating the maximum discharge Q_{max} are given in Table 4. The parameters in these equations are lake volume (V in m³) or potential energy (PE) of the lake. PE is expressed as the product of dam height (m), volume (m³), and the specific weight of water (98000 N/m³) (Costa and Schuster 1988).

Figure 2. Retreat map of the glacier in different time periods



Discussion and Conclusion

Estimation of discharge from the lake was done using empirical equations (Table 4).

Table 4. List of models used for estimation of maximum discharge (Q_{\max}).

Code	Formulae or models	References	Results (m ³ /sec)
1	$Q_{\max}=75V^{0.67}$	[6]	118.2
2	$Q_{\max}=0.72V^{0.53}$	[7]	10.3
3	$Q_{\max}=0.0048V^{0.896}$	[8]	88.12
4	$Q_{\max}=0.045V^{0.66}$	[9]	70.40
5	$Q_{\max}=0.063PE^{0.42}$	[10]	12.20
6	$Q_{\max}=70.00077V^{1.017}$	[11]	15.34

For all the equations the lake volume is assumed as 1.97 million m³, average depth as 25 m and PE as 4.82×10^{11} . The resultant maximum instantaneous discharge from the lake is given in the Table 4. Subsequent to the development of the above formulas many physical based models were developed to estimate peak discharge. Due to non-availability of other parameters such as ice thickness, lake temperature, length of drainage tunnel, bathymetry of the lake etc., it is difficult to apply such models for this kind of investigations. Therefore, above mentioned models are used for initial assessment of lake discharge.

As mentioned in the earlier section, maximum possible lake volume is 1.97 million m³, and lake depth is 25m; peak discharge is estimated by using the formulas (Table 4). Due to the lack of field data the modeled discharge error is unknown. In Indian Himalayan region flash floods from sudden downpour due to cloudburst is very common in monsoon period. The formation of cloudburst over glacial lakes can cause dangerous GLOFs.

This paper presents the utility of remote sensing in detecting and monitoring the hazardous nature of glacial lakes in highly glaciated terrain of Indian Himalaya. Empirical models allow an approximate estimate of a potential GLOF hazard. If the preliminary study indicating a severe hazard potential, more detailed field survey may be required to establish the risk of GLOF. In view of fast retreating glaciers in Himalaya to establish the hazard potential of glacial lakes a systematic inventory of glacial lakes using remote sensing and in situ field survey is recommended and adaptation

measures like early warning systems and mitigation measures are required in potential GLOF areas.

Acknowledgements

The author would like to thank Director, NRSC and Deputy Director (RS & GIS), NRSC for providing support during the course of work. Thanks to GLCF, University of Maryland, USA for the Landsat MSS and TM data, Swiss Foundation of Alpine Research, Zurich for providing the Garhwal Himalaya OST Map and ERSDAC for ASTER GDEM.

References

1. Clague, J.J. and Evans, S.G.(1994) Formation and failure of natural dams in the Canadian Cordillera, Geological Survey of Canada Bulletin(464).
2. Shen, Y. (2004) An Overview of Glaciers, Retreating Glaciers and Their Impact in the Tibetan Plateau, Chinese Academy of Sciences (CAS) Report(42).
3. Richardson, S. D. and Quincey, D.J.(2009) Glacier outburst floods from Ghulkin Glacier, Upper Hunza Valley, Pakistan, Geophysical Research Abstracts, EGU2009-12871, EGU General assembly, 19-24 April 2009, Vienna, Austria.
4. Bajracharya, R.S., Mool, P.K. and Shrestha B.R.(2006) The impact of global warming on the glaciers of the Himalaya. International symposium on Geo-disasters, infrastructure management and protection of world heritage sites proceedings :231 - 242.
5. Richardson, S.D. and Reynolds, J.M.(2000) An overview of glacial hazards in the Himalayas, Quaternary International (65-6): 31-47.
6. Clague, J.J. and Mathews, W.H.(1973) The magnitude of Jökulhlaups, Journal of Glaciology (12): 501-504.
7. Evans, S.G. (1986) The maximum discharge of outburst floods caused by the breaching of man-made and natural dams, Canadian Geotechnical Journal (23): 385-387.
8. Popov, N.(1991) Assessment of glacial debris flow hazard in the north Tien-Shan, In Proceedings of the Soviet-China-Japan Symposium and field workshop on natural disasters :384-391.
9. Walder, J.S., and O'Connor, J.E.(1997) Methods for predicting peak discharge of floods caused by failure of natural and constructed earthen dams, Water Resources Research (33): 2337-2348.
10. Clague, J.J. and Evans, S.G.(2000) A review of catastrophic drainage of moraine-dammed lakes in British Columbia, Quaternary Science Reviews (19): 1763-1783.
11. Huggel, C.; Kääh, A.; Haeblerli, W.; Teysseire, P. and Paul, F.(2002) Remote sensing based assessment of hazards from glacier lake outbursts: a case study in the Swiss Alps, Can. Geotech. Journal (39):316-330.
12. Costa J.E. and Schuster, R.L.(1988) The formation and failure of natural dams, Geological Society of America Bulletin (100): 1054-1068.
13. Kulkarni, A. V. (1996) Moraine- Dammed Glacial Lake Studies using Remote Sensing Technique, Himalayan Geology (17): 161-164.



Manuscript Submission Guidelines: Notes for Authors

1. Contributions may be submitted in any language, but will be published only in English.
2. Contributions are considered for publication only on the understanding that they are not published already elsewhere, that they are the original work of the authors (s), and that the authors assign copyright to the National Institute of Disaster Management, New Delhi.
3. Standard length of papers is 6000 words, but shorter/longer contributions are also welcomed. They should be typed, double spaced on one side of the paper with margins of 3 cm.
4. Papers should normally be submitted as e-mail attachments to the Editor. The subject of the e-mail should be typed 'CONTRIBUTION FOR DISASTER AND DEVELOPMENT'.
5. Papers may also be sent in hard copies by registered post but these must always be accompanied by a virus-free 3½ inch disk with manuscript formatted in Word for Windows. Disks should be labeled with the name of the article and the author.
6. Title, author's name, full address and brief biographical note should be typed on a separate sheet.
7. an abstract of 100-200 words and about 5 key words should also be typed on a separate sheet.
8. Figures, maps and diagrams should be precisely and boldly drawn to permit photographic reproduction. Use single quotation marks (except for quotes within quotes).
9. Notes should appear at the end of the text.
10. Referencing in the text should be as follows: (Brinkley 2006:157).
11. Recommended style for the bibliography is: Brinkley, D (2006) The Great Deluge-Hurricane Katrina, New Orleans and the Mississippi Gulf Coast. New York. Harper Coillins.
Weibull, A. (1994) 'European Officers' Job Satisfaction and Job Commitment', Current Sociology 42 (3): 57-70.
12. Authors receive proofs of their articles, 25 offprints of the published version and one copy of the journal. Authors are responsible for obtaining copyright permission for reproducing any illustrations, tables, figures or lengthy quotations published elsewhere.



National Institute of Disaster Management
IIPA Campus, I.P. Estate, Mahatma Gandhi Marg, New Delhi -110002
Phone: 91- 11 -23702445, Fax: 91- 11- 23702446